

# **Regulation of mTOR and its Role in Reproduction**

- Invasion-related Signal Transduction in Human Trophoblast Cells

## **Dissertation**

zur Erlangung des akademischen Grades *doctor rerum naturalium* (*Dr.rer.nat.*)

vorgelegt dem Rat der Biologisch-Pharmazeutischen Fakultät der Friedrich-Schiller-Universität Jena

von Susann Busch

geboren am 05.05.1980 in Jena

1. Gutachter: PD Dr. med. Udo R. Markert, Friedrich-Schiller-Universität Jena
2. Gutachter: Prof. Dr. rer. nat. Claus Liebmann, Friedrich-Schiller-Universität Jena
3. Gutachter: PD Dr. rer.nat. Udo Jeschke, Ludwig-Maximilians-Universität München

Verteidigung: 15.10.2008

Die wahre Entdeckungsreise  
besteht nicht darin,  
dass man neue Landschaften sucht,  
sondern dass man mit neuen Augen sieht.

Marcel Proust<sup>1</sup>



Wenn der Kontrollierende das Kontrollierte ist, [...] dann entsteht eine  
vollkommen andere Art von Energie, die das, was ist, verwandelt.

Krishnamurti<sup>2</sup>

---

<sup>1</sup> Valentin Louis Georges Eugène Marcel Proust (\* 10. Juli 1871 in Auteuil; † 18. November 1922 in Paris) war ein französischer Schriftsteller, Kritiker und Intellektueller [Wikipedia]. Zitat aus „Auf der Suche nach der verlorenen Zeit“ (*À la recherche du temps perdu*)

<sup>2</sup> Jiddu Krishnamurti (\* 12. Mai 1895 in Madanapalle, Indien ; † 17. Februar 1986 Ojai, Kalifornien) war ein indischer Brahmane, Autor und spiritueller Lehrer [Wikipedia]. Zitat aus „Vollkommene Freiheit“ (*Total Freedom*)

# Table of contents

<b>Motivation</b>	<b>1</b>
<b>1 Introduction</b>	<b>2</b>
<b>1.1 Pregnancy – Puzzle of fine regulation</b>	<b>2</b>
1.1.1 Immunological paradoxon between mother and foetus	2
1.1.2 Placenta – Platform for life	3
1.1.2.1 Aspects of placental development	3
1.1.2.2 Placental signal transduction induced by growth factors and chemokines	4
1.1.3 Trophoblast “Pseudo-tumourigenesis”	5
1.1.3.1 Trophoblast proliferation and differentiation	5
1.1.3.2 Molecular features of migration and invasion	7
1.1.3.3 Restriction of trophoblast invasion	8
1.1.4 Trophoblastic cell line models	9
<b>1.2 Welcome to the TOR signalling network</b>	<b>10</b>
1.2.1 Structure and function of mTOR	10
1.2.2 Upstream effectors and regulation of mTOR	11
1.2.2.1 Upstream signalling events	11
1.2.2.2 Positive regulator of mTOR: Rheb GTPase	13
1.2.3 Downstream targets	14
1.2.4 Feedback and cross-talk signalling	14
1.2.5 Inhibitor of mTOR: Rapamycin	15
1.2.6 mTOR and cancer	16
1.2.7 mTOR and reproduction	16
<b>1.3 Objectives</b>	<b>17</b>
<b>2 Material and Methods</b>	<b>19</b>
<b>2.1 Regulation of mTOR by Rheb in HEK293T</b>	<b>19</b>
2.1.1 Generation of Rheb mutants	20
2.1.1.1 Primer design	20
2.1.1.2 PCR mutagenesis	21
2.1.1.3 Transformation	22
2.1.1.4 Plasmid preparation	22
2.1.1.5 Subcloning	23

2.1.2 Cell culture and transfection	24
2.1.3 Cell lysis and protein isolation	25
2.1.4 Gel electrophoresis and Western blot	25
2.1.5 Analysis of Rheb functions	26
2.1.5.1 Functional assay: Amino acid withdrawal	26
2.1.5.1 Binding assay: GST pull down	26
<b>2.2 Role of mTOR in trophoblast invasion</b>	<b>27</b>
2.2.1 Cell line and cell culture	27
2.2.2 Manipulation of cells	27
2.2.2.1 RNA interference	27
2.2.2.2 Chemical inhibitors	29
2.2.3 Cell lysis and protein isolation	30
2.2.4 Gel electrophoresis and Western blot	31
2.2.5 MTS proliferation assay	32
2.2.6 Apoptosis assay: Cleaved PARP	32
2.2.7 Invasion-related analysis	33
2.2.7.1 Substrate zymography	33
2.2.7.2 Immunocytochemistry of PAI-1	33
2.2.7.3 PAI-1 ELISA	34
2.2.7.4 <i>In vitro</i> Matrigel invasion assay	34
2.2.8 Immunohistochemistry of placental tissue	35
<b>2.3 Data presentation and statistics</b>	<b>36</b>
2.3.1 Standard deviation	36
2.3.2 Student t-Test	36
<b>3 Results</b>	<b>37</b>
<b>3.1 Regulation of mTOR by Rheb in HEK293T</b>	<b>37</b>
3.1.1 Expression level of created Rheb mutants	37
3.1.2 Mutagenic Rheb function upon amino acid withdrawal	38
3.1.3 Binding properties of Rheb mutants	40
<b>3.2 Role of mTOR in trophoblast invasion</b>	<b>41</b>
3.2.1 Transfection with siRNA	41
3.2.2 Phosphorylation of p70 <sup>S6K</sup> to monitor mTOR kinase activity	43
3.2.3 Stat3 phosphorylation	45
3.2.4 Proliferationrate	46
3.2.5 Level of apoptosis induction	50

3.2.6 Invasion-related assays	52
3.2.6.1 Zymolytic activity	52
3.2.6.2 Expression and secretion of PAI-1	55
3.2.6.3 Cell invasiveness	59
3.2.9 Immunohistochemistry of placental tissue	61
<b>4 Discussion</b>	<b>64</b>
<b>4.1 Regulation of mTOR by Rheb in HEK293T</b>	<b>64</b>
4.1.1 Severe loss-of-function for Rheb switch 1 and 2 mutants	64
4.1.2 The Rheb switch 2 segment is critical for mTORC1	65
<b>4.2 Role of mTOR in trophoblast invasion</b>	<b>66</b>
4.2.1 Establishment of siRNA transfection in HTR8/SVneo	66
4.2.2 Rapamycin inhibits proliferation and apoptosis whereas mTOR knockdown promotes apoptosis	67
4.2.3 Role of mTOR signalling in trophoblast invasion through uPA and PAI-1 secretion	69
4.2.4 Cross-talk between mTOR and Stat3 signalling in trophoblast cells	72
4.2.5 No differential expression of mTOR in human first-trimester and term placenta	73
<b>4.3 Model: Role of mTOR regulation in human reproduction</b>	<b>73</b>
<b>4.4 Perspective</b>	<b>75</b>
<b>5 Appendix</b>	<b>78</b>
<b>5.1 Material list</b>	<b>78</b>
<b>5.2 Supplementary densitometric analysis</b>	<b>82</b>
<b>5.3 Summary</b>	<b>94</b>
<b>5.4 Bibliography and Index of Tables</b>	<b>96</b>
<b>5.5 References</b>	<b>97</b>
Zusammenfassung	105
Curriculum vitae	<b>Fehler! Textmarke nicht definiert.</b>
Danksagung/Acknowledgement	107
Ehrenwörtliche Erklärung	108

## Motivation

Pregnancy is known to be a tolerated semi-allogenic event and therefore considered an immunological paradoxon. It has been debated whether the maternal immune system is “tricked” to fail recognizing the “foreign” foetus by an immunological inert barrier. It is now well accepted that immune-competent cells of the mother at the foeto-maternal interface are required for successful pregnancy as a functional immune system will trigger signals allowing the foetus to grow and also to induce the essential tolerance [1-3].

The foetus anchors and nourishes itself by the placenta, which is an autonomous unit comprised of maternal and foetal cells. The foetal cells will invade the maternal tissue by means that resemble the invasive behaviour of tumour cells. Once foetal trophoblast cells are rendered into an invasive state, they infiltrate the maternal tissue and replace endothelial cells of the maternal spiral arteries, thereby contributing to placental remodelling. Unlike to cancer, invasion of trophoblast cells is under physiological control in terms of temporal and spatial limitations. Nevertheless, cancer attributes such as immune suppression, proliferation, migration and invasion account for a “pseudo-tumourigenesis” process as part of the pregnancy [4].

If the fine regulation of those mechanisms is disturbed, pregnancy pathologies such as pre-eclampsia, intra-uterine growth retardation (IUGR), trophoblast moles, choriocarcinoma or even miscarriage can occur. Of special importance regarding adverse pregnancy outcome is trophoblast invasiveness as for instance pre-eclampsia is characterized by shallow trophoblast invasion resulting in small placentae, whereas increased invasiveness might lead to the formation of trophoblast moles [5, 6].

Therefore, it is of high scientific interest to aim for a better understanding of the regulation of the temporally and spatially restricted trophoblast invasion. So far, very little is known about the regulation of trophoblast invasion and the involved intracellular signalling events.

In this study, the focus was set on functional aspects of trophoblast invasion by manipulating signalling pathways of a first-trimester trophoblast cell line model (HTR8/SVneo). Hereby, special interest was focussed on the regulation of and by the signalling molecule mTOR. It was already demonstrated that mTOR plays a role in murine trophoblast outgrowth *in vitro* and mTOR knockdown was shown to be post-implantational lethal in mice [7].

The presented work contributes just a small piece to the puzzle to unravel the regulative mechanisms which arise during the paradoxon pregnancy.

# Chapter 1 | Introduction

## 1.1 Pregnancy – Puzzle of fine regulation

Several mechanisms at the foeto-maternal interface (decidua) contribute to the maintenance of pregnancy. The fine regulation of the communication between maternal and foetal cells is of great importance and dysregulation results in pregnancy-related diseases such as pre-eclampsia, intra-uterine growth retardation (IUGR) and choriocarcinoma or even in the loss of the foetus (miscarriage, recurrent spontaneous abortion; RSA). It is to note that detailed knowledge of implantation and trophoblast invasion in humans is elusive and therefore makes extrapolation from other mammals necessary.

### 1.1.1 Immunological paradoxon between mother and foetus

The semi-allogenic foetus bears half of the paternal antigens which are foreign to the maternal immune system and which is therefore a potential target of an immunological attack. Tolerance failure of the maternal immune system will consequently lead to the rejection of the foetus.

The immune system is assessed with a distinct set of MHC receptors which will allow a determination of self and non-self antigens. Lack of self or non-self/foreign antigens will hence trigger an immune reaction, exerted by immune cells such as T-, B-, NK cells, macrophages, dendritic cells and many others.

It was believed for a long time that the foeto-maternal interface is, similar to the eye or brain, an immunological inert site in order to evade any contact with the maternal immune system. It is now accepted that in fact the opposite is more likely. Recognition of the foetus by the mother's immune system is required to achieve a successful pregnancy while also inducing immunological tolerance [1-3]. Without that recognition, early events of pregnancy, such as the implantation of the blastocyst might already be disturbed.

During pregnancy the pre-dominant immune cells within the placenta are NK cells, which will largely increase until the end of the first trimester and then decline again towards term. NK cells make up to 70% of the decidual lymphocytes and exhibit the cytokine-secreting phenotype with less CD16 receptors on the cell surface which are important for NK cytotoxicity [8]. It has been proposed that the decidual NK cells play therefore a role not in immune defence but in the maintenance of pregnancy by chemokine and receptor expression supporting foetal growth and invasion of the foetal cells (trophoblasts) [9]. This idea is supported by



the fact that certain isoforms of NK receptors are markers for higher risk of pre-eclampsia, a severe pregnancy pathology which is manifested by small placentae and shallow trophoblast invasion [10].

In order to maintain pregnancy and avoid an immunological rejection, various further mechanisms account for the survival of the foetus. Of special importance are hereby the secretion of non-classical MHC class I molecules (HLA-E, G) which inhibit NK cytotoxicity, the secretion of indoleamine 2,3-dioxygenase (IDO) which depletes tryptophan and thereby inhibits T cell activity and the secretion of cyto-/chemokines favouring a non-inflammatory environment (Th2 shift) [11-13] and the expression of Galectin-1 [14].

### 1.1.2 Placenta – Platform for life

#### 1.1.2.1 Aspects of placental development

As soon as implantation of the blastocyst occurs (around day 6 post-conception), foetal cells start to infiltrate the maternal tissue. The start of this trophoblast invasion leads to the decidualization of the mother's uterine epithelium, finally resulting in the development of the placenta, which will anchor the foetus and supply it with all demands for nutrients and oxygen.

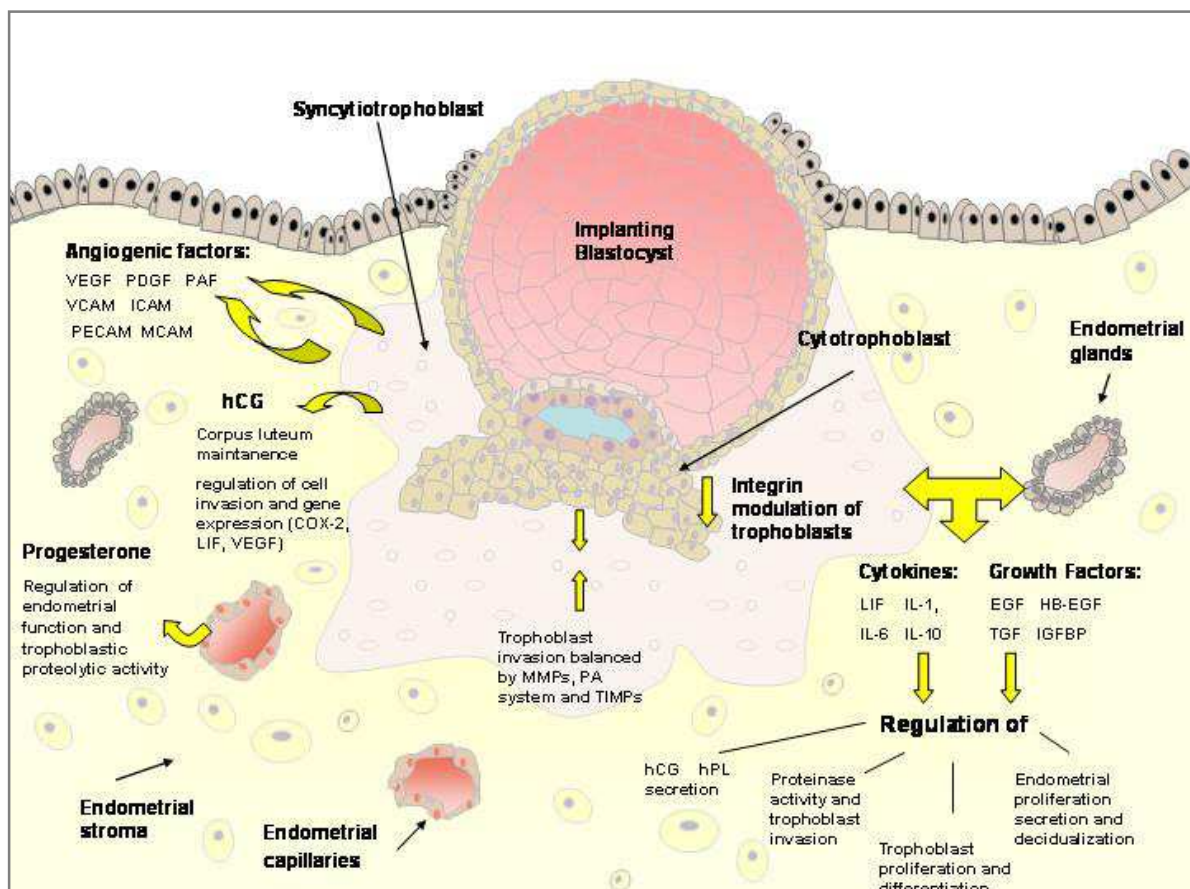


figure 1. Schematic presentation of an implanting blastocyst, highlighting invasion-regulating interactions between trophoblast and endometrial cells, including integrins, growth factors, cytokines, hormones and proteases (taken from Staun-Ram and Shalev 2005).

Around day 7 to 9 post-conception the first erosion of maternal tissues by invasive trophoblast takes place and uterine epithelium regrows over the conceptus until it is fully embedded. From gestational week 2 until term, trophoblasts invade into the connective tissue (day 14 to term) and into the walls of maternal spiral arteries (gestational week 3 to term) with its peak around gestational week 12. From this on, the flow of maternal plasma and blood into the intervillous space of the placenta can arise. During the course of placentation the villous surface expands to 12.5 m<sup>2</sup> at the end of term [15].

Trophoblast cells develop in parallel to the embryo and are therefore a non-somatic cell population with a distinct protein expression. A schematic picture that summarizes the anatomy of the implantation site and localization of trophoblast subtypes can be seen in figure 1. The placenta represents an autonomous and self-sufficient unit capable of modulating its own growth and function [4].

### 1.1.2.2 Placental signal transduction induced by growth factors and chemokines

The regulation of the placental microenvironment evolves from cyto-/chemokines, growth factors, hormones, enzymes secreted by maternal and foetal cells which are required for tissue remodelling, trophoblast invasion, as well as for tolerance induction [16].

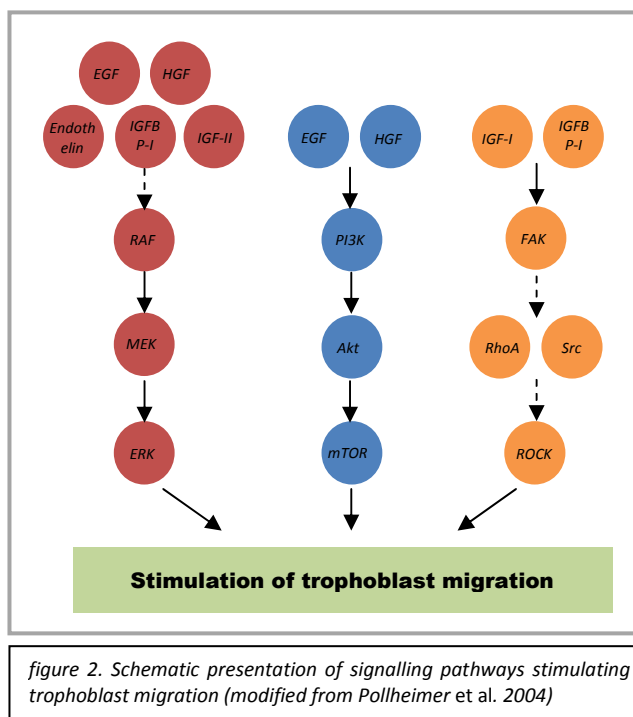
Growth factors and cyto-/chemokines which are expressed within the placenta and which were shown to have a special role in trophoblast growth, differentiation, spreading and/or invasion are: leukaemia inhibitory factor (LIF) [11], hepatocyte growth factor (HGF) [17], insulin-growth factor-I (IGF-I) [18], IGF-II [19], epidermal growth factor (EGF) [20], transforming growth factor- $\alpha$  (TGF- $\alpha$ ) [21] and placental growth factor (PIGF) [22] and various others. The source and effect on trophoblast cells by several factors can be seen in table 1.

Factors	Source	Effect		
		Proliferation	Migration	Invasiveness
<b>Adhesion molecules</b>	Trophoblast		↑↓	↑↓
<b>Angiopoietins</b>	Decidua, trophoblast		↑	
<b>Colony Stimulating Factor-I</b>	Placenta, decidua	↑		
<b>Decorin</b>	Decidua	↓	↓	↓
<b>Epidermal Growth Factor</b>	Decidua, trophoblast	↑		↑
<b>Endothelin</b>	Placental blood vessels, CT, ST, EVT		↑	
<b>Hepatocyte Growth Factor</b>	Decidua, trophoblast		↑	↑
<b>Insulin-like Growth Factor II</b>	Trophoblast		↑	↑
<b>Insulin-like Growth Factor Binding Protein-I</b>	Decidua		↑	↑
<b>Melanoma Cell Adhesion Molecule</b>	Uterine smooth muscle cells		↓	
<b>Metalloproteinases</b>	Trophoblast			↑
<b>Nodal</b>	Placenta	↓		
<b>Hypoxia</b>				↑↓
<b>Urokinase-type Plasminogen Activator</b>	Trophoblast		↑	↑
<b>Prostaglandin E<sub>2</sub></b>	Decidua, trophoblast		↑	
		↓	↓	
<b>8-iso-PGF<sub>2<math>\alpha</math></sub></b>	Decidua			↓
<b>Placental Growth Factor</b>	Trophoblast	↑		
<b>TGF-<math>\beta</math></b>	Decidua, trophoblast, uNK cells	↓	↓	↓
<b>TNF-<math>\alpha</math></b>	Decidua, uNK cells, decidual macrophages		↓	
<b>VEGF</b>	Decidua, trophoblast	↑		

table 1. Some of the key factors regulating EVT cell function (taken from Luhnghi et al. 2007)

These factors trigger cascades of signals in trophoblasts. Those pathways include signal molecules such as G-proteins, mitogen-activated proteinkinases (MAPKs), focal adhesion kinase (FAK), PI3K, Akt, mTOR, TGF- $\beta$ -dependent Smads, signal transducer and activator of transcription (Stat) and nuclear factor-kappa B (NF $\kappa$ B). A summary of several signalling molecules induced by the appropriate growth factors is schematically depicted in figure 2 [23].

A lack or aberrant expression of growth factors can cause pathologies or may be symptoms of pathologies such as pre-eclampsia which was correlated with a low level of HGF. A low level of HGF was also linked to placental defects with diminished trophoblast growth and embryonic lethality in mice [24].



### 1.1.3 Trophoblast “Pseudo-tumorigenesis”

As mentioned before, trophoblasts resemble cancer cells in many aspects as they exhibit tumour-like attributes such as rapid proliferation, migration, invasion and immune suppression mechanisms. However, unlike cancer the invasion process of trophoblast cells is kept in check. Also, their differentiation is not a consequence of a multi-step progression of genetic alterations within tumour suppressor genes or proto-oncogenes as it happens in cancer, but manifested by physiological means.

#### 1.1.3.1 Trophoblast proliferation and differentiation

Upon blastocyst implantation, trophoblast cells begin to differentiate in two different subtypes, cytotrophoblasts and syncytiotrophoblasts. The latter are formed by fusion of trophoblast cells which make contact with the uterine epithelium generating a syncytium. This multinucleated cell layer covers the placental

villi, possesses endocrine activity and is in direct contact with the maternal blood and is thus, capable for foeto-maternal exchanges. It is fully differentiated and therefore lacks any generative activity. The cytotrophoblast cells are mononucleated and represent the proliferating pool of trophoblasts (also referred to as trophoblast stem cells). They divide rapidly and give rise to other subtypes and by subsequent differentiation through syncytial fusion expand and maintain the syncytium. A schematic presentation of the anatomy of the implantation site/foeto-maternal interface is given by figure 3.

Around day 12 to 14 post-conception, cytotrophoblast start to penetrate the syncytium reaching the outer part and coming into contact with the maternal tissue. Here, they form cylinder-shaped cell accumulations called trophoblastic cell columns from which invading trophoblast termed extravillous trophoblast cells (EVTs) start to invade.

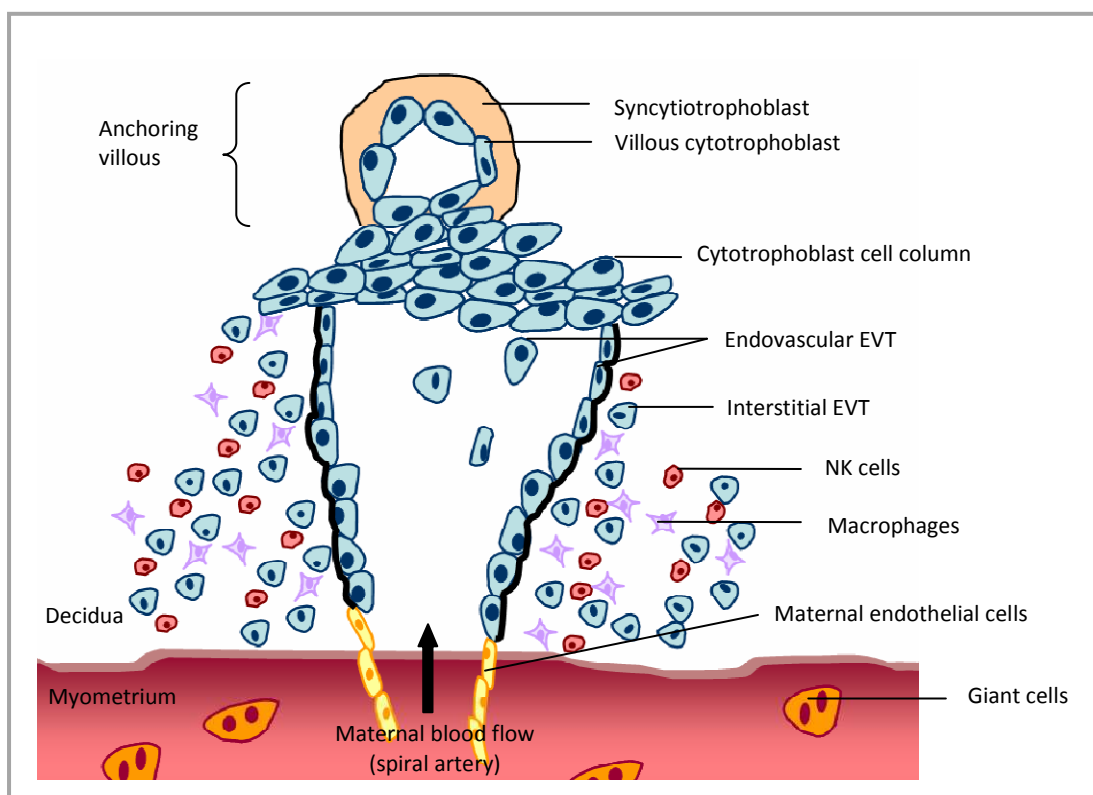


figure 3. Placental implantation site (modified after Lunghi et al. 2007).

EVTs are a discrete set of trophoblast with difference in phenotype and function compared with the villous type. EVT's originate from trophoblast cells which are in proximity of the basement membrane of the villi. Daughter cells of this subtype exhibit no longer proliferative capacity but start to differentiate and migrate. This feature is a major difference to malignant tumour cells which still show proliferative activity during the invasive process. EVT's that migrate through the decidual stroma are referred to as interstitial EVT's and come in contact with maternal cells such as lymphocytes. The exact interplay between both populations is not well understood. For instance, it seems that certain NK cell receptors play a role in stimulating trophoblast growth.

During their course of invasion, EVT<sub>s</sub> undergo phenotypical changes and switch their repertoire of integrins favouring the migration process. EVT<sub>s</sub> can also be subdivided structurally in three different subtypes; large polygonal EVT<sub>s</sub>, small spindle-shaped EVT<sub>s</sub> and multinucleated giant cells.

Some EVT<sub>s</sub> take a side route in their way of invasion and reach the walls of maternal spiral arteries. They are referred to as endovascular EVT<sub>s</sub>. They are either located inside the media or lining their lumina. They replace the maternal endothelial cells leading to extravasation of the vessel. Thereby, the arteries undergo a dilation which is several times of the original diameter. The transformation of the spiral arteries into dilated and large capacity vessels together with a reduced activity of the smooth muscles surrounding the arteries ensures an adequate utero-placental circulation, the prerequisite of a normal growth and development of the foetus.

The differentiation of the trophoblast cells is controlled by various factors such as transcription factors, hormones growth factors, cytokines and oxygen level [15].

#### 1.1.3.2 Molecular features of migration and invasion

The key components along the invasive course of cells are the extra-cellular matrix (ECM) proteins (such as fibronectin, laminin, collagen, vitronectin), their receptors (integrins) and ECM-degrading enzymes (such as matrix-metalloproteinases; MMPs). In order to migrate and invade, cells have to overcome the basal lamina, digest the surrounding matrix leading to destruction or remodelling of the tissue and also to acquire independence of their anchorage-attachment.

Trophoblasts modulate their integrin repertoire during invasion and differentiation. Integrins are heterodimeric membrane glycoproteins, composed of  $\alpha$ - and  $\beta$ -subunits. Depending on the type of  $\alpha/\beta$  combination, they are able to bind to various ECM components and cell adhesion molecules (CAM) and mediate cell-cell interaction. Upon binding they affect cell adhesion, spreading, migration, reorganisation of the cytoskeleton and cell signalling.

Upon their integrin expression EVT<sub>s</sub> can be discriminated into invasive and non-invasive cells. Invading EVT<sub>s</sub> upregulate  $\alpha 5\beta 1$  (vitronectin receptor) and  $\alpha 1\beta 1$  (collagen receptor) integrins and vascular cell adhesion molecule (VCAM), whereas  $\alpha 6\beta 4$  (probably a laminin receptor) is downregulated. This progression of the phenotype is also designated as integrin switch. The integrin  $\alpha 1\beta 1$  and VCAM expressed by endovascular EVT<sub>s</sub> enables the cells to blend with the endothelial cells and penetrate the walls of the spiral arteries. The endothelial cell adhesion molecules ICAM (intercellular adhesion molecule), VCAM and PECAM (platelet endothelial cell adhesion molecule) are important in endothelial activation and were found to be elevated expressed by the maternal endothelium during pregnancy [25].

When invading into the maternal tissue and penetrating the uterine wall of spiral arteries, trophoblast cells are confronted with ECM proteins. The composition of the ECM components affects cell adhesion, migration, differentiation and spreading and thereby influences trophoblast behaviour and function. Trophoblast cells secrete matrix-metalloproteinases (MMPs) which break down all components of ECM, both interstitial matrix and basement membrane. They also secrete the tissue inhibitors of matrix-metalloproteinases (TIMPs) [25].

TIMPs are secreted by maternal endometrial cells as well as by trophoblast and restrain MMP activity thus contributing a mechanism to control trophoblast invasion [26].

So far, 22 human MMPs are known which are subdivided in five classes according to their structure and substrate specificity. MMPs regulate cell-matrix and cell-cell interactions, and also the release, activation or inactivation of signal molecules or receptors. They are themselves regulated at transcriptional level, by secretion, activation, inhibition and degradation. MMP expression is cell-, tissue- and MMP-specific and can be induced by cytokines and growth factors. They are secreted as pro-enzymes (zymogens) and activated by cleavage of the pro-peptide domain via other MMPs or several serine proteases including urokinase-type plasminogen activator (uPA).

MMP9 and MMP2 are gelatinases, degrading collagen IV, and regarded as key molecules in embryo implantation, allowing trophoblast invasion through the decidua and into maternal vessels. MMP2 is already secreted by the embryo at the blastocyst stage. There is a differential expression of MMP2 and -9 throughout the first trimester, with MMP2 being pre-dominantly expressed in the early and MMP9 in the late first trimester. It could be shown that MMP9 is secreted in the inactive form by pre-eclamptic trophoblasts. Nevertheless, knock-out mice deficient in MMP2 or -9 are fertile and only mild effects have been reported [27].

The uPA system represents a family of serine proteases that are involved in the degradation of the basement membrane and ECM components and also in fibrinolysis. Various enzymes are able to activate uPA such as plasmin, kallikrein, factor XIIa, and cathepsin B. Activated uPA converts plasminogen into plasmin, which, in turn, activates a variety of substrates, including matrix metalloproteases (MMPs) and uPA itself [28]. UPA binds to its receptor uPAR which is a 50 to 65 kDa cell surface glycoprotein expressed by activated leukocytes, keratinocytes, monocytes/macrophages, endothelial cells, fibroblasts, trophoblasts, and many cancer cells [29-31]. High endogenous levels of uPA and uPAR could be linked with tumourigenicity and metastatic capacity of tumour cells whereas reduced levels of uPA and increased concentrations of PAI-1 have been reported in pre-eclampsia, characterized by impaired trophoblast invasion [32].

There are two subtypes of uPA inhibitors, called PAI-1 and PAI-2. The uPA system and its inhibitors are thought to play a role in trophoblast invasion through regulation of the proteolysis and the remodelling of maternal tissue. The localisation of the expression of its components could be demonstrated in human placenta [33]. Interestingly, PAI-1 appears not to solely inhibit cell invasion by inhibiting uPA activity but also to promote cell spreading by mediating cell detachment [34]. PAI-1 is mainly expressed by first-trimester trophoblast and was found concentrated where detachment from maternal tissue occurs [33] whereas interstitial and endovascular EVT are PAI-1 negative [35]. A summary of the described mechanisms that are involved in trophoblast invasion is outlined in figure 1.

#### 1.1.3.3 Restriction of trophoblast invasion

When invading trophoblast cells reach the upper luminal third of the myometrium, their invasiveness slows down and finally comes to a halt. The reason for this is unclear, but several hypotheses try to explain it either

by extrinsic or intrinsic factors. Extrinsic factors accounting for invasion stop could be a certain interaction with the surrounding cells in the myometrium, a gradient of a signal that is no longer available or in a too low concentration to trigger invasion not any more when too far from the source of the signal. Alternatively, trophoblast cells may be able to invade only for a certain period of time or for a certain distance which would follow an intrinsic program. Additionally, apoptosis induction, polyploidization leading to a non-invasive but matrix-secreting phenotype and syncytial fusion may also lead to the limitation of invasion [15].

Another recently discussed hypothesis suggests that the oxygen level accounts for the restriction of trophoblast invasiveness. In early pregnancy, a low level of oxygen (hypoxia) is present. Later, the oxygen level rises with the establishment of the utero-placental circulation. Hypoxia leads to the expression of hypoxia-inducible factor (HIF), which could be detected in EVT<sub>s</sub>, villous cytotrophoblast as well as in the syncytiotrophoblast. The expression of HIF declines with gestational age and thereby reflects the increase of the oxygen level [36].

To what extent all of these hypotheses contribute to the transient nature of trophoblast invasiveness remains to be answered. Taken together, on the one hand placental cells possess the capacity of indefinite growth and extensive invasion, and are on the other also bestowed with mechanisms to regulate and restrict these tumour-like attributes. This unique feature implicates that trophoblast cells might be a useful model to study cell growth, differentiation as well as tumourigenesis [4].

#### 1.1.4 Trophoblastic cell line models

Isolation of primary trophoblast cells is a difficult cell stress-inducing procedure often yielding in low cell numbers and their culture is only possible for a short-time which might not be suitable for certain analysis. There are several cell lines utilized as model for human trophoblast cells. Some are derived from choriocarcinoma cells, such as JEG-3, JAR and BeWo cell lines. Other cell lines originate from a hybridization of a choriocarcinoma cell line with trophoblast cells, such as AC1M59 and ACH3P (both JEG-3 hybrids). In spite of their trophoblastic origin those cell lines may have distinct differences in morphogenic and functional phenotype as they are cancer cells as well.

The cell line HTR8/SVneo is widely used as a model for first-trimester trophoblast cells. The cell line was generated in 1993 by Charles H. Graham and Peeyush K Lala in Canada [37]. The cell line originates from first-trimester trophoblast cells which were immortalized by introducing the gene encoding simian virus (SV) 40 large T antigen. The selection could be performed through induction of neomycin resistance. The trophoblastic identity after transfection was confirmed by various morphological and functional markers such as cytokeratin-7. The cell line secretes MMP2 and human Gonadotropin (hCG), the pregnancy marker hormone, and is susceptible to TGF- $\beta$  as shown for normal first-trimester trophoblast cells. As HTR8/SVneo cells share various similarities to trophoblast cells and are not of tumour origin, they seem to be a very good tool in order to analyze placental function and tumour progression.

## 1.2 Welcome to the TOR signalling network

Target of Rapamycin (TOR) is a signalling molecule which is well conserved among species. It was first discovered as two polypeptides, named TOR 1 and TOR 2 in budding yeast *Saccharomyces cerevisiae* during a screen for resistance towards the drug Rapamycin. Later, it was also found in drosophila (dTOR) and mammals (mTOR). In mammals, a single TOR protein is present which shows about 42% identity with the amino acid sequence to the yeast TOR homologues [38].

### 1.2.1 Structure and function of mTOR

Mammalian target of Rapamycin (mTOR), also designated as FKBP12-Rapamycin associated protein (FRAP) and Rapamycin target (RAFT), belongs to the phosphoinositide kinase-related kinase (PIKK) family [39]. MTOR kinase is a high-molecular weight protein consisting of 2549 amino acids and containing several distinct and conserved domains. Schematic presentations of structural features of mTOR and its complex binding partners are depicted in figure 4.

MTOR possesses a C-terminal serine/threonine protein kinase activity domain [40, 41], an FKBP12-Rapamycin binding domain (FRB), a toxic effector domain and an N-terminal region that features 20 tandem HEAT repeats which have been proposed to mediate protein-protein interactions [42].

Phosphorylation sites of mTOR are threonine at position 2446 (Thr<sup>2446</sup>) and serine at 2448 (Ser<sup>2448</sup>). It was shown that intrinsic kinase activity leads to autophosphorylation. Whether this intrinsic activity is sufficient for full activity *in vivo* is not known. The significance of the phosphorylations themselves is unclear as well since it could be demonstrated that substitution of both phosphorylation sites with alanine did not affect mTOR activity [43].

MTOR can be found in two protein complexes, mTOR complex 1 (mTORC1) and complex 2 (mTORC2), both different in binding partners and functions. In mTORC1, mTOR is associated with the regulatory-associated protein of mTOR (Raptor), proline-rich Akt substrate of 40kDa (PRAS40) and mLST8 (also known as G protein  $\beta$ -subunit-like protein; G $\beta$ L), whereas in mTORC2, it interacts with Rapamycin-insensitive companion of mTOR (Rictor; also named as mAVO3), mLST8 and recently found with Sin1 and PRRL5 [44]. The well characterized targets of mTORC1 are p70 S6 kinase (p70<sup>S6K</sup>) and 4E-binding protein 1 (4E-BP1) whereas mTORC2 possibly acts via Rho signalling pathway which is less understood [45]. Those downstream events are further described in 1.2.3.

In general, mTOR integrates nutritional and mitogenic signals as well as stress-induced signals to coordinate cell growth (accumulation of cell mass), protein synthesis, cell proliferation and survival. It is essential for the regulation of protein translation in response to the extracellular signals allowing the progression from the G1 to S phase within the cell cycle [46]. MTOR also controls protein degradation by macro-autophagy, which is a catabolic process degrading cytoplasmic contents upon starvation, by ubiquitination, internalization and



turnover of specific nutrient transporters [47]. It was also shown that mTORC1 regulates trafficking of nutrient transporters and thereby promoting nutrient uptake such as of glucose, amino acids, lipoprotein and iron [48].

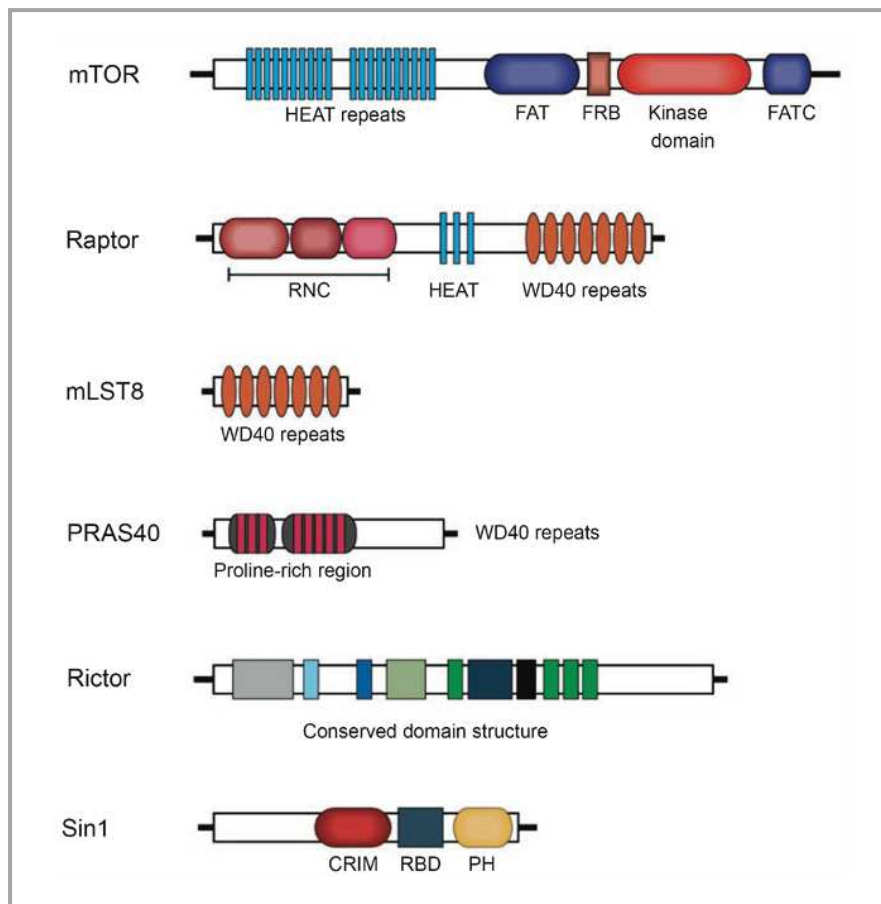


figure 4. Schematic structure of mTOR complex components. (HEAT: protein-protein-interaction structure of two tandem anti-parallel  $\alpha$ -helices found in huntingtin, elongation factor 3, PR65/A and TOR, FAT: domain structure shared by FRAP, ATM And TRRAP, FRB: FKBP12/Rapamycin binding domain, FATC: FAT C-terminus, RNC: Raptor N-terminal conserved domain, WD40: about 40 amino acids with conserved W and D forming four anti-parallel  $\beta$ -strands, CRIM: conserved region in the middle, RBD: Ras binding domain) (taken from Yang et al. 2008)

## 1.2.2 Upstream effectors and regulation of mTOR

### 1.2.2.1 Upstream signalling events

mTOR controls cell proliferation, growth and survival by regulation of many aspects of the cellular metabolism [44]. Four major inputs have been associated with the regulation of mTOR signalling including growth factors, nutrients, energy and stress. A schematic summary of signalling events occurring in the mTOR pathway can be seen in figure 5.

Growth factors such as insulin-like growth factor-I (IGF-I) and -II (IGF-II) trigger the mTOR pathway via the phosphatidylinositol 3-kinase (PI3K)/Akt axis. Upon binding to the according growth factor receptor the insulin

receptor substrate (IRS) is recruited and phosphorylated which then leads to the recruitment of PI3K. The PI3K/IRS complex converts phosphatidylinositol-4,5-phosphate (PIP2) to phosphatidylinositol-3,4,5-phosphate (PIP3) which co-recruits 3-phosphoinositide-dependent kinase-1 (PDK1) and Akt (also known as protein kinase B; PKB) to the membrane. PDK1 then activates Akt by phosphorylation [47]. The accumulation of PIP3 can be reversed by phosphatase and tensin homolog deleted on chromosome 10 (PTEN) which is a known tumour suppressor.

The tuberous sclerosis heterodimer complex which is comprised of TSC1 (Hamartin) and TSC2 (Tuberin) is a GTPase-activating protein (GAP). Mutations in TSC proteins cause the formation of benign tumours (hamartomas) in various tissues and organs known as tuberous sclerosis complex syndrome which is characterized by very large cells within the tumours [49]. TSC1 and TSC2 are therefore also known as tumour suppressors [50]. TSC2 is phosphorylated and thereby inactivated by Akt. The TSC heterodimer is a negative regulator of mTOR, inhibiting its kinase activity through Rheb inhibition which is a positive mTOR effector protein (described in more detail in section 1.2.2.2).

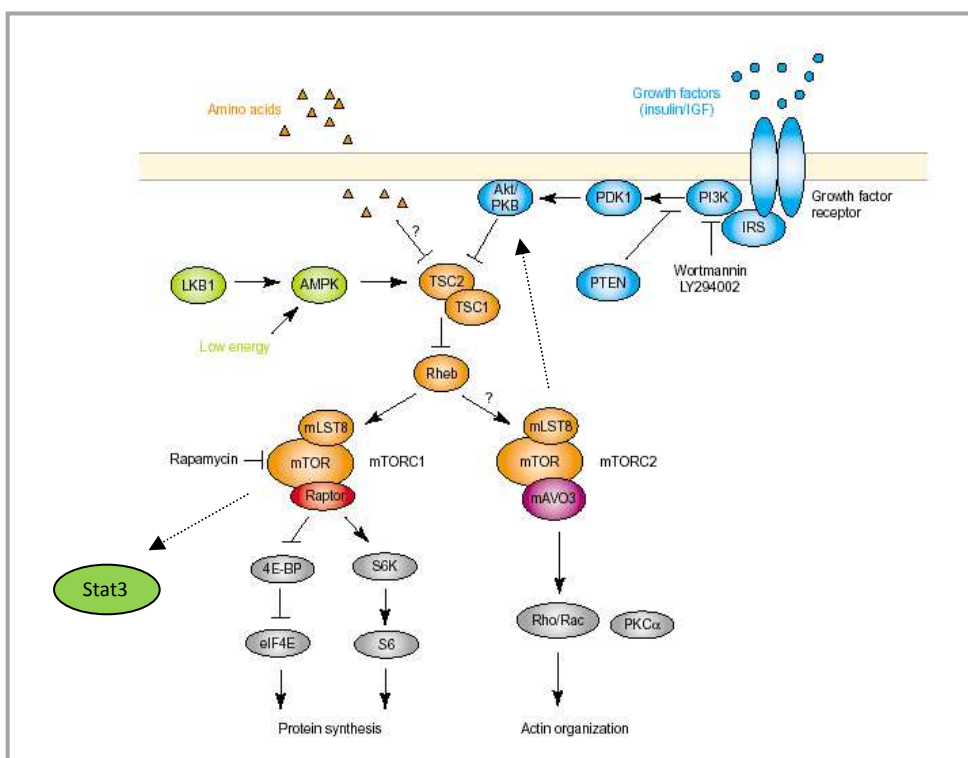


figure 5. TOR signalling network (modified after Martin and Hall 2005)

It was shown that the absence of amino acids, in particular leucine, leads to a rapid dephosphorylation of the mTORC1 substrates p70<sup>S6K</sup> and 4E-BP1 which can be restored upon readdition of amino acids [51] or Rheb overexpression [52]. Several mechanisms by which the nutrient status communicates to mTOR have been proposed which function either by inhibition of the TSC1/2 complex [53] or stimulation of Rheb [52].

Alternatively and independently of both mechanisms, either via TSC or Rheb regulation, nutrient sensing might directly arise via mTORC1 through alteration of Raptor-mTOR binding [54].

The energy level of a cell is manifested by the AMP:ATP ratio which is sensed by the AMP-activated protein kinase (AMPK). High AMP:ATP activates AMPK which in turn activates TSC1/2 GAP activity resulting in an inhibition of mTOR signalling in response to a low cellular energy level [55].

Upon stress such as hypoxia or DNA damage the cell downregulates energy-demanding processes and arrests its growth [56]. It was demonstrated that mTOR plays also a role in such a stress-induced cell response [57].

#### 1.2.2.2 Positive regulator of mTOR: Rheb GTPase

Rheb (Ras homolog enriched in brain) is a small G-protein and an upstream regulator of mTOR. There are two Rheb molecules in human, Rheb1 and Rheb2. It is ubiquitously expressed and particularly abundant in brain and muscle [58]. Rheb consists of 184 amino acid residues whereof the 169 N-terminal residues form the GTPase domain and the 15 C-terminal amino acids, which are hypervariable, comprise a conserved motif important in farnesylation and association with the membrane [59].

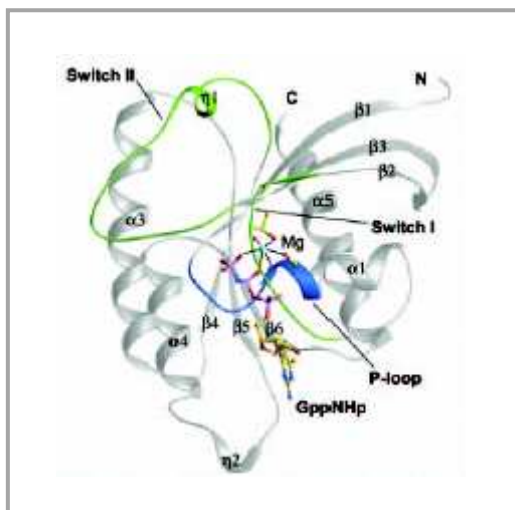


figure 6. Overall structure of Rheb-GppNHp complex (taken from Yu et al. 2005)

Mutations in Rheb can lead to cell growth inhibition, whereas overexpression promotes an increase in cell size and also leads to an insensitivity of mTOR kinase activity when growth factors and amino acids are absent [52, 60]. Rheb binds to mTOR complex 1 (mTORC1) and thereby affects mTOR kinase activity. Transient expression of Rheb leads to mTOR-mediated activation of p70<sup>S6K</sup> and phosphorylation of 4E-BP1. Rheb is negatively regulated by the TSC1/2 heterodimer. Rheb functions as an important mediator between TSC and mTOR to stimulate cell growth [50]. Recently, the structural properties of Rheb, when bound to its nucleotides (GTP/GDP), have been described. It was suggested that Rheb forms a new group within the Ras/Rap subfamily and uses a novel GTP hydrolysis mechanism [61]. The result of the structural analysis can be seen in figure 6.

### 1.2.3 Downstream targets

Substrates of mTORC1 are p70 S6 kinase (p70<sup>S6K</sup>) and eukaryotic initiation factor 4E-binding protein 1 (4E-BP1) [62], which are involved in the regulation of translation initiation [62]. Raptor has been proposed to be a scaffold protein for the mTOR substrates. The mTOR substrate binding to Raptor is mediated via the five amino acids TOR signalling (TOS) motif that is located in the N-terminus of both substrates [63].

In recent studies, PRAS40 was shown to be a physiological target of mTORC1 [64] and to be required for downstream signalling [65]. PRAS40 also possesses a TOS motif and is predominantly bound to Raptor, in a competitive manner towards p70<sup>S6K</sup> and 4E-BP1. Upon mTOR activation, PRAS40 is phosphorylated and dissociates from Raptor, thus relieving PRAS40-mediated substrate competition [66].

The p70<sup>S6K</sup> phosphorylates the 40S ribosomal protein S6 which is involved in the initiation of the translation of 5'-terminal oligopyrimidine (TOP) tract mRNAs which encode ribosomal proteins and components of the translation apparatus [67, 68]. The phosphorylation of 4E-BP1 leads to a release of eIF4E that binds the 5' cap structure of mRNA. Released eIF4E is a component of a functional translation initiation complex also comprised of eIF4G, eIF4A and eIF3 [69, 70].

mTORC2 meanwhile is thought to play a role in the organization of the actin cytoskeleton [45]. TORC2 also plays a role in a regulatory feedback loop of TOR signalling by phosphorylation of Akt, which is upstream in the mTOR signal pathway [71]. Additionally, mTORC1 is conferred to as being Rapamycin-sensitive whereas mTORC2 is Rapamycin-insensitive although prolonged Rapamycin treatment will disturb mTORC2 assembly [72]. Mechanisms of signalling events downstream of mTORC2 to the actin cytoskeleton are largely unknown but might involve PKC $\alpha$  and the small GTPases Rho and Rac [73].

### 1.2.4 Feedback and cross-talk signalling

A constitutive activation of the mTOR kinase activity induces a negative feedback loop to attenuate PI3K via inhibition of IRS1. Studies demonstrated that p70<sup>S6K</sup> regulates IRS1 at transcriptional level and through direct phosphorylation thereby interfering with the adaptor function of IRS1 and the consequent PI3K signalling [74].

The existence of a positive feedback loop caused via mTORC2 activating Akt has already been mentioned above (see paragraph 1.1.3). It was shown that the Rictor-mTOR complex directly phosphorylates Akt at a serine residue at position 473 *in vitro* and facilitates the phosphorylation of threonine at position 308 by PDK1. Hence, mTORC2 was identified as the long-sought PDK2, phosphorylating Akt.

Moreover, the phosphorylation of mTOR at Thr<sup>2446</sup> and Ser<sup>2448</sup> was shown to be PI3K-dependent and increased with constitutively activated Akt, but it could be shown that the responsible kinase is not Akt but the mTOR substrate p70<sup>S6K</sup> [75, 76]. It is still unclear whether the phosphorylation of this feedback loop is positive, negative or inconsequential and whether it occurs in mTORC1 or mTORC2 or both.

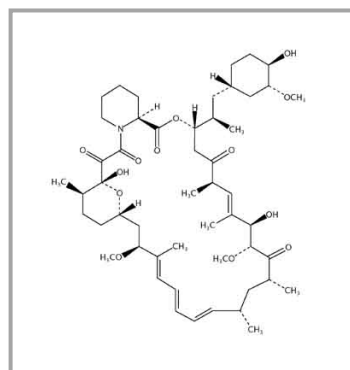
In addition, mTOR was shown to phosphorylate the signal transducer and activator of transcription (Stat) -3 at its serine residue 727 (Ser<sup>727</sup>) [77]. Janus kinase (Jak)/Stat signalling is a rapid transcription-activating pathway leading to a cell response upon cytokine stimulation. The phosphorylation of Stat3 at the tyrosine residue 705

(Tyr<sup>705</sup>) regulates the Stat dimerization which is an essential prerequisite for the establishment of a classical Jak/Stat signalling path. However, there is a second phosphorylation site at the serine residue within the C-terminus and mutation of this residue alters transcriptional activity [78]. However, the role of the serine phosphorylation of Stat3 is still controversially discussed in the literature [79].

#### 1.2.5 Inhibitor of mTOR: Rapamycin

Rapamycin (or Sirolimus), a microbial natural product with potent anti-proliferative activity and known to be used as an immunosuppressant applied to graft recipients after transplantation, is a specific potent mTOR inhibitor. Rapamycin was originally isolated from the bacterial strain *Streptomyces hygroscopicus* found in a soil sample from Easter Island (Rapa Nui in local language) [47]. Rapamycin is a macrocyclic lactone and binds with high affinity to FKBP12, which is a prolyl isomerase, to form an active drug-protein toxin [80, 81]. The chemical structure can be seen in figure 7.

figure 7. Structure of Rapamycin.



mTOR directly binds to the FKBP12-Rapamycin complex [38, 82]. It was shown that the FKBP12-Rapamycin complex inhibits the binding of the mTOR substrates p70<sup>S6K</sup> and 4E-BP1 to Raptor, which results in the aforementioned sensitivity of mTORC1 to Rapamycin treatment. Thus, mTORC1 is disabled to phosphorylate and thereby activate its substrates which are important factors for protein synthesis. As follows, Rapamycin is an inhibitor of cell proliferation which promotes it as a candidate drug target for anti-cancer therapy and led to the development of Rapamycin analogues, explained further in the next section (see 1.2.6).

mTORC2 is considered as Rapamycin-insensitive, but upon prolonged Rapamycin treatment a disassembly of the complex takes place. Newly synthesized mTOR proteins bind to FKBP1-Rapamycin preventing an assembly of mTORC2, whereas already-existing complexes break down, eventually leading to a Rapamycin-induced mTORC2 inhibition [72].

### 1.2.6 mTOR and cancer

In various human cancers, pathways that regulate mTOR are transformed [51]. Mutations in the tumour suppressor PTEN is one of the best described and frequently found genetic alteration that affects mTOR signalling in tumour cells. Loss-of-function PTEN is associated among various cancers such as in prostate, breast, lung, brain or bladder [83]. Furthermore, genes encoding the catalytic subunit of PI3K and Akt were found to be amplified in ovarian and breast cancer [84]. Mutations in the tumour suppressors TSC1 or TSC2 lead to hamartomas as already mentioned. It was also observed that Rheb activity is elevated in many tumour cell lines [85].

It can be assumed that an activation of mTOR signalling contributes to tumourigenesis by providing cancerous cells with a growth advantage through promotion of protein synthesis and cell cycle progression. Therefore, mTOR is an attractive target for cancer therapy. At the moment three Rapamycin analogues, named CCI-779 (Wyeth), RAD001 (Novartis) and AP23573 (Ariad Pharmaceuticals) are in clinical trials. Preliminary results showed that the Rapamycin derivatives are particularly effective in tumours with PTEN inactivation [83]. But there is a need for biomarkers predicting tumour sensitivity to Rapamycin and its analogues. One study on breast cancer demonstrated that Akt phosphorylation and p70<sup>S6K</sup> overexpression might be those markers rather than PTEN status or p70<sup>S6K</sup> phosphorylation [86].

It is also noteworthy that long-term treatment of Rapamycin implicates induction of apoptosis possibly by impairing the positive feedback loop from mTORC2 to Akt. As said before, mTORC2 is Rapamycin-insensitive but its assembly is disrupted upon prolonged treatment. Tumours upregulating mTORC1 signalling thereby also activate the negative feedback loop to IRS1, which prevents full activation of Akt signalling. A diminished activation of Akt-dependent survival mechanism might render those cancer cells more susceptible to apoptosis. Hence, inhibitors against mTOR-Rictor (TORC2) might also be beneficial in cancer therapy [83]. Others studies demonstrated that the application of Rapamycin derivatives showed improved effects on cancer when combined with other chemotherapeutical agents; cutting off intracellular pro-survival signals at diverse and distinctive sites [87].

### 1.2.7 mTOR and reproduction

It was reported that children of transplant recipients who received Rapamycin-based immunosuppressiva during pregnancy showed no maltransformations although case number was very low (n=7) and three out of the seven pregnancies resulted in spontaneous abortion [88]. Otherwise, another study mentioned that Rapamycin treatment was avoided during pregnancy of women undergoing transplantation [89]. Otherwise Rapamycin is considered teratogenic since it was reported that treatment of early embryos in mice with Rapamycin led to a phenotype highly similar to mTOR mutant embryos [90].

In a mouse model, it could be demonstrated that disruption of the mTOR gene was implicated with a limited level of trophoblast outgrowth *in vitro* and post-implantational lethality of homozygotes [7]. Rapamycin treatment of mouse embryos also inhibited trophoblast outgrowth [7]. A deletion of six amino acids in the C-

terminal part, essential for mTOR kinase activity, demonstrated reduced cell size and a proliferation arrest in early mouse embryos and embryonic stem cells [91].

Furthermore, mTOR has been described as a placental growth signalling sensor [92]. In the presence of extracellular amino acids, particularly leucine, mTOR gets activated in early mice blastocysts leading to trophoblast spreading [93]. Another study in mice showed that leucine uptake occurs by the amino acid transport system B<sup>0+</sup> which triggers mTOR signalling and development of trophoblast motility *in vivo* and *in vitro* [94]. A study on humans demonstrated, that mTOR regulates placental leucine transport and was found downregulated in intra-uterine growth restriction (IUGR) leading to the proposal that mTOR functions a nutrient sensor, matching fetal growth with maternal nutrient availability by regulation of the nutrient transport [95]. On the whole, very little is known of the role of mTOR in reproduction especially in human.

### 1.3 Objectives

The aim of the study is to further unravel the role of mTOR signalling in trophoblast invasion choosing the cell line HTR8/SVneo as model. Special question was raised concerning the contributions of both mTOR complexes to trophoblast response, especially when deprived of nutrients and growth factors, performed by serum-starvation. Additionally, the influence of mTOR upstream effector proteins such as Rheb, Akt and PI3K was to elucidate as well as its cross-link to Stat3. In our laboratory it was already shown that Stat3 plays a role in trophoblast invasion, demonstrated in other cell lines than HTR8/SVneo [96].

Experimental approaches:

- (1) In order to investigate the role of single signal molecules within the mTOR pathway (Rheb, mTOR, Raptor, Rictor), their expression was knocked down (silenced) by RNA interference (RNAi) through transfection with small interfering (si) RNA.
- (2) Rapamycin, a specific inhibitor against mTOR, was used to allow comparison with knockdown effects. Thereby two time points of Rapamycin exposure were applied; acute (2 h) and prolonged (24 h). It was expected that acute Rapamycin treatment solely affects mTORC1 whereas that prolonged Rapamycin also impairs mTORC2.
- (3) Pharmacological inhibitors against mTOR upstream effector Akt and PI3K were utilized in order to further analyze possible feedback mechanisms which might impact the differential outcome induced by Rapamycin.
- (4) The withdrawal of serum was used as a tool to mimic absence of “energy” signals by growth factors and nutrients.
- (5) Assays were performed to determine proliferation rate and apoptosis induction upon treatment by RNAi or inhibitors.

- (6) Invasion-related functional assays were used as read-outs for trophoblast invasiveness. Those assays included substrate zymography indicating the secretion of matrix-degrading enzymes, PAI-1 ELISA and immunocytochemistry and *in vitro* matrigel invasion assay.
- (7) The existence of mTOR expression within the decidua was confirmed by immunohistochemical staining of placental tissue.

Supplementary data obtained during a scientific sojourn at the Massachusetts General Hospital in the laboratory of Joseph Avruch (MD PhD) are specially indicated. This work comprised the regulatory effects of Rheb mutants on mTOR activity and binding using a human embryonic kidney cell line (HEK293T). This project should be considered separately, but still demonstrates the regulation of mTOR activity which is part of the study.



## Chapter 2 | Material and Methods

### 2.1 Regulation of mTOR by Rheb in HEK293T

Regulation of mTOR requires Rheb to be in its active GTP-bound form, which enables it to bind and/or induce mTOR kinase activity. It could be shown that two regions within the Rheb molecule, named switch 1 (residues 33-41) and switch 2 (residues 63-79) are important for mTOR activation, highlighted in figure 8. The overall structure of Rheb when bound to GTP and GDP has recently been described [61]. When Rheb harbours GTP, structural changes are induced and critical amino acids will be exposed resulting in functional Rheb. In order to identify those critical amino acids, a set of Rheb mutants was created. The putative changes were selected by prediction of solvent-exposure at the threshold when all residues of both switches are fully accessible.

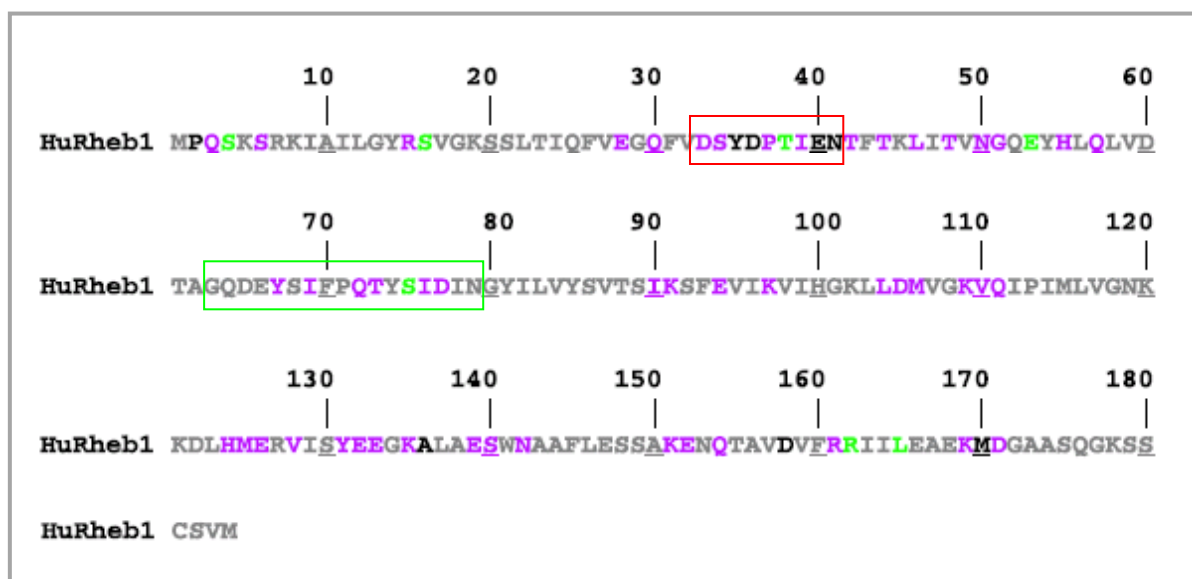


figure 8. Sequence of human Rheb1 (taken from Long et al. 2007). Colours indicate solvent accessibility in X-ray crystallographic structures of Rheb1 either to GTP or GDP, calculated by the DeepView program (gray: not solvent exposed, purple: exposed in both Rheb-GTP/GDP, black: exposed only in Rheb-GTP, green: exposed only in Rheb-GDP, red box: switch 1, green box: switch 2).

The sequence of human Rheb1 wildtype can be seen in figure 8. The solvent accessibility of each residue was calculated by the DeepView program, available at the Swiss Protein Database. At a setting of 25% it could be ensured that all residues of switch 1 and switch 2 were exposed. At that setting, 58 amino acid residues of

Rheb1 are solvent-exposed in the GTP-bound form. Those residues were substituted by alanine. Several (up to five) mutated residues were clustered leading to the generation of 20 mutants in total. The five residues that are only surface-exposed in the GDP-bound form were individually changed. All residues were also changed to alanine. The functional capacities of these mutants were monitored by their potential to restore substrate phosphorylation by mTOR upon amino acid withdrawal. Additionally, their binding properties to mTOR and its interaction partners were tested.

### 2.1.1 Generation of Rheb mutants

The desired mutations, selected as described above, were introduced in two vectors comprising the wildtype Rheb1 and an additional N-terminal tag; pCMV5-Flag and pEBG, consisting of a Flag- and glutathione sepharose (GST)-tag, respectively. Both vectors also encode Ampicillin-resistance (vector map of pCMV5 can be seen in the appendix). In the table below (table 2) all designed mutant constructs are listed with the corresponding abbreviations.

No.	Mutation	Abbreviation	No.	Mutation	Abbreviation
1	G3/S4/S6	3-6	14	I76/D77	76, 77
2	R15	15	15	I90/K91	90, 91
3	S16	16	16	E94/K97	94, 97
4	E28/Q30	28, 30	17	L104/D105/M106	104-06
5	D33/S34/Y35/D36/P37	33-37	18	K109/V110/Q111	109-11
6	I39/E40/N4/T42	39-42	19	H124/M125/E126/V128	124-28
7	T44/L46	44, 46	20	Y131/E132/E133/K135	131-35
8	T48/N50/G51	48-51	21	E139/S140/N142	138-142
9	E53	53	22	K151/E152	151, 152
10	H55/Q57	55, 57	23	Q154/D158/R161	154-61
11	Y67/I69	67, 69	24	R161/R162/I163/I164	161-64
12	Q72/Y74	72, 74	25	K169/M170/D171	169-71
13	S75	75			

table 2. Set of Rheb1 mutants (Capital letters indicate changed residues at given position number: G glycine, S serine, R arginine, E glutamic acid, Q glutamine, D aspartic acid, Y tyrosine, P proline, I isoleucine, N asparagine, T threonine, L leucine, H histidine, K lysine, M methionine, V valine). All residues were substituted with alanine (A).

#### 2.1.1.1 Primer design

A set of 25 pairs of primers were designed according to the guidelines given by the manual of the QuikChange site-directed mutagenesis kit (Stratagene). The mutagenic primer pairs were designed in a way that both

primers, sense and anti-sense, contained the desired mutation and annealed to the same sequence on opposite strands of the plasmid. They were about 25 to 45 bases in length with a melting temperature ( $T_m$ ) of slightly higher or equal to 78° C. With following formula was used to estimate  $T_m$ :

$$T_m = 81.5 + 0.41 (\% \text{ GC}) - 675 / N - \% \text{ mismatch}$$

(*N*: primer length in bases, % GC: percentage of guanine G and cytosine C bases; values are whole numbers rounded down, % mismatch: percentage of bases creating mismatches /mutation number; values are whole numbers rounded up)

The desired mutation was preferred to be in the middle of the primer. Ideally, the content of guanine (G) and cytosine (C) was 40% at minimum and primers terminated with one or more C or G bases. Primers encoded for several point mutations, adjacent or close-by of each other, leading to a switch of one or several amino acids to alanine. Primers with the mutagenic sequences were generated by the MGH DNA Core Facility and obtained as lyophilized powders. Primers (sense, anti-sense) were separately resuspended in deionized water to achieve 125 µg/ml as final concentration. Primers were stored at -20° C. DNA manipulations were introduced in a single step using the generated pair of primers of each mutant in a polymerase chain reaction (PCR).

#### 2.1.1.2 PCR mutagenesis

The QuikChange site-directed mutagenesis kit was used according to the instruction manual. Designed primer pairs were applied to introduce mutations within both vectors: pCMV5-Flag and pEBG, encoding wildtype Rheb protein fused with Flag- or GST-tag, respectively.

Reactions were prepared as follows:	40 ng (1 µl)	Template (pCMV plasmid [40 µg/ml])
	or 50 ng (1.25 µl)	Template (pEBG plasmid [40 µg/ml])
	125 ng (1 µl)	Sense primer
	125 ng (1 µl)	Anti-sense primer
	5 µl	10x reaction buffer
	1 µl	dNTP mix
	40 µl	ddH <sub>2</sub> O
	1 µl	<i>PfuTurbo</i> DNA polymerase (2.5 U/µl)

Sample reactions with different primer pairs were run simultaneously because of similar melting temperature, but only when the same template was used since plasmids either encoding Flag- or GST-tag have different sizes, 6 kilobases (kb) and 7 kb, respectively. Cycling was run with following parameters.

PCR parameter setting:	1 cycle	95° C	30 s
	16 cycles	$\left\{ \begin{array}{l} 95^\circ \text{ C} \\ 55^\circ \text{ C} \\ 68^\circ \text{ C} \end{array} \right.$	30 s
			1 min
			2 min/kb (pCMV5-Flag: 12 min, pEBG: 14 min)
	1 cycle	72° C	10 min
		4° C	

Upon PCR, amplification samples were incubated with 1  $\mu$ l of *Dpn I* (10 U/ $\mu$ l) restriction enzyme for 1 h at 37° C. This enzyme targets methylated DNA and is thereby useful to digest original (non-mutated) strands. Sample reactions were stored at -20° C until further use for transformation into competent bacteria.

#### 2.1.1.3 Transformation

*Escherichia coli* (*E.coli*) strain XL-1 Blue supercompetent cells (Stratagene, provided with QuikChange Site-directed Mutagenesis PCR Kit) were thawed on ice and 50  $\mu$ l were aliquoted into pre-chilled tubes for each transformation, taking 1  $\mu$ l of sample reaction. Transformation samples were incubated on ice for 30 min and subsequently heat-pulsed for 45 sec at 45° C. Afterwards samples were put on ice again for 2 min. Pre-heated LB media (1% tryptone, 0.5% yeast extract, 1% NaCl) was added and the whole reaction sample was incubated for 1 h at 37° C. Ampicillin-containing (50  $\mu$ g/ml) agar plates (1% tryptone, 0.5% yeast extract, 1% NaCl, 1.5% agar) were prepared by spreading 100  $\mu$ l of 10 mM isopropyl-1-thio- $\beta$ -D-galactopyranoside (IPTG) and 2% 5-bromo-4-chloro-3-indolyl- $\beta$ -D-galactopyranoside (X-gal) about 30 min prior to spreading of 100 to 200  $\mu$ l transformation reaction. Next day, colour screening was performed and white clones were selected and grown over night at 37° C in 3-5 ml LB media containing 75  $\mu$ g/ml Ampicillin. Next day, bacteria cultures were used to isolate plasmids. In order to keep a glycerol stock of selected clones, 400  $\mu$ l of media was taken of overnight culture and 150  $\mu$ l of 70% glycerol was added and kept at -80° C.

#### 2.1.1.4 Plasmid preparation

Purification of plasmids was performed by use of a mini-prep kit (Marligen) according to the manufacturer's instructions. Briefly, 3 ml bacterial overnight cultures were taken and centrifuged (14.000 rpm for 1 min or 4.000 rpm for 10 min), all media were removed and pellets were resuspended in an RNase A (20 mg/ml)-containing buffer. Lysis buffer (200 mM NaOH, 1% SDS) was added, followed by an incubation of 5 min at room temperature. Afterwards neutralisation buffer was added and the mixtures were centrifuged at high speed (12.000 g) for 1 min. Supernatant were applied onto columns which were loaded on 2 ml tubes and again centrifuged at high speed for 1 min. The flow-through was discarded and the columns were washed with an ethanol-containing buffer and centrifuged as before. DNA was eluted from the columns by pre-warmed (about 65-70° C), deionized water. DNA concentrations of purified plasmids were measured by Nanodrop 1000 spectrophotometer (Thermo Scientific) and stored at -20° C.

To verify correct sequence after mutagenesis PCR, 1  $\mu$ g of the purified plasmid constructs was taken and supplemented with the according sequencing primer pair, either for pCMV5-Flag or pEBG, flanking the Rheb sequence within the plasmids and sent to the MGH DNA Sequencing Core Facility. DNA sequences were verified using the BLAST 2 Sequences program.

Clones of mutant constructs with correct mutations were used for a maxi-preparation of plasmids in order to obtain high amounts of plasmid DNA for further experiments. Therefore, the appropriate glycerol stocks were

taken to inoculate 200-300 ml LB media. Bacterial cultures were grown over night and by use of a maxi-prep kit (Marligen), plasmids were purified by similar procedure as already described for mini-prep but on higher scale. In difference, columns required equilibration before use and after the elution from the columns, DNA was precipitated with isopropanol, centrifuged at 15.000 g for 30 min and the precipitates were then washed with 70% ethanol and again centrifuged. Pellets were air-dried and then finally dissolved in deionized water. DNA concentrations were measured by Nanodrop and constructs were stored at -20° C until further use for cell transfection.

#### 2.1.1.5 Subcloning

For constructs that failed to be generated by mutagenesis PCR or failed to be expressed in the following experiments, subcloning was used as another approach to generate desired mutagenic constructs. An insert from one construct was cloned into the other vector. Generally, pCMV5-Flag-Rheb vectors with correct mutations were taken to create the according pEBG construct.

Therefore, about 2 µg of purified plasmids from selected clones were digested with the restriction enzymes *Kpn I* and *BamH I* with respective recommended buffer, simultaneously for 2 h at 37° C (see restriction sites of vector in the appendix). Afterwards the restriction reaction samples were loaded onto a 1.5% agarose gel (1.5% agarose, 0.008% ethidium bromide) to identify and separate the inserts by its size from undigested (circular) or partly digested (linear) plasmid. The gel was run approximately for 1 h at 90 V. At the according bp length (552 bp) in respect to 1 kb DNA ladder (Invitrogen), gel was cut out under UV light and the inserts were purified from the gel piece by use of a gel extraction kit (Marligen). Briefly, gel was solubilised by warming up with the according buffer and the resulting solution was then loaded onto a column which was centrifuged at 13.000 rpm for 1 min, washed twice and DNA (mutagenic Rheb insert) was eluted with deionized water. To estimate concentrations of inserts, 2 µl were loaded onto 1.5% agarose gel and compared to the kb ladder with known concentration (1 µg/µl).

Following digestion of vector to obtain inserts with correct mutation, the inserts were ligated into the other vector which was digested with the same restriction enzymes allowing recombination of “sticky” ends of vector and inserts. In addition to digestion of 1 to 2 µg vector, recirculation of vector was prevented by incubation with calf intestine alkaline phosphatase (CIAP) for 1 h at 37° C. Afterwards, vector was purified by use of gel purification kit. To estimate concentration of digested vector, 2 µl of mix was loaded onto a 1.5% agarose gel and compared to kb ladder.

A ratio of 3:1 was used for vector-insert ligation also considering the bp ratio (pCMV5-Flag: 6 kb, pEBG: 7 kb, Rheb insert: 552 bp). Therefore, the following equation was used:

$$V_{\text{insert}} = 3 * (C_{\text{insert}} * X_{\text{insert}}) / C_{\text{vector}} \quad (V: \text{volume}, c: \text{concentration}, X: \text{bp ratio})$$

Ligation was performed using the Quick Ligation Kit (New England Biolabs) according to the manufacturer’s instruction. To verify if enzymes worked properly, a negative control reaction was prepared by adding only

vector and no insert to the ligase reaction. Religation of vector should be circumvented due to the dephosphorylation of the 3' and 5' end by CIAP.

Ligase reaction was mixed as follows:	10 $\mu$ l	Quick ligase buffer (2x)
	1 $\mu$ L	Vector
	$V_{\text{insert}}$	Insert
	1 $\mu$ l	Quick ligase
	9 $\mu$ l - $V_{\text{insert}}$	Deionized water

Reactions were incubated for 5 min on ice and subsequently used for transformation into the *Escherichia coli* strain DH5 $\alpha$  competent cells (Life Technologies). DH5 $\alpha$  competent cells are suitable for subcloning procedures and capable of being transformed with large plasmids (Life Technology manual). Transformation was done as recommended by instruction manual; 1 to 5  $\mu$ l of ligation product was added to a 50  $\mu$ l aliquot of DH5 $\alpha$  and incubated for 30 min on ice and afterwards, reactions were heat-pulsed for 20 sec at 37° C and then put on ice for 2 min. Upon addition of 1 ml pre-heated LB media, the mixtures were incubated for 1 h at 37° C while shaking. Then 300 to 500  $\mu$ l of media was spread onto Ampicillin-containing agar plates and incubated over night at 37° C. Next day, clones were selected for mini-prep which was done as already explained. Obtained plasmids were subjected to control digestion. Therefore, 7.5  $\mu$ l of plasmid solutions were incubated with restriction enzymes *BamH I* and *Kpn I* for 1 to 1.5 h at 37° C and applied onto a 1.5% agarose gel in the same manner as described before. If bands appeared at correct sizes compared to kb ladder, clones were sent for sequencing.

### 2.1.2 Cell culture and transfection

The Rheb mutants were transiently transfected into a human embryonic kidney cell line referred to as HEK293T. HEK293T cells were cultured in Dulbecco's modified Eagle's medium (DMEM) supplemented with 10% FBS, 100 U/ml penicillin and 0.1 mg/ml streptomycin at 37° C in 10% CO<sub>2</sub>. Cells were prepared for transfection experiments by seeding them into 30 mm dishes at a confluency of 30-50%.

The transfection was performed by the lipofection method. With this method the administered cationic lipids are thought to facilitate the mediation of DNA into mammalian cells by forming DNA-lipid complexes which fuse with the cell membrane allowing DNA uptake by endocytosis. Lipofectamine (Invitrogen) was used as transfection agent and applied following the instruction manual.

In order to verify if plasmids are expressed properly, several clones encoding correct mutation were chosen to transfect HEK293T. Prior to transfection, 200 ng of pCMV5-Flag-Rheb constructs or 300 ng of pEBG-Rheb constructs were diluted with 150  $\mu$ l OPTI-MEM and a solution of 13  $\mu$ l Lipofectamine and 137  $\mu$ l OPTI-MEM was prepared and incubated for 30 min at room temperature. In the meantime, media of cells were removed and the cells were rinsed twice with OPTI-MEM. Then 1.5 ml OPTI-MEM was added and the 300  $\mu$ l DNA-Lipofectamine mix was added dropwise. Next day, media was changed to complete growth media.

Cells were harvested 48 h post-transfection, lysed and used for SDS-PAGE and Western blot as described below. The resulting membranes were incubated accordingly with anti-Flag or anti-GST specific antibodies to detect the overall expression of the Rheb mutants. The expression was compared to the expression of the recombinant wildtype Rheb expression.

When constructs failed to express in HEK293T cells, subcloning an insert with correct mutation into a new lot of vector was also the method of choice to rule out possible mutations during PCR which could have occurred within the vector in other parts than the insert resulting in an adverse expression level.

For functional analysis and for binding assay, 0.5 µg of constructs were used for transfection and amino acids were withdrawn as described in paragraphs below.

### 2.1.3 Cell lysis and protein isolation

Two days after transfection, cells were harvested by rinsing them twice in ice-cold PBS and while left on ice, cells were scraped off with 200- 400 µl lysis buffer (20 mM Tris-Base pH 7.9, 20 mM NaCl, 25 mM EGTA, 20 mM β-glycerol, 1 mM DTT, 1 mM PMSF, 1 protease inhibitor cocktail tablet/50 ml, 0.25% CHAPS, 0.025% calyculin, 2 mM Na<sub>3</sub>VO<sub>4</sub>, 1 mM EDTA, 100 mM NaF) and kept cold. After a centrifugation of 10 min at 12.000 rpm, the supernatants were collected and protein concentrations were measured by Bradford assay. Lysates were prepared for gel electrophoresis by supplementing the same amount of protein (15-20 µg) of each sample with lysis buffer and gel loading buffer. Lysates were stored at -80° C.

### 2.1.4 Gel electrophoresis and Western blot

Protein lysates of transfected pCMV5-Flag-Rheb and pEBG-Rheb constructs were run on 11% and 13% sodium dodecyl sulphate-polyacrylamide gels (SDS-PAGE), respectively (11% or 13% acrylamid/bisacrylamid, 375 mM Tris-Base pH 8.8, 0.1% SDS, 0.1% APS, 0.004% TEMED). The electrophoresis separates proteins by molecular weight and the percentage of the gel depends on the size of the protein of interest. Gels were run in according running buffer (125 mM Tris-Base, 1 M glycine, 0.5% SDS) at 200 V until running front reached the end of the gel. Electrophoresis was followed by an immediate protein transfer onto a nitrocellulose membrane through vertical Western blotting. Therefore the stacking gel was cut off and discarded and the separation gel was applied onto the membrane which was equilibrated before in blotting buffer (20 mM Tris-HCl, 200 mM glycine, 20% methanol). Air bubbles were removed and then gel and membrane were put within two wet filter papers and sponges. Subsequently, this sandwich was set up accordingly in the blotting chamber filled with cold blotting buffer and an iced tank was added to keep protein transfer process cold. The blotting was run at 70 V for 90 min. Following protein transfer, membranes were blocked for 30 min in 5% milk-containing TBS-T buffer (250 mM Tris-Base, 27.1 mM KCl, 1.37 M NaCl pH 7.5). After blocking, membranes were washed three times with TBS-T for 5 min before incubation with primary antibody over night at 4° C. In a 1:1000 or 1:500 dilution of antibody in TBS-T, the primary antibodies specific for p70<sup>S6K</sup>, phosphorylated p70<sup>S6K</sup>, GST- and Flag-tag were

used. Next day, membranes were washed thrice again with TBS-T for 5 min. The secondary antibody specific for mouse (used for primary antibody specific for phosphorylated p70<sup>S6K</sup> and Flag-tag) or rabbit (used for all other primary antibodies) which are linked to horse-radish peroxidase (HRP) were used in a 1:10.000 dilution with TBS-T and incubated for 1 h at room temperature. Thereafter, membranes were again washed as before and incubated with HRP substrate solution for 1 min before membranes were subjected to film detection in the dark room.

#### 2.1.5 Analysis of Rheb functions

##### 2.1.5.1 Functional assay: Amino acid withdrawal

As it was shown previously, overexpression of wildtype and thus functional Rheb can rescue inactivation of mTOR kinase activity when deprived of amino acids [52]. Such mutants, which failed to show rescue ability, are hence of interest since the changed amino residues caused a disruption in function and must therefore be involved in mTOR regulation. As a functional read-out, the phosphorylation level of the mTOR substrate p70<sup>S6K</sup> was used, and therefore cells were co-transfected with a p70<sup>S6K</sup>-encoding reporter.

Clones of the Flag-tagged constructs with optimal expression were selected to transfect HEK293T for functional analysis. In order to screen the Rheb mutants for their functional ability, transfected cells were withdrawn of amino acids prior to harvesting of the cells.

Following transfection of 0.5 µg of pCMV5-Flag-Rheb constructs, cells were allowed to express mutagenic and wildtype Rheb for 24 hours. Next day, cells were deprived of amino acids for 90 min by replacing complete culture media with Dulbecco's PBS (D-PBS). Subsequently, cells were harvested and lysed as already described. Protein samples were prepared and subjected to gel electrophoresis with following Western blot, which was performed as explained before.

Transfection with wildtype Rheb-encoding plasmid was used as control to show rescue ability of overexpressed Rheb on mTOR activity upon absence of amino acids. As additional control, cells were also transfected with the "empty" pCMV5-Flag vector encoding no Rheb protein. This control, which results in no Rheb overexpression which can rescue mTOR activity upon amino acid withdrawal, points out the loss of p70<sup>S6K</sup> phosphorylation by inactive mTOR caused by the amino acid deprivation.

The primary antibody specific for phosphorylated p70<sup>S6K</sup> at position threonine 389 (Thr<sup>389</sup>) was used and signals much lower than compared to control with transfected wildtype Rheb were considered as deficient in rescue ability.

##### 2.1.5.1 Binding assay: GST pull down

The next question addressed whether the switched amino residues of Rheb mutants that lost capability of restoring mTOR activity, also cause a malfunctioning binding towards mTOR.



HEK293T cells were transfected with selected pEBG-Rheb constructs with best expression and additionally with a vector encoding for the catalytic domain of mTOR (Flag-tagged). Cells were again allowed to express the mutant proteins for 24 h and amino acid withdrawal was performed for 120 min prior to harvesting. Cell extraction and Bradford assay was performed as already been described above. An aliquot of the lysates was used to verify the expression of GST-tagged Rheb by gel electrophoresis, Western blot and subsequent immuno-detection.

For the binding assay, the same amount of protein (100-200 µg) of the remaining lysates was incubated with GSH-sepharose beads (GE-Healthcare) at 4° C for 1 h, and adsorbed proteins were washed three times in lysis buffer and eluted with glutathione elution buffer (10 mM glutathione, 50 mM Tris-base pH 8.0). The beads bind to the GST-Rheb fusion proteins and thereby “pull down” all proteins that bound to Rheb. The bound proteins in the eluate can be identified by Western blot.

## 2.2 Role of mTOR in trophoblast invasion

### 2.2.1 Cell line and cell culture

The immortalized human first-trimester trophoblast cell line HTR8/SVneo was cultured in RPMI supplemented with 5% fetal bovine serum (FBS). The cell line was kindly provided by Charles H. Graham. Cells were splitted every two or three days according to confluency. For detaching of cells Trypsin/EDTA (BioWhittaker) was used after washing the cells with phosphate buffered saline (PBS). Cells were stored in freezing media (92% FBS, 8% DMSO) in liquid nitrogen.

### 2.2.2 Manipulation of cells

For further analysis HTR8/SVneo cells were treated accordingly: transfection with small interfering RNAs (siRNAs), addition of chemical inhibitors and supplementation with serum or in the absence of serum. A schematic presentation of the experimental design can be seen in figure 9.

#### 2.2.2.1 RNA interference

RNA interference (RNAi) is a post-transcriptionally induced gene silencing mechanism induced by viral infection or artificially through introduction of double-stranded RNA leading to mRNA degradation. RNAi can be caused either by synthetically designed small interference RNA (siRNA) oligonucleotides or by viral vectors which possess a genetically encoded short hairpin RNA (shRNA) which will be further processed within the cell by an enzyme called Dicer to generate siRNA molecules with a 3' overhang. Briefly, the siRNA duplexes bind to a multi-protein complex termed RNA-induced silencing complex (RISC) which firstly unwinds the siRNA double-

strand by its helicase activity, and then leads the anti-sense strand to its homologous mRNA which will finally result in a cleavage within the target mRNA by the RISC nuclease activity. The cleaved mRNA will be further degraded by exonucleases and the siRNA-RISC complex can bind to another mRNA. The frequent destruction of the mRNA molecules causes the silencing of the expression of the respective gene also referred to as knockdown.

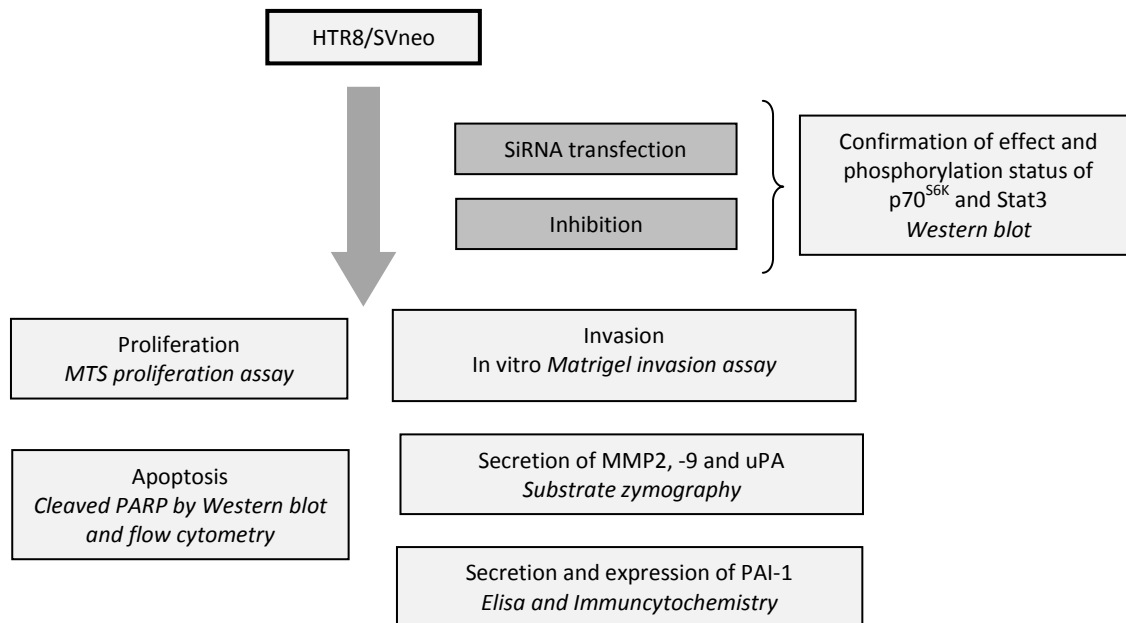


figure 9. Schematic presentation of experimental design. Applied methods are highlighted with italic letters.

siRNAs consist of 21 to 23 base pairs (bp) and can be introduced in eukaryotic cells by lipophilic agents such as Oligofectamine (Invitrogen) forming vesicles which will fuse with the cell membrane or by electroporation which causes short-time holes in the cells' membrane.

Cells were transfected by pipette-type electroporation using the MicroPorator (PeqLab). Therefore, one million cells per 100  $\mu$ l resuspension buffer with no or 0.1 nmol siRNA (according to 1  $\mu$ M siRNA in 100  $\mu$ l) were electroporated with one pulse at 1700 V for 20 msec. Cells were counted and accordingly applied for subsequent assays as proliferation or invasion or cultured for protein isolation and media collection.

The used siRNAs were purchased pre-designed from Ambion. siRNAs were not validated, except for mTOR-specific siRNA (a) which showed 7.3 and 8.45% remaining mRNA in HeLa and 16.13% in DU145 and for mTOR-specific siRNA (b) which showed 18.56% remaining mRNA in HeLa (data taken from Ambion data sheets). siRNA with a non-genomic sequence was used as control in order to verify possible unspecific effects due to the transfection procedure itself.

The following sequences represent the anti-sense strand of siRNAs in 5' to 3' direction, the 3' overhang is depicted by small letters:

Rheb-specific siRNA sequence:	CCG AGC AUG AAG ACU UGC Ctt
mTOR-specific siRNA sequence (a):	AGU UCA UCA ACC CAU UUC Ctc
mTOR-specific siRNA sequence (b):	AUA GAA GCG AGU AGA CUC Ctc
Raptor-specific siRNA sequence:	GUU CAG AAA UAU UUG GUC Gtc
Rictor-specific siRNA sequence:	AUA UAA UUU ACU GCU GGG Ctt
Non-genomic (scrambled; Scr) siRNA:	GAA CGA AUU UAU AAG UGG Ctt

siRNAs were either already pre-annealed and ready to use (as for both mTOR siRNAs) or they were annealed by diluting the same amount of sense and anti-sense strand with 5x Annealing buffer and nuclease-free water to a final concentration of 10  $\mu$ M. The mix was incubated for 1 min at 95° C and subsequently for 1 h at 37° C. Annealed oligonucleotides were aliquoted and stored at -20° C

#### 2.2.2.2 Chemical inhibitors

Cells were incubated with inhibitors against mTOR (Rapamycin), Akt (Akt-I X) and PI3K (LY249002) the following day, after cells were seeded in 6-well plates or 24 h after siRNA transfection. Incubation of inhibitors lasted 24 h until analysed for proliferation and zymolytic activity in the absence of serum. Additionally, Rapamycin treatment was also applied for invasion experiments with and without the presence of serum.

Rapamycin was pre-dissolved in sterile-filtered methanol and further diluted (1:10) with serumfree RPMI media obtaining a 100  $\mu$ M stock solution. It was used in a final concentration of 100 nM and cells were incubated for two time points, 2 h and 24 h. After 2 h incubation, media was changed to serum-containing or serumfree and further cultured for 24 h. Media was also changed for untreated samples and 24 h incubation to ensure the same condition of media by the cells which secret molecules continuously. Therefore, Rapamycin was added again to the according samples.

Akt-I X is a cell-permeable and selective inhibitor of the Akt phosphorylation and the Akt *in vitro* kinase activity. It has minimal effect on PI3K and PDK1 and was shown to prevent activation of Akt downstream targets as mTOR and p70<sup>S6K</sup> (Calbiochem manual). It was reconstituted in sterile deionized water as recommended, achieving a stock solution of 1 mg/ml which approximately corresponds to 2.5 mM. It was examined for its efficiency of inhibiting mTOR kinase activity (read-out: p70<sup>S6K</sup> phosphorylation) and finally used with a final concentration of 5  $\mu$ M. Akt-I X was added after 2 h treatment with Rapamycin and not removed upon the following overnight incubation.

LY249002 is a highly selective inhibitor of PI3K *in vitro* and *in vivo*. It abolishes PI3K activity without affecting other lipid kinases such as PI4K, MAPK and C-Src. It was shown to block PI3K-dependent Akt phosphorylation

and activity (Cell Signaling Technology manual). LY249002 was pre-dissolved in DMSO as recommended and further diluted (1:5) with sterile distilled water to get a 10 mM stock solution. The final concentration used in cell culture was 10  $\mu$ M after evaluation of the inhibiting effect on mTOR kinase activity (read-out: p70<sup>S6K</sup> phosphorylation). Like Akt-I X, LY249002 was added after 2 h Rapamycin treatment and not removed upon the following overnight incubation. A representation of the combination with the according incubation time is given in table 3.

	Control			Akt-I X			LY294002			Inc.- time
	-	2h	24h	-	2h	24h	-	2h	24h	
<b>100nM Rapamycin</b>	-	x	x	-	x	x	-	x	x	2h
<b>100nM Rapamycin</b>	-	-	x	-	-	x	-	-	x	} 24h
<b>5<math>\mu</math>M Akt-I X</b>	-	-	-	x	x	x	-	-	-	
<b>10<math>\mu</math>M LY294002</b>	-	-	-	-	-	-	x	x	x	

table 3. Combination and incubation time of used inhibitors.

The molecular formula of used inhibitors:

Rapamycin:  $C_{31} H_{79} NO_{13}$

Akt-I X:  $C_{20} H_{25} ClN_{20} \times HCl$  (10-(4'-(N-diethylamino)-butyl)-2-chlorophenoxazine, HCl)

LY249002:  $C_{19} H_{17} NO_3$

### 2.2.3 Cell lysis and protein isolation

Prior to cell harvesting, media was taken off and centrifuged at 3.000 rpm for 10 min to remove dead, detached cells and cell debris. Collected media were aliquoted and stored at -20° C. Cells were washed once with cold PBS and then scraped off with 100  $\mu$ l lysis buffer (Cell signalling technology: 20 mM Tris-HCl pH 7.5, 150 mM NaCl, 1 mM Na<sub>2</sub>EDTA, 1 mM EGTA, 1% Triton-X, 2.5 mM sodium pyrophosphate, 1 mM  $\beta$ -glycero-phosphate, 1 mM Na<sub>3</sub>VO<sub>4</sub>, 1  $\mu$ g/ml Leupeptin) diluted 1:10 with PBS and supplemented with 0.1% protease inhibitor cocktail (Sigma) on ice. Samples were further lysed by repeating freeze and thaw cycles using liquid nitrogen and finally cell debris were spun down at 13.000 rpm for 20 min at 4° C. Cell lysates were stored at -20° C. Protein concentrations were determined by Bradford. Briefly, 5  $\mu$ l of lysates or standards of known concentrations of bovine serum albumin (BSA) were mixed with 995  $\mu$ l Bradford assay solution and incubated in the dark for about 10 min at room temperature and subsequently measured photospectrometrically at 595 nm using the Cary WinUV Simple Reads software program for monitoring. The creating of a standard curve by BSA sampled allows the calculation of the protein concentration of the cell lysate samples.

#### 2.2.4 Gel electrophoresis and Western blot

Sample preparation involved denaturation of 10-20 µg of whole cell extract or media (amount was extrapolated from the according cell extracts, allowed detection of secreted PAI-1) with 5x Laemmli gel loading buffer (312.5 mM Tris-HCl, 2% SDS, 13.5% glycerol, 1% bromophenol blue, 5% β-Mercaptoethanol) and subsequent incubation at 95° C for 10 min. Samples were loaded onto an SDS-polyacrylamide gel which consisted of a stacking gel (4% acrylamid/bisacrylamid, 125 mM Tris-HCl, 0.1% SDS, 0.07% APS, 0.18% TEMED) and a 7.5% separating gel (7.5% acrylamid/bisacrylamid, 375 mM Tris-Base pH 8.8, 0.1% SDS, 20% glycerol, 0.08% APS, 0.12% TEMED). In case of detecting Rheb expression, a 12% separating gel (12% acrylamid/bisacrylamid, 375 mM Tris-Base pH 8.8, 0.1% SDS, 20% glycerol, 0.08% APS, 0.12% TEMED) was cast due to the low molecular weight of Rheb (21 kDa). Samples and a molecular weight marker were run with according electrophoresis buffer (24 mM Tris-Base, 19 mM glycine, 0.01% SDS pH 8.5) at 125 V or 25 mA/gel, depending on the used electrophoresis apparatus (Life Technologies: Blot-Module Mini-V8x10 or PeqLab Model Twin S), until the running front reached the end of the gel.

Immediately following the gel electrophoresis, proteins were transferred onto a nitrocellulose membrane, a process termed Western blot. The gel, filter papers and membrane were equilibrated in blotting buffer (12 mM Tris-Base, 96 mM glycine, 20% methanol) and then placed in layers according to the instructions. The transfer was performed at 200-250 mA (5 mA/cm<sup>2</sup> membrane) for 12 (for Rheb detection) or 25 min according to the molecular weight of the desired protein. After blotting, the membrane was stained with Ponceau S (0.1% Ponceau S, 5% acetic acid) to prove whether the protein transfer was successful. Ponceau S staining could be removed with 0.2 M NaOH.

Membranes were further washed with NET-G buffer (150 mM NaCl, 5 mM EDTA, 50 mM Tris-Base pH 7.5, 0.05% Triton-X, 0.02% gelatine) which also has mild blocking effects and subsequently incubated with the according primary antibody over night at 4° C. Used primary antibodies were specific for detection of Rheb, mTOR, Raptor, Rictor, cleaved PARP, PAI-1, Stat3 and p70<sup>S6K</sup> expression as well as for detection of serine (Ser<sup>727</sup>) or tyrosine (Tyr<sup>705</sup>) Stat3 and threonine (Thr<sup>378</sup>) p70<sup>S6K</sup> phosphorylation. Antibodies were diluted 1:1.000 with NET-G buffer.

Next day, membranes were washed thrice with NET-G buffer for 5 min and subsequently incubated with horse-radish peroxide (HRP)-conjugated secondary antibody for 1 h at room temperature. The used secondary antibodies were either specific for mouse IgG (used for p70<sup>S6K</sup> and cleaved PARP-specific antibodies) or rabbit IgG (all other used antibodies) and diluted with NET-G 1:5.000 or 1:10.000, respectively. Afterwards, membranes were washed again as before.

Membranes were then incubated with a substrate solution for HRP for one minute. The resulting chemiluminescent signal was detected by exposure to a hypersensitive film in the dark. Film was developed manually by dipping it into developer solution followed by a fixation solution, then washed and dried.

In order to re-use a Western blot membrane, all antibodies were removed by incubation with the stripping buffer (0.7% β-mercaptoethanol, 2% SDS, 0.6% Tris-HCl pH 6.7) and heated at 50° C for 30 min. After that,

membranes were washed with NET-G and incubated with the next primary antibody following the same procedure as described above.

#### 2.2.5 MTS proliferation assay

In order to monitor effects on the proliferation rate due to cell manipulations by inhibitor treatment or upon siRNA transfection, the cell numbers were determined by use of MTS tetrazolium compound (also called Owen's reagent). MTS is reduced by metabolically active cells into a coloured formazan product which can be measured photometrically at 490 nm.

Therefore 10.000 cells per well were seeded in a 96-well plate. The seeding of cells was performed either with freshly trypsinized cells from cell culture or subsequently after siRNA transfection. For each sample, triplicates were prepared. Cells were left over night under normal growth conditions and next day media was changed to fresh culture media with serum or serumfree media and treated with inhibitors and incubated another 24 h. Next day, the MTS solution (Promega; CellTiter 96 Aqueous One Solution) was added and as soon as the colour changed from yellow to orange/red the absorbance was measured.

#### 2.2.6 Apoptosis assay: Cleaved PARP

Apoptosis was measured in two ways through the cleavage of poly-ADP-ribose polymerase (PARP) which is a DNA-repairing enzyme, important for cells to maintain their viability. Upon triggering the caspase cascade which results in apoptosis, caspase 3 cleaves PARP, which separates its DNA-binding domain from its catalytic domain. With the use of a fluorescein-conjugated antibody specific for the large cleaved PARP product, specifically the C-terminal catalytic domain, the rate of apoptosis could be measured flow cytometrically with a modified protocol from the Cell Signaling Technology manual.

Therefore, 200.000 cells were seeded in a 6-well plate and treated accordingly with 100 nM Rapamycin for 2 h and 24 h with or without serum. Additionally, a sample for negative and positive control was prepared. For positive control, cells were incubated with 60 U DNase I over night and for negative control, cells were left untreated. Next day, cells were scraped off with a rubber spatula and washed with PBS. Centrifugation steps were carried out at 1.500 rpm for 5 min. Cells were fixed by resuspension in 4% paraformaldehyde for 10 min at room temperature. Cells were then washed with TBS (50 mM Tris-HCl, 150 mM NaCl). Then cells were permeabilized with a 0.2% Triton-X solution for 5 min at room temperature with a following TBS washing step. In order to incubate the cells with the antibody over night at 4°C, they were resuspended in 50µl TBS. Cells of negative control were incubated with 1.5 µl triple negative antibody (Dako) instead of Fluorescein-conjugated cleaved PARP-specific antibody (Cell signalling technology) which was added to the samples. The following day cells were resuspended with FACS flow buffer (BD Biosciences) and flow cytometry parameters were set up with negative and positive control, measuring the signal in fluorescence channel 1. Then the samples were analyzed by counting 100.000 events. Apoptosis rate could be calculated by subtraction of negative signal

which gives rise to unspecific binding. Obtained values were set to relation of basic apoptosis which is given by the untreated sample.

Detection of cleaved PARP could also be achieved by Western blot using an unconjugated PARP-specific antibody (Cell Signaling Technology).

## 2.2.7 Invasion-related analysis

### 2.2.7.1 Substrate zymography

Cells were harvested and media was taken off as described in 3.2.3. Protein concentrations of cell extracts were determined by Bradford and extrapolated for cell culture media. 2x non-denaturing buffer (0.5 M Tris-HCl, 20% glycerol, 4% SDS, 0.05% bromphenol blue) was added to media samples corresponding to 10-20 µg which were applied on a 7.5% SDS-polyacrylamide gel containing 2 mg/ml (0.02%) casein plus 0.025 U/ml plasminogen for examining uPA activity, or 2 mg/ml (0.02%) gelatine for MMP2 and MMP9 activity. The gel was run at 125 V or 25 mA/gel according to used electrophoresis system until running front reached end of the gel. Gels were taken and subsequently washed twice for 15 min in 2.5% Triton-X to allow renaturation of proteins and then left over night in incubation buffer (50 mM Tris-HCl, 5 mM CaCl<sub>2</sub>) at 37° C. The next day, gels were stained with Coomassie solution (0.25% Coomassie, 30% methanol, 10% acetic acid) and destained (30% methanol, 10% acetic acid) until lysed bands were obvious. Gels could be preserved by a 1 h incubation in a glycerol-containing solution (10% acetic acid, 10% glycerol). Gels were dried by vacuum gel dryer system.

### 2.2.7.2 Immunocytochemistry of PAI-1

To obtain additional data concerning the effect of Rapamycin on PAI-1, the expression of PAI-1 was monitored by immunocytochemical staining.

Slides were coated with poly-L-lysine and cells were left over night at 37° C to adhere. The following day, media were changed and cells were treated with or without Rapamycin for 2 h or 24 h. Next day, cells were fixed with 4% paraformaldehyde for 1 h at 4° C, washed with 0.1 M PBS, unspecific antigens were blocked with 5% normal goat serum diluted with PBS/Tween20 (0.3%) solution for 1 h at room temperature and Cas-Block solution (Zymed) for 10 min. Primary antibody mouse anti-human PAI-1 (American Diagnostica Inc.) was diluted 1:20 with the PBS/Tween20 solution and incubated over night at 4° C. Slides were washed again and incubated with RPE-conjugated anti-mouse antibody (Dako), which was diluted 1:400 in 0.1 M PBS, for 1 h at 4° C. Eventually, mounting media that contains 4,6-Diamidin-2-phenyl-indol (DAPI) (Vector) was applied which will stain DNA and thereby visualize cell nuclei. The slides were sealed and stored at 4° C until analyzed with fluorescence microscope Axioplan 2 (Zeiss) and the according software Axiovision.

### 2.2.7.3 PAI-1 ELISA

Obtained media as described in 3.2.3 was also used for enzyme-linked immunosorbent assay (ELISA) to detect levels of secreted PAI-1. ELISA is a common antigen-binding test allowing quantitative conclusions about the detected molecule. The AssayMax human PAI-1 ELISA kit (AssayPro) was used according to the manufactures' instructions. Briefly, 50  $\mu$ l of media and standards of known PAI-1 concentrations were applied on 96-well strips for 2 h at room temperature. Wells were washed five times in between all following steps of incubation with; biotinylated detection antibody for 1 h, streptavidin-peroxidase-conjugate for 30 min, and chromogene substrate for 10 min until optimal blue colour developed which was stopped by a stop solution causing a colour change from blue to yellow which was measured immediately at a wavelength of 450 nm. The used ELISA was shown to have a sensitivity of detecting a minimal dose of less than 50 pg/ml and its intra-assay and inter-assay coefficients of variation were about 5% and 8%, respectively (AssayPro manual).

Cell culture media containing serum was diluted 1:50 upon first trial whereas serumfree media and later samples were applied undiluted. Value of blank was subtracted from measured standard and sample values. The standard curve was performed in duplicates and analyzed by linear regression for calculating concentrations of media samples.

### 2.2.7.4 *In vitro* Matrigel invasion assay

In order to assess the ability of cells to digest and invade through extracellular matrix (ECM), Matrigel-coated well inserts were applied. Matrigel is a solubilized basement membrane preparation extracted from Engelbreth-Holm-Swarm (EHS) mouse sarcoma which is a tumour rich in extracellular matrix proteins (specification sheet of BD Biosciences) and hence can be used to mimic ECM.

Aliquoted growth factor-reduced Matrigel (BD Biosciences) was diluted 1:10 with serumfree RPMI media and 100  $\mu$ l were added to the 8  $\mu$ m 24-well plate inserts (Millipore) and left to dry at room temperature for 4 h. Residual Matrigel was taken off and 50.000 cells, taken upon trypsinization or siRNA transfection, were applied into the inserts. Exposure of Rapamycin for 2 h was performed prior to adding the cells into the inserts whereas 24 h treatment was continued throughout the assay until insert membrane preparation next day. Transfected cells were applied with or without serum for 48 h. For each sample, triplicates were set up. After incubation time, inserts were washed in PBS and Matrigel was removed by using a wet cotton swab. Cells were fixed with methanol: acetic acid (3:1) solution for 10 min, washed three times and stained with 1% crystal violet for 10 min and washed again. The membrane of the inserts was cut out with a scalpel and put onto a slide adding mounting media (Microscopy Aquatex, Merck) and a cover slip. Amount of invaded cells which are stained in blue/violet was monitored by a bioimaging system (DNR MF-ChemiBIS 3.2) and evaluated by the Totallab TL100 software.



### 2.2.8 Immunohistochemistry of placental tissue

The performance and establishment of placental staining for mTOR detection was done by Prof. Sebastian San Martin and Maja Weber (diploma student).

Collected tissue was taken from decidual side from placentas which were obtained directly after Ceasarian section or from selective abortion. Thus, gestational age of placentas varied from 11<sup>th</sup> to 41<sup>st</sup> week. Tissue was washed with PBS and fixed with 4% paraformaldehyde in 0.1 M PBS for 48 h at 4° C. Afterwards, tissue was washed with 0.1 M glycine in PBS of 30 min or over night at 4° C. An ethanol-based hydration followed with an incubation of 30 min with each ethanol concentration starting with 50% to 70%, 95% and finally to absolute ethanol at room temperature. The last two concentrations were carried out three times. Then tissue was cleared of ethanol by Xylol incubation three times for 15 min. Thereafter, the tissue was infiltrated with paraffin (Histosec) by incubation for 30 min at 56-60° C for three times. The final embedding was achieved with the fourth paraffin incubation. The embedded tissue was then cut with a microtome gaining 5 µm thick slices which were placed on a slide and kept at 4° C until further immuno-staining.

Cut tissue slices needed to get deparaffinized and rehydrated which was performed by two Xylol incubations for 30 min and ethanol solutions, starting from absolute ethanol two times for 30 min, to 95% once for 30 min, to 70% once for 30 min and finally to distilled water for 15 min. Antigenic retrieval was achieved in 10 mM citrate sodium buffer (pH 6.0) at 95° C for 10 min and cooling down in the same buffer for 30 min. Slides were then washed with distilled water three times for 5 min and with 0.1 M PBS twice for 15 min. Unspecific binding was blocked with 5% normal goat serum diluted in 0.3% Tween20 in PBS for 1 h at room temperature in a humid chamber with subsequent blocking by Cas-Block (Zymed) for 10 min. Upon blocking, the incubation with the primary antibody could be performed over night at 4° C in the humid chamber. The mTOR specific antibody (Cell signaling technology) was diluted 1:50 in 0.3% Tween20 in PBS. Next day, slides were washed with 0.1 M PBS three times for 5 min. Subsequently, tissue samples were incubated for 1 h at room temperature in a humid chamber in the dark with the secondary antibody, a Cy3-conjugated goat anti-rabbit IgG (Dianova) antibody, which was diluted 1:400 in 0.1 M PBS. Slides were washed with 0.1 M PBS and mounted with DAPI-containing mounting media (Vector). A cover slip was added on top of the slide and sealed with nail enamel. Slides were stored at 4° C until analysis with fluorescence microscope.

For hematoxylin-eosin staining, cut slices were dried for 1 h at 56-60° C in incubator and subsequently deparaffinized by a graded xylol/ethanol series, rehydrated, stained and dehydrated by the following procedure (at room temperature): twice xylol for 2 min, absolute ethanol for 2 min, 95% ethanol for 2 min, 70% ethanol for 2 min, 50% ethanol for 2 min, distilled water for 2 min, Mayer's hemalaun solution for about 1 min, washing with distilled water for 5 to 10 min, again washed with distilled water for 2 min, 0.5% Eosin G solution for 1 min, washing with 70% ethanol, twice with 95% ethanol, twice with absolute ethanol, ethanol/xylol mix and finally twice with xylol for 5 min. HE-stained slices were mounted with Histofluid (Marienfeld) on a slide and a coverslip was added on top. Slides were stored at 4° C until analysis with fluorescence microscope Axioplan 2 (Zeiss) and the software Axiovision.

## 2.3 Data presentation and statistics

Results were evaluated and are graphically presented by Microsoft Excel software. Given error bars indicate standard deviation (S.D.) and significance was determined through Student's t-Test.

### 2.3.1 Standard deviation

In order to consider the range of error factors, standard deviations were calculated by the following equations (done by Excel).

$$S.D. = \sqrt{\sum_{s=1}^m \sum_{i=1}^n (y_{is}-M)^2 / (ny-1)}$$

$$M = \frac{\sum_{s=1}^m \sum_{i=1}^n y_{is}}{ny}$$

*(S.D.: standard deviation, s: data series, i: data point within data series s, m: number of data series of point y in diagram, n: number of points per data series, y<sub>is</sub>: value of data series s and of point i, ny: total number of values of all data series, M: arithmetic median)*

### 2.3.2 Student t-Test

The Student t-Test demonstrates the probability (p) that two sets of data are not significantly different from each other. If p value is below 5% (p<0.05), the difference is significant. Data were highly significantly different when p<0.005.

The two-tailed Student t-Test for paired samples was applied since in all cases data were related accordingly. Student t-Test for paired samples is calculated as follows (performed by Microsoft Excel).

$$\sum d_z^2 = \sum z^2 - ((\sum z)^2 / n)$$

$$\sigma_d^2 = \sum d_z^2 / n-1$$

$$\sigma_n = \sum d_z^2 / (n-1)$$

$$t = \bar{z} / \sigma_n$$

$$p (T \leq t)$$

*(z: difference between control from corresponding treatment value, n: number of pairs, d: difference,  $\sigma_d^2$ : difference of variance, t: calculated t-value)*

In case of enzyme activity analysis, by three data points minimum, the arithmetic median was depicted which is less susceptible to outliers.

## Chapter 3 | Results

### 3.1 Regulation of mTOR by Rheb in HEK293T

#### 3.1.1 Expression level of created Rheb mutants

A set of Rheb1 mutant plasmids could be generated by PCR mutagenesis, which was then cloned in *E.coli* in order to amplify and isolate the DNA-plasmids. The desired mutagenic sequences were verified by DNA sequencing. Whereas some mutants were easily obtained by mutagenesis PCR and subsequent cloning, for others more obstacles were to overcome. Interestingly, fusion proteins with GST-tag were in general harder to create and therefore, subcloning from an already-made Flag-construct with the appropriate mutation was undertaken, by cutting out the mutant Rheb insert with restriction enzymes and ligation in another vector.

For one Rheb mutant, two or more clones were selected and transfected in HEK293T cells. The expression level of the selected mutants was tested by Western blot (data not shown). Some Rheb mutants showed low expression levels, making a screening of more clones necessary. Generally, one clone with optimal expression was chosen for functional analysis.

Expression levels were again verified when Rheb function was tested by amino acid withdrawal by use of anti-Flag antibody (figure 10, abbreviation of clones is explained in the material and methods part). As seen in figure 10 there is still a low expression for six clones observed, which are (48-51), both (94, 97) clones, (131-135) and both (139-142) clones. Also shifts and double bands of Rheb-Flag expression could be observed for clones (33-37), (48-51) and (161-164), respectively. The shift possibly indicates an effect on running during gel electrophoresis caused by a change of the protein net charge of mutagenic Rheb molecules. Some mutants replaced a charged amino residue (tyrosine and aspartate in mutant 33-37, asparagine in mutant 48-51, arginine in mutant 161-164) by an uncharged one (alanine) which might induce the change of the net charge of the whole protein. The double bands of the p70<sup>S6K</sup> detection might account for the S6K isomer p85<sup>S6K</sup>, whereas the higher band is p85<sup>S6K</sup> and the lower the mTOR substrate p70<sup>S6K</sup>.

The functional analysis was performed twice and the results are summarized in table 4. However, some mutants indicated also ambiguous expression levels between the two functional analysis experiments, requiring further analysis either by testing more clones or setting up another stock of cell extract by maxi-prep to achieve equal expression which is required for a reproducible functional outcome. Clones of GST-tagged Rheb mutants, which could already be created, were also tested for expression level.

3.1.2 Mutagenic Rheb function upon amino acid withdrawal

After verification of the expression levels of the Flag-tagged Rheb mutants, two experiments with the selected clones of all mutants have been carried out to test their ability of rescuing mTOR kinase activity after deprivation of amino acids. Therefore, plasmids of selected clones were co-transfected with p70<sup>S6K</sup>-encoding vectors and 48 h after transfection culture media was replaced by PBS for 90 min. The results of the first experiment are demonstrated in figure 10 which shows Rheb expression levels (by anti-Flag antibody) and p70<sup>S6K</sup> expression and phosphorylation.

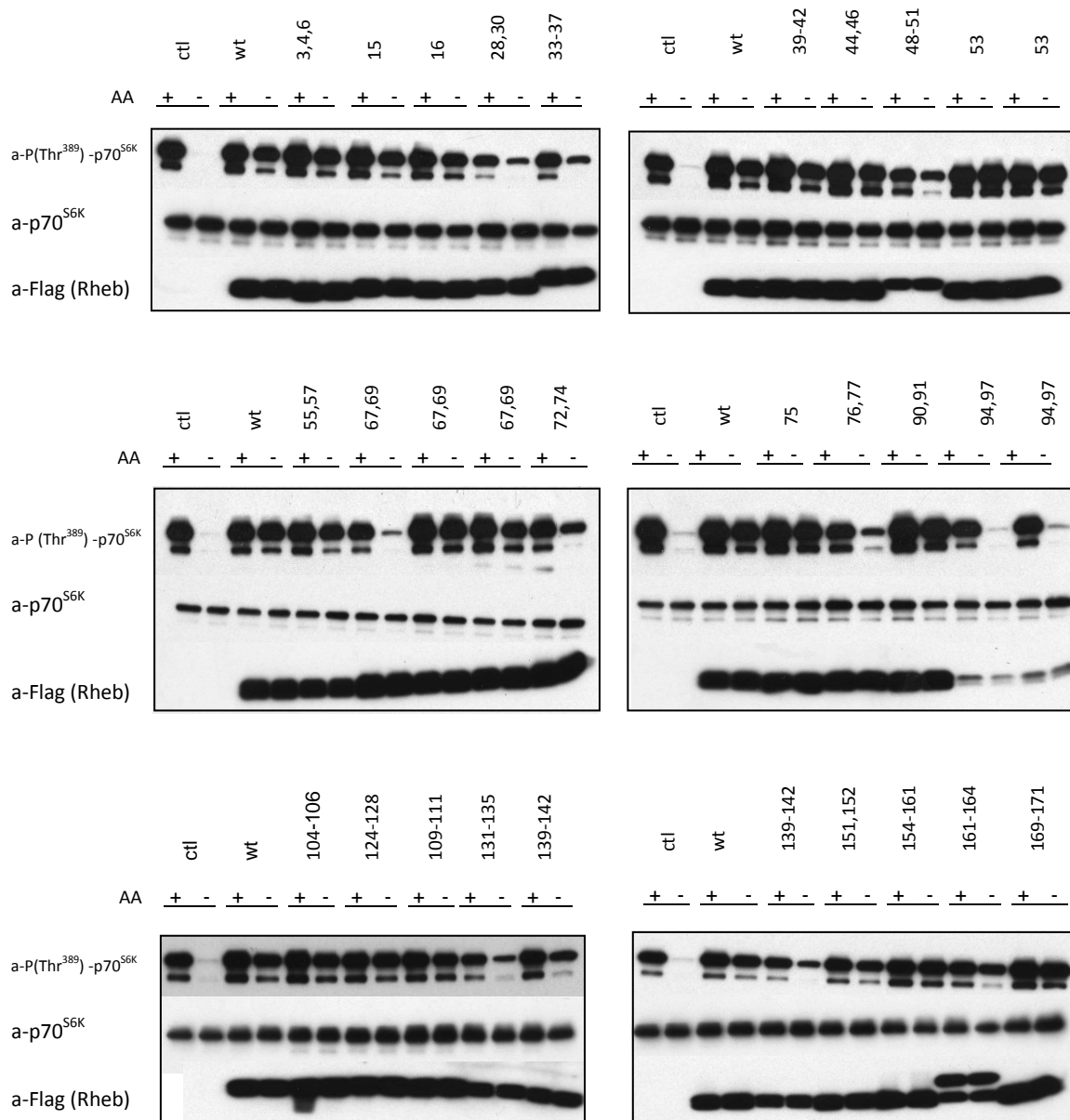


figure 10. Western Blot of functional analysis (first experiment as an example) of Flag-tagged Rheb mutants in HEK293T. (AA: amino acid presence; + yes/ - no, ctl: control with "empty" pCMV5 vector, wt: wildtype Rheb, numbers according to Rheb mutation sites; explained more in detail see table 2 in material and methods part, a-P(Thr<sup>389</sup>)-p70<sup>S6K</sup>: antibody specific against phosphorylated p70<sup>S6K</sup> at threonine residue 389, a-Flag: antibody specific against Flag-tag which indicates here total Rheb expression)

As controls an “empty” vector encoding no Rheb protein and a vector encoding wildtype Rheb were transfected. The “empty” vector results in a diminished p70<sup>S6K</sup> phosphorylation upon amino acid withdrawal whereas the vector with the wildtype Rheb leads to the rescue of mTOR kinase activity and therefore to no decrease in p70<sup>S6K</sup> phosphorylation upon amino acid withdrawal due to the overexpression of functional Rheb. This allowed a comparison of functionality of wildtype Rheb with the mutagenic Rheb molecules. Loss-of-function was stated when Rheb mutants were not capable of restoring p70<sup>S6K</sup> phosphorylation more than 50% compared to wildtype.

MUTATION	1. Functional analysis			2. Functional analysis	
	FUNCTION	RESCUE	EXPRESSION	RESCUE	EXPRESSION
3-6	+	+	+	+	+
15	+	+	+	+	+
16	+	+	+	50%	70%
28, 30	<b>Loss</b>	20-30%	80%	0%	80%
33-37	<b>Loss</b>	40%	+ (shift)	0%	70% (shift)
39-42	+	+	+	+	+
44, 46	<b>Ambiguous</b>	+	+	0%	+
48-51	?	50%	50% (shift)	10%	10%
53	+	+	+	+	+
55, 57	<b>Ambiguous</b>	+	+	0%	70%
67, 69	<b>Loss</b>	10%	+	0%	+
72, 74	<b>Loss</b>	50%	+	0%	+
75	+	+	+	+	+
76, 77	<b>Loss</b>	20%	+	10%	+
90, 91	+	+	+	+	+
94, 97	?	10%	<10%	0%	<10%
104-06	<b>Ambiguous</b>	+	+	0%	70%
109-11	<b>Ambiguous</b>	+	+	0%	+
124-28	+	+	+	80%	80%
131-35	?	30%	50%	0%	<10%
138-142	?	40%	50%	10%	10%
151, 152	+	+	+	+	80%
154-61	+	+	+	+	+
161-64	+	+	+ (2 bands)	80%	+ (2 bands)
169-71	+	+	+	+	+

table 4. Summary of results from two functional analysis experiments of Rheb mutant expression and their mTOR kinase rescue ability. 2. Functional analysis was repetition of selected clones from 1. Functional analysis. Highlighted in the red box is switch 1 (residues 33-41) and green box switch 2 (residues 63-79). (+: expression/rescue as wildtype, %: percentage of expression/rescue property compared to wildtype Rheb,?: rescue ability uncertain due to lower expression)

In figure 10 can be seen that for the nine mutants (28, 30), (33-37), (48-51), (67, 69), (72, 74), (76, 77), (94, 97), (131-135), (139-142) p70<sup>S6K</sup> is less phosphorylated after amino acid deprivation than with transfected wildtype

Rheb. For the four clones (48-51), (94, 97), (131-135), (139-142), this outcome might be due to the low Rheb expression.

In order to achieve a comparison in function between poorly expressed mutant Rheb and wildtype, a dose-response experiment was carried out (data not shown). Thereby wildtype Rheb plasmid was transfected in several concentrations, ranging from 0.031 to 1  $\mu\text{g}$  per 2 ml cell culture media. Mutant Rheb vectors were also applied with two different amounts (0.5 and 1  $\mu\text{g}$ ) to increase chance of comparable expression levels. As result, for all tested mutants the expression was still lower than the lowest applied amount of wildtype Rheb plasmid. The rescue of this low mutagenic Rheb expression turned out to lead to very faint bands, making it difficult to verify functional activity and showing the limit of the assay as it is not reasonable to go even lower in vector concentration to transfect. A summary with the estimated expression or phosphorylation level can be seen in table 4 of two independent experiments. Second functional analysis was a repetition with the same clones of first functional analysis. When comparing the outcome of both experiments, it is obvious that for some mutants either the expression level or the rescue ability or both were ambiguous.

The putative loss-of-function mutants as well as unknown or ambiguous results are outlined in table 4.2. The mutants that are located within the two Rheb switch regions are highlighted (red: switch1, green: switch2). Clearly, all loss-of-function mutants harbor mutation sites adjacent or within those regions.

### 3.1.3 Binding properties of Rheb mutants

In order to test whether defect phosphorylation rescue was due to an impaired interaction between mTORC1 and mutant Rheb, a binding assay was performed. Therefore, GST-tagged Rheb proteins with their according binding partners were “pulled down” by use of GSH sepharose which binds to GST. Prior to “pull-down” constructs of selected clones encoding mutagenic Rheb were co-transfected with one of the mTORC1 components; either the catalytic domain of the mTOR polypeptide, LST8 or Raptor, which were all Flag-tagged. Eluates of “pull-down” as well as cell extracts were examined by Western blot.

As a negative control, an “empty” pEBG vector encoding no Rheb protein was transfected, which will lead to no GST-tagged fusion protein. This should ensure no “pull-down” of any protein with GSH-Sepharose. Strikingly, with the GSH eluate there was a band observed comparable to the “pulled down” Flag-tagged mTOR of the transfected wildtype Rheb indicating a high background. A representative Western blot seen in figure 4.3 shows expression level of mTOR polypeptide (cell extract) and binding to GST-tagged mutagenic Rheb proteins in the GSH eluate in presence and absence of amino acids. Also the high background of “empty” pEBG vector is obvious. Interestingly, when comparing band intensities of “pulled down” mTOR (eluate) there seems to be a higher binding to Rheb mutants than Rheb wildtype except for clone (28, 30). The high background was seen in several experiments and in addition with the unequal Rheb expression, seen by Coomassie stain of membranes (data not shown) made it difficult to evaluate the data.

Nevertheless, preliminary results indicated that binding to mTOR might be independent from the functional outcome since some loss-of-function Rheb mutants showed mTOR binding despite low expression or loss of function. As can be seen for the loss-of-function mutant (33-37) (seen in figure 4.1), the GST-tagged Rheb mutant shows higher binding to mTOR catalytic domain obvious by a stronger band in the GSH eluate compared to wildtype (figure 11).

Because of the mentioned difficulties, experiments for binding properties of Rheb to several interaction partners were carried out *in vitro*. Those and additional experiments indicating GTP binding and *in vitro* mTOR kinase activity were performed later on and were published in the Journal of Biological Chemistry 2007 [97] (for more information see paragraph 5.1.2 in the discussion part).

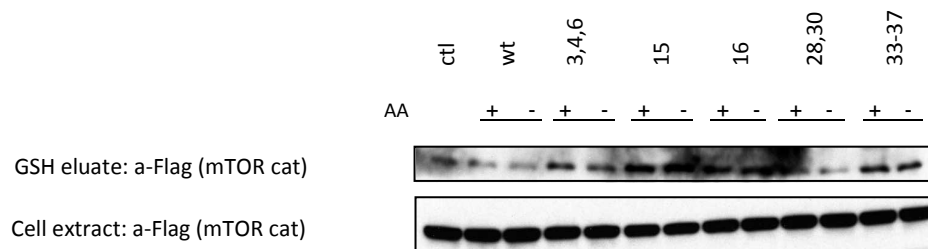


figure 11. Western blot of binding assay (exemplary). Co-transfection of GST-Rheb and Flag-mTOR polypeptide (catalytic domain). (AA: amino acid presence; + yes/ - no, ctl: control with "empty" pEBG vector, wt: wildtype Rheb, numbers according to Rheb mutation sites; explained more in detail see table 2.x in material and methods part)

## 3.2 Role of mTOR in trophoblast invasion

### 3.2.1 Transfection with siRNA

The transfection with siRNA in HTR8/SVneo had to be established. Results with use of lipophile transfection agents were poorly successful (data not shown). With electroporation, for all used siRNAs (Rheb, mTOR (a) and (b), Raptor and Rictor) a good knockdown effect was observed after 48 h by Western blot. The figures of densitometric analysis can be seen in the appendix chapter.

The transfection rate for Rheb knockdown was about 80% which was a significant reduction of Rheb expression (figure 13 and densitometric figure 49 in the appendix). For both mTOR sequences a knockdown effect of approximately 80% was received (figure 14 and densitometric figure 50 in the appendix), but was only significant for sequence (a) due to a higher variability of mTOR expression level when transfected with mTOR siRNA sequence (b). Also the phosphorylation level of the mTOR substrate p70<sup>S6K</sup> was more decreased with the use of mTOR siRNA (a). Transfection with mTOR siRNA (b) led to a phosphorylation level of p70<sup>S6K</sup> similar to

that of control cells. Since silencing effect was better with siRNA sequence mTOR (a) regarding both, mTOR expression and substrate phosphorylation level, this siRNA was preferentially used for further analysis. Additionally, for mTOR (a) a phenotypical change of cells could be observed whereas no such change was seen with the other siRNAs (figure 15). Transfected cells with mTOR (a) showed less pronounced development of filopodia.

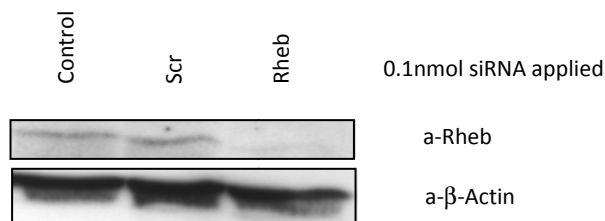


figure 13. Western blot detecting level of Rheb 48h after transfection. (Control: no siRNA, Scr: "scrambled" non-genomic control siRNA)

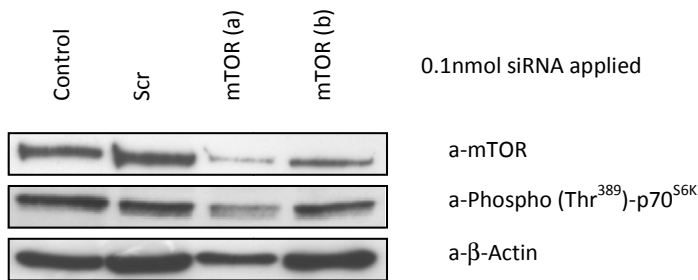


figure 14. Western blot detecting level of mTOR 48h after transfection mTOR (a) and mTOR (b) are mTOR-specific siRNAs with different sequences. (Control: no siRNA, Scr: "scrambled" non-genomic control siRNA)

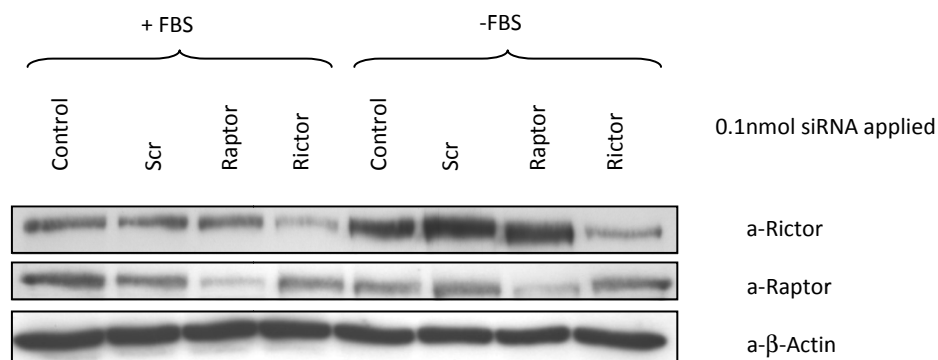


figure 12. Western blot detecting level of Raptor and Rictor 48h after transfection cultured with or without serum. (Control: no siRNA, Scr: "scrambled" non-genomic control siRNA)



The transfection with Raptor siRNA led to a decrease of about 80% of Raptor expression and with Rictor siRNA to a decrease of about 60% lower expression (figure 12 and densitometric analysis seen in figure 51 and figure 52 in the appendix). Both transfection rates were highly significant.

No difference of transfection rate of used siRNAs was seen between serum-supplemented and serumfree cell culture. Interestingly, it could be observed that Rictor expression was increased when no serum was available (figure 12). Raptor expression was unaffected by serum availability.

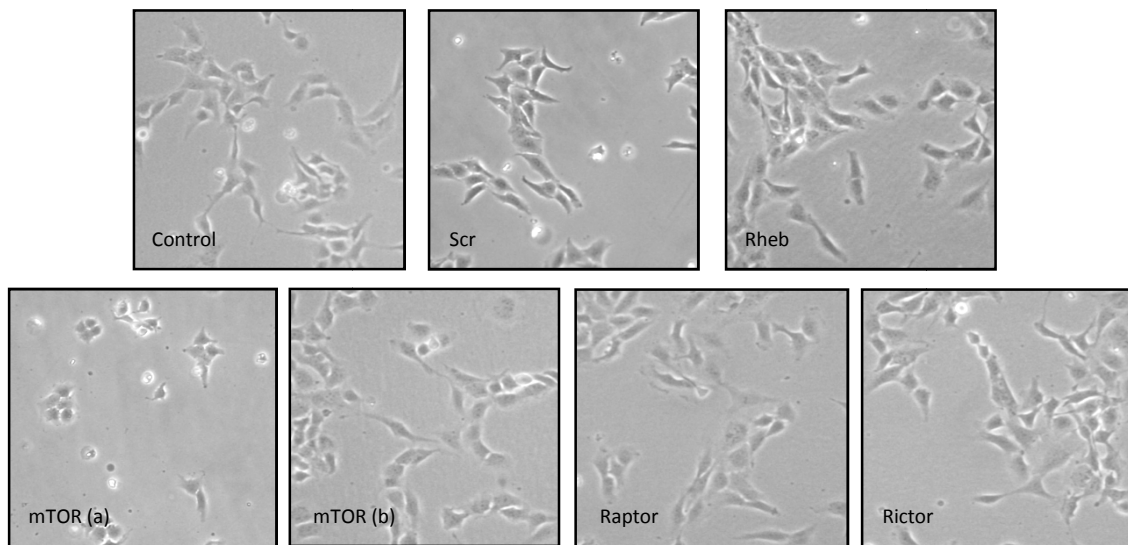


figure 15. Light microscopy showing cell phenotype 48h after transfection of 0.1nmol siRNA (cultured with serum). mTOR (a) and mTOR (b) are mTOR-specific siRNAs with different sequences. (Control: no siRNA, Scr: "scrambled" non-genomic control

### 3.2.2 Phosphorylation of p70<sup>S6K</sup> to monitor mTOR kinase activity

In order to verify the effect of Rapamycin, Akt-I X and LY294002 inhibitors as well as of silenced proteins by siRNA transfection on mTOR kinase activity, the phosphorylation of mTOR substrate p70<sup>S6K</sup> was used as read-out.

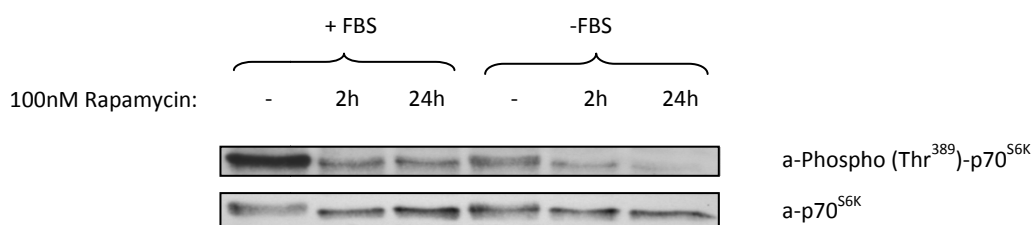


figure 16. Western blot detecting p70<sup>S6K</sup> and its phosphorylation status upon Rapamycin treatment when cultured with or in the absence of serum.

In the absence of serum, there is a significantly lower basal level in p70<sup>S6K</sup> phosphorylation which is about 40% of the phosphorylation level seen in the presence of serum (see densitometrical analysis figure 53 in the appendix). Hence, the lack of serum within the cell culture media influences mTOR kinase activity which was already mentioned to be a nutrient sensor. Also there is tendentially but not significant increase of total p70<sup>S6K</sup> expression when serum was absent.

As seen in figure 16, Rapamycin very efficiently abolishes p70<sup>S6K</sup> phosphorylation after 2 h and 24 h treatment to the same extent (about 80% less). This effect was observed for both, with and without serum in the media, but was only significant for the latter (see densitometric figure 58 in the appendix).

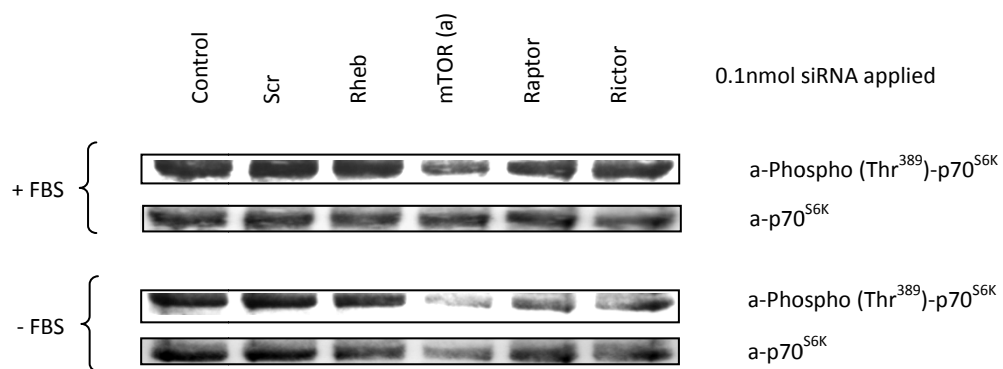


figure 17. Western blot detecting p70<sup>S6K</sup> and its phosphorylation status upon siRNA transfection when cultured with or in the absence of serum. (Control: no siRNA, Scr: "scrambled" non-genomic control siRNA)

As for transfection, only mTOR knockdown with mTOR-specific siRNA (a) showed a reduction of p70<sup>S6K</sup> phosphorylation (figure 17) when serum was available. Under serumfree condition, also Raptor and Rictor knockdown showed a slightly diminished phosphorylation of p70<sup>S6K</sup> (densitometric analysis is seen in figure 64 in the appendix). Transfection with Rheb siRNA and control with non-genomic siRNA (Scr) did not affect phosphorylation level of p70<sup>S6K</sup>. Expression of total p70<sup>S6K</sup> was observed to be highly variable (densitometric analysis see figure 65 in appendix).

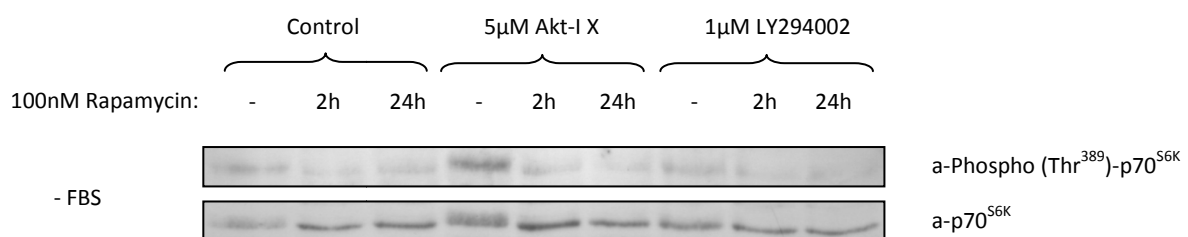
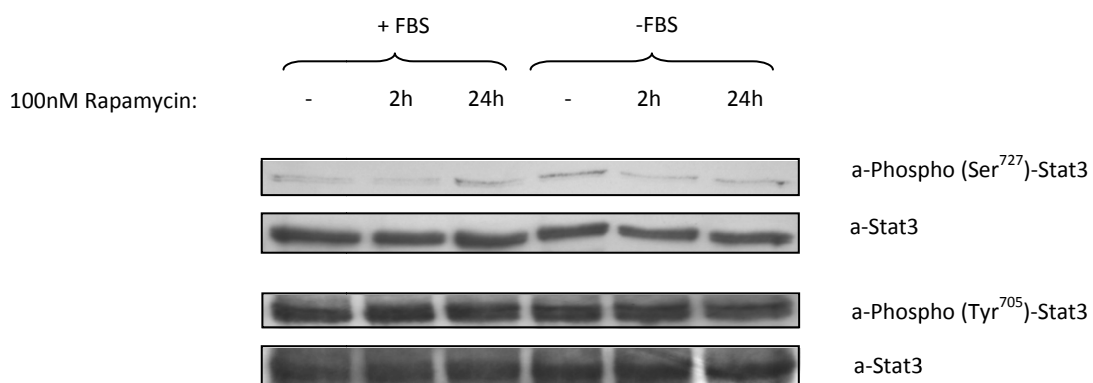


figure 18. Western blot specific for mTOR kinase substrate p70<sup>S6K</sup> detecting p70<sup>S6K</sup> and its phosphorylation status upon inhibition of mTOR (Rapamycin), Akt (Akt-I X) and PI3K (LY294002) when cultured in the absence of serum.

For the use of specific inhibitors of Akt (Akt-I X) and PI3K (LY294002), first the optimal concentration for inhibiting effect on mTOR activity was determined in absence and presence of serum (data not shown). As seen clearly in figure 18, the PI3K inhibitor LY294002 seemed more efficient in abrogation of p70<sup>S6K</sup> phosphorylation whereas the Akt inhibitor Akt-I X did not decrease but rather increase basal p70<sup>S6K</sup> phosphorylation. This effect was also seen when determining optimal concentration of inhibitor in the absence but not in the presence of serum.

### 3.2.3 Stat3 phosphorylation

Stat3 possesses two phosphorylation sites, at position 705 (tyrosine) and 727 (serine). The effect of Rapamycin and siRNA transfection was examined on both phosphorylation sites. Serum did not affect total expression of Stat3 and also basal phosphorylation level on either site (see densitometric analysis figure 53 in the appendix). Generally, it is to note that a high variability for both phosphorylation levels was observed, especially for Rapamycin treatment. Therefore, the represented pictures have to be considered with caution.



*figure 19. Western blot detecting Stat3 and its phosphorylation status upon Rapamycin treatment when cultured with or in the absence of serum.*

In figure 19, the phosphorylation status of Stat3 is seen when cells were exposed to Rapamycin. As for serine phosphorylation, there seems to be a slight decrease when cells were treated for 2 h and an increase when treated for 24 h with Rapamycin in the presence of serum whereas under serumfree conditions there is a decrease in the phosphorylation level with acute and prolonged Rapamycin treatment. Tyrosine phosphorylation seems to be unaffected by Rapamycin (also densitometry in figure 56 in appendix). In contrast, densitometric analysis which summarizes two (with serum) and four (without serum) independent experiments revealed that only acute Rapamycin in the absence of serum significantly diminished serine phosphorylation (see figure 55 in the appendix).

The Stat3 phosphorylation status upon transfection is demonstrated in figure 20 which represents two experiments. It can be seen, that mTOR siRNA (a) abolished serine phosphorylation in the presence and absence of serum in a significant manner (densitometric analysis is seen in figure 61). Rictor knockdown decreased serine phosphorylation only under serumfree condition whereas serine phosphorylation seems to be unaffected by Raptor knockdown. The use of Rheb-specific siRNA led to an increase of serine phosphorylation when cells were cultured with serum and has no effect in the absence of serum. Phosphorylation level remained the same in respect to untransfected control when non-genomic siRNA (Scr) was used.

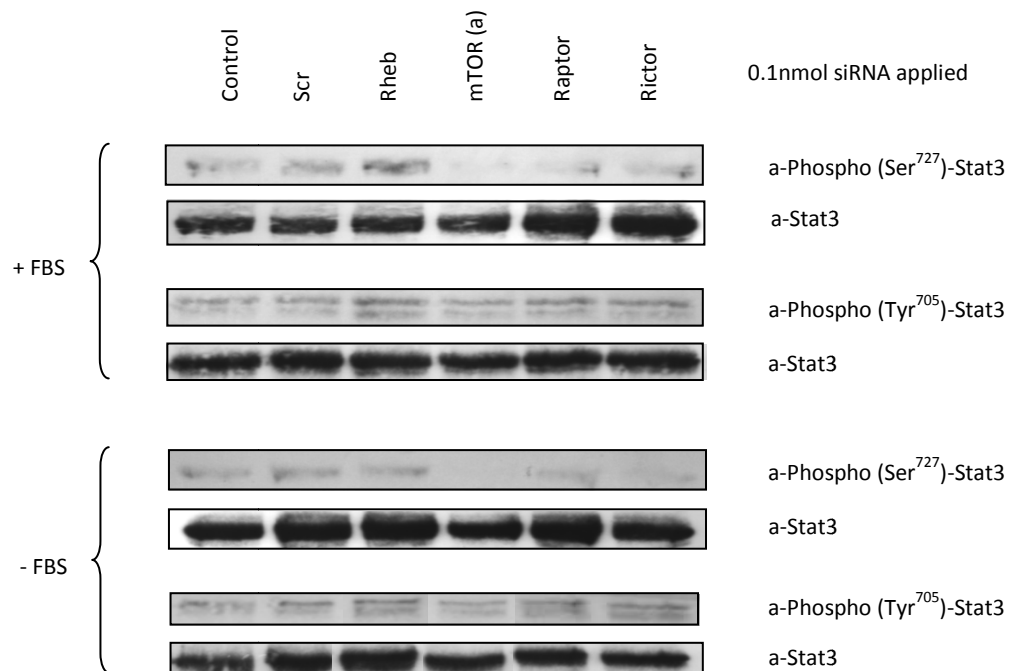


*figure 20. Western blot detecting Stat3 and its phosphorylation status upon siRNA transfection when cultured with or in the absence of serum. (Control: no siRNA, Scr: "scrambled" non-genomic control siRNA)*

Tyrosine phosphorylation does not seem to be strongly affected by any used siRNA but there was a slight, but not significant decrease for mTOR, Raptor and Rictor obvious in the densitometric analysis, presented in figure 62. There was slight decrease in the Tyr<sup>705</sup> phosphorylation level in mTOR (a) transfected cells. The overall Stat3 expression was also not influenced 48 h after siRNA transfection.

#### 3.2.4 Proliferationrate

The MTS proliferation assay was used to verify effects on cell number upon inhibitor treatment or siRNA transfection. Whether observed results are indeed due to changes in cell proliferation or maybe a consequential effect by apoptosis cannot be elucidated with this assay.

Rapamycin was applied with or without the presence of serum in the cell culture media for 2 h with subsequent incubation for 24/48 h or it was incubated throughout the assay. Because of the absorbance divergence between serum-containing and serumfree media, values were related to according control which was set as 100% in both cases.

As seen in figure 21, all samples treated with Rapamycin were significantly different from controls. In the presence of serum cell number was reduced about 15-20% after 24 h and 35-40% after 48 h of incubation for acute and prolonged Rapamycin exposure. There was no difference seen between acute and prolonged treatment with Rapamycin unlike when serum was absent which showed significantly different cell numbers between both exposure time-points. When no serum was available in the cell culture media, cell number was less decreased when Rapamycin exposure was prolonged. For both time points it was about a 20% reduction. After 24 h, acute Rapamycin treatment diminished cell number about 30% and after 48 h, it was about 40%. Calculated standard deviations were small for all samples probably due to seeding from one cell batch which is less prone to errors in cell numbers between each sample.

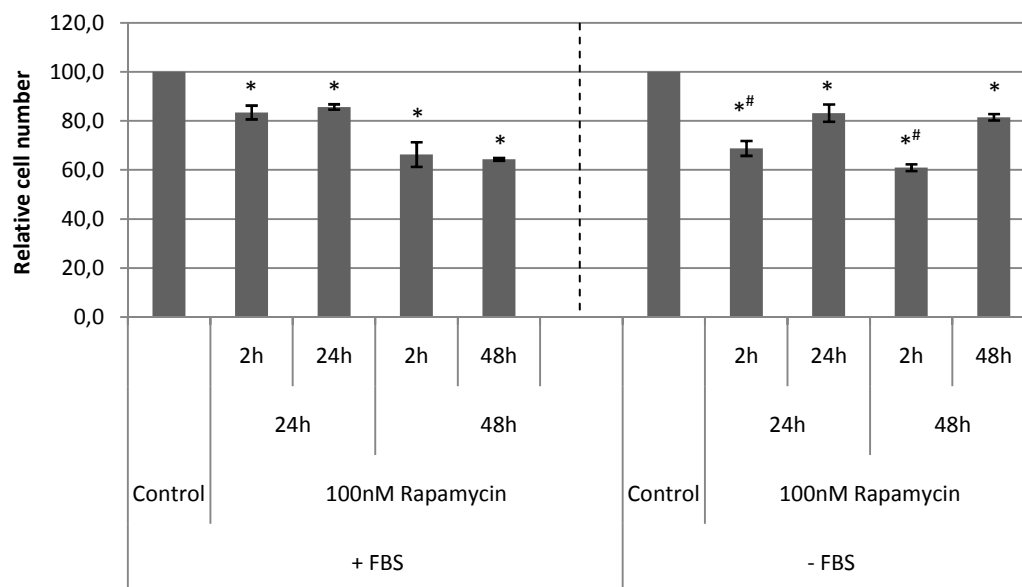


figure 21. Relative cell number upon Rapamycin treatment when supplemented with or without serum. MTS measurement was performed 24 h and 48 h after inhibition (acute Rapamycin treatment was 2 h with subsequent Rapamycin-free culture for 24 h or 48 h accordingly, prolonged Rapamycin treatment was accordingly 24 h or 48 h). Error bars indicate standard deviation of three independent experiments with triplicates. Controls were set independently as 100%. (Student t-Test: \*  $p < 0.02$  [versus control], #  $p < 0.01$  [2h versus 24h])

Subsequently to transfection of cells with siRNA, cells were seeded for proliferation assay, changing media next day and measuring another 24 h later. In figure 22, the relative proliferation rate or cell number is depicted. There was no significant change when Rictor was knocked down whereas Raptor knockdown showed high significant decrease in cell number of about 10% and 20% with and without presence of serum, respectively.

Rheb knockdown only showed high significance with no serum in media of which relative cell number declined down to 75%.

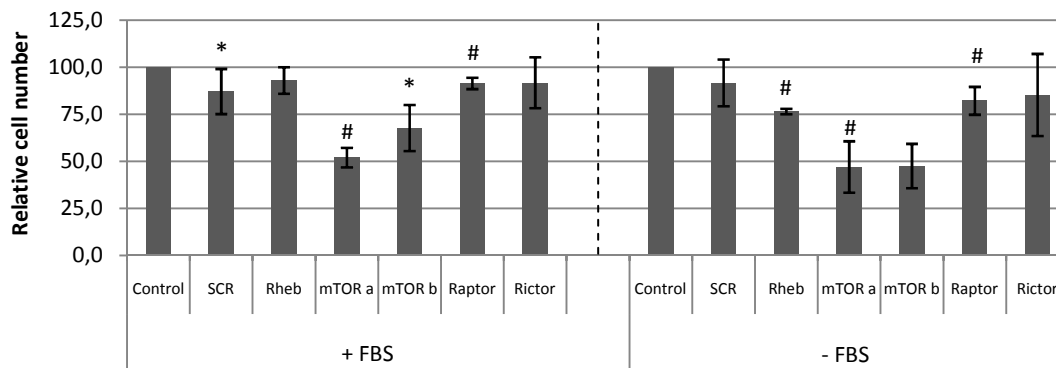


figure 22. Relative cell number upon 0.1nmol siRNA transfection when supplemented with or without serum. Error bars indicate standard deviation of at least three independent experiments (except for mTOR (b) -FBS, n=2) with triplicates. mTOR (a) and mTOR (b) are mTOR-specific siRNAs with different sequences. (Control: no siRNA, Scr: "scrambled" non-genomic control siRNA, Student t-Test: \*  $p < 0.05$  [versus control], #  $p < 0.005$  [versus control])

With the use of mTOR siRNA sequence (a), a highly significant reduction down to the half of control was seen for both cultures, with and without serum. The other sequence (b) showed a less pronounced effect of a 30% reduction when serum was present. Under serumfree condition the reduction of about 50% compared to control by mTOR (b) was not significant due to low experiment number (two independent experiments).

Standard deviation values were higher compared to Rapamycin treatment probably due to inhomogenous seeding of cells which may result from counting errors; all cells have to be counted separately after transfection whereas the batch of cells seeded for inhibitor treatment is for all samples the same.

In order identify a mechanism which can reverse the observed differential effect of acute and prolonged treatment in absence of serum, Rapamycin treatment was also performed when cells were transfected to knock down molecules within the mTOR pathway.

In figure 23 can be seen that for both controls, untransfected and transfected with non-genomic siRNA (Scr), a significant decrease in relative cell number upon acute Rapamycin treatment was observed as before. Strikingly, this effect is minor (about 10% reduction) in respect to previous experiments (20-30% reduction). Also there is no significance between acute and prolonged Rapamycin treatment anymore. Tendentiously, cell numbers are reduced when treated with Rapamycin for all transfected cells. Significance of reduction of knockdowns in respect to untransfected cells is according to results shown before. Only for Raptor knockdown a significant change by acute Rapamycin exposure to its untreated knockdown was apparent. Also just tendentiously, it was observed that there is a reversion of differential cell number reduction by 2 h or 24 h treatment seen for Rheb and Raptor knockdown.

In another approach to identify a mechanism which potentially can reverse the observed effect by Rapamycin, the mTOR upstream molecules Akt and PI3K were inhibited. Akt is already known as target for positive feedback loop via the mTOR-Rictor (TORC2) complex.

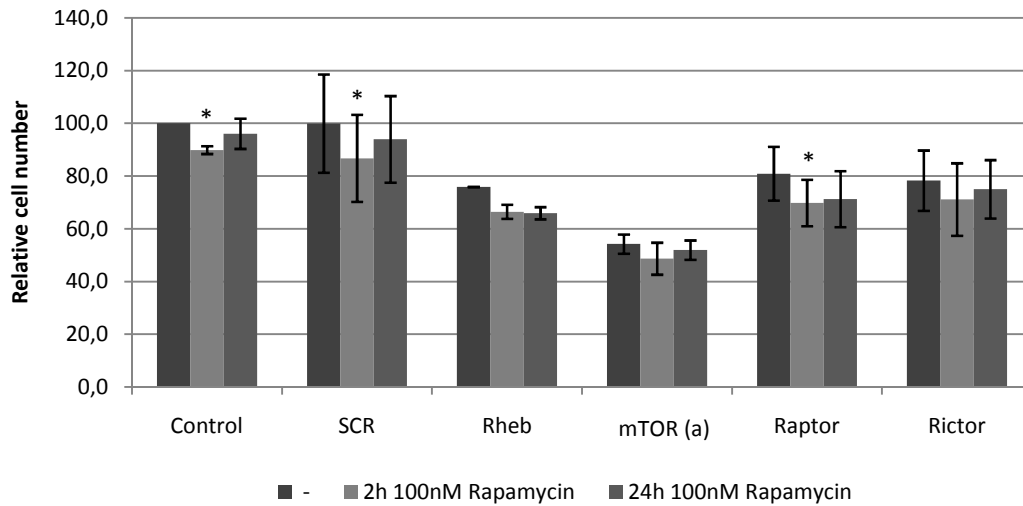


figure 23. Relative cell number upon 0.1nmol siRNA transfection and Rapamycin treatment in the absence of serum. Error bars indicate standard deviation of at least three independent experiments with triplicates. (Control: no siRNA, Scr: "scrambled" non-genomic control siRNA, Student t-Test: \* p<0.04 [untreated versus 2h Rapamycin treatment])

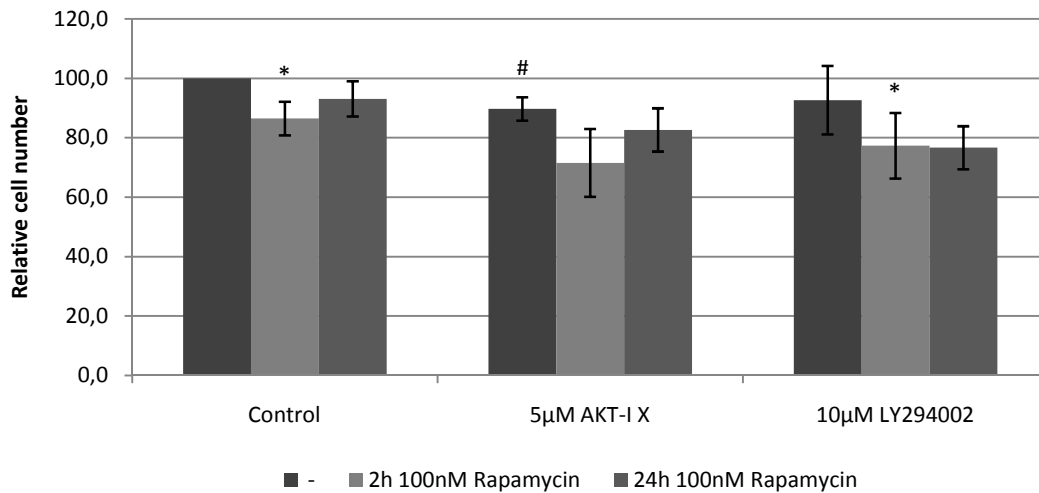
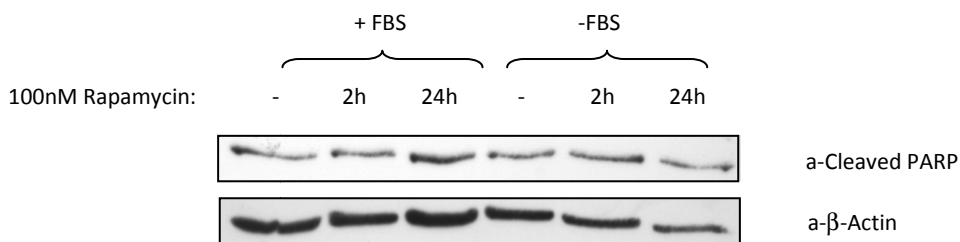


figure 24. Relative cell number upon inhibition of mTOR (Rapamycin), Akt (Akt-I X) or PI3K (LY294002) under serumfree condition. Error bars indicate standard deviation of three independent experiments with triplicates. (Student t-Test: \* p<0.02 [untreated versus 2 h Rapamycin treatment], # p=0.02 [versus untreated control], no significances 2 h versus 24 h Rapamycin treatment)

Incubation of the cells with Akt-I X and LY294002 led to a decreased cell number to 90% compared to untreated cells, but which was only significant for the Akt inhibitor. Decrease of cell number in respect to non-Rapamycin treated cells through acute Rapamycin exposure was only significant for control and PI3K-inhibited cells. Yet again for control cells, only a tendentious a difference could be seen from acute to prolonged Rapamycin exposure. This tendentious effect was also seen when cultured with Akt, but not with PI3K inhibitor. This observation hints that PI3K but strikingly not Akt is involved in Rapamycin-induced differential outcome on cell proliferation.

### 3.2.5 Level of apoptosis induction

In order to find out whether effects seen with MTS proliferation assay are not due to cell death, an assay was performed using an apoptosis marker; the big cleavage product of PARP. This cleaved PARP product, which is a sign of early apoptosis, was detected by Western blot and additionally by flow cytometry.



*figure 25. Western blot detecting cleaved PARP upon Rapamycin treatment when cultured with or in the absence of serum. Pictures represent two independent experiments.*

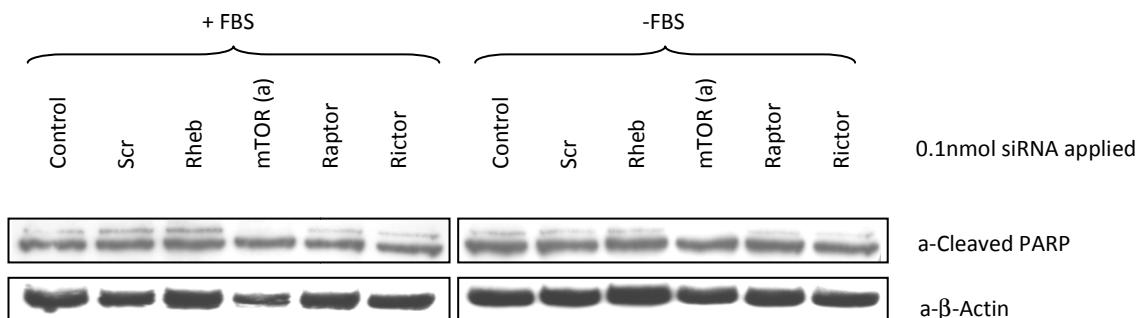


*figure 26. Western blot detecting cleaved PARP upon siRNA transfection when cultured with or in the absence of serum. Pictures represent three independent experiments. (Control: no siRNA, Scr: "scrambled" non-genomic control siRNA)*



Western blot showed no influence of serum on the level of cleaved PARP products (densitometric analysis in figure 53 in the appendix). Regarding Rapamycin-treated cells, no major difference in cleaved PARP level was seen with or without the presence of serum by Western blot (figure 25) (differences seen in figure upon Rapamycin treatment might be due to different protein load as obvious when considering  $\beta$ -Actin bands). Densitometric analysis revealed a slight, but not significant increase of cleaved PARP upon Rapamycin-treatment (figure 54 in appendix).

Western blot detecting cleaved PARP after siRNA transfection showed repeatedly a double band which was not observed for untransfected cells. According to the data sheet of the cleaved PARP antibody, the antibody does not detect full-length PARP (116 kDa), hence both bands must be related to cleaved PARP indicating apoptosis induction. Possibly, the electroporation procedure might have had an effect. There were no major changes in levels of cleaved PARP except for mTOR knockdown (figure 26) since the upper band of the double band was not detectable for both serum conditions.

Flow cytometry revealed a basal apoptotic rate of about 20% which seems to be decreased upon Rapamycin (see figure 27). But results varied strongly so that no significance could be affirmed and which also led to high standard deviations and is therefore depicted only in upwards direction. Interestingly, upon the absence of serum, the apoptotic rate was decreased about one quarter.

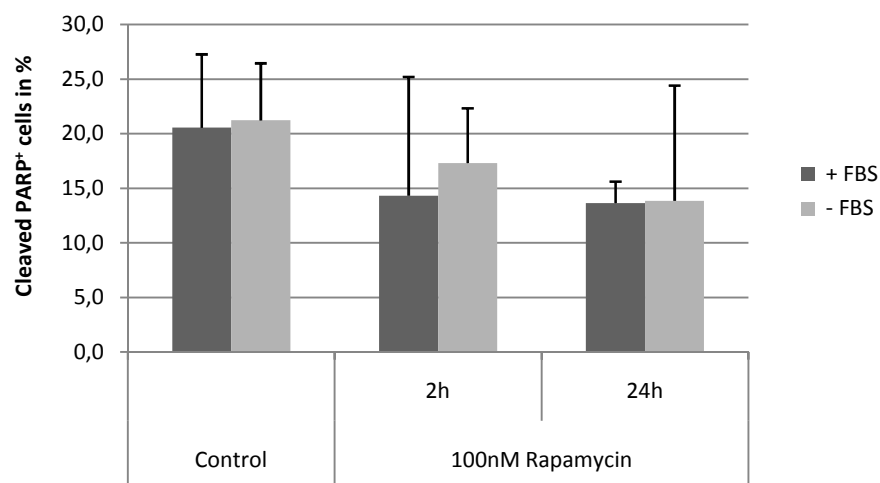


*figure 27. Apoptosis rate measured by flow cytometric analysis of fluorescein-conjugated cleaved PARP upon Rapamycin treatment when cultured with or in the absence of serum. Error bars indicate standard deviation of two independent experiments.*

The same basic apoptotic rate of around 20% was seen with transfected cells (figure 28). Strikingly, the withdrawal of serum increased apoptosis around one third, possibly due to a higher sensitivity of cells after electroporation procedure for transfection. Here, it is obvious that with transfection of mTOR siRNA sequence (a) the apoptosis rate % was increased with and without serum by the double and two-thirds, respectively. Also

there is a decrease down to the half for Raptor knockdown but only when cultured with serum. Otherwise there are only slight changes seen with transfected cells compared to control.

Since Western blot monitors apoptosis rate without any quantitative statement about apoptotic cell numbers, flow cytometric analysis was chosen to allow a quantification of cell numbers which are positive for cleaved PARP and hence apoptosis induction. However, a high variability was observed with both methods.

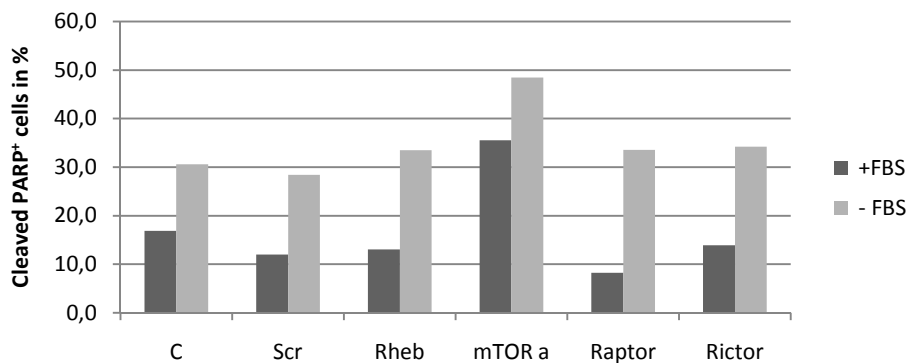


figure 28. Apoptosis rate measured by flow cytometric analysis of fluorescein-conjugated cleaved PARP upon 0.1nmol siRNA transfection when cultured with or in the absence of serum from one experiment.

### 3.2.6 Invasion-related assays

#### 3.2.6.1 Zymolytic activity

Using zymographic analysis the activity of gelatinases (MMP9, MMP2) and the plasminogen-converting enzyme uPA can be monitored by addition of the appropriate substrate to the electrophoresis gels. Here, the activity of secreted enzymes indicating the matrix-degrading potential was examined by taking conditioned cell culture media for analysis.

As for untreated cells, it could be observed that there was a lower zymolytic activity of the gelatinases MMP2 and MMP9 when there was no serum available in the medium whereas uPA activity seemed to be unaffected although there was a high variability among different experiments (densitometric analysis seen in figure 29). The values of zymolytic activity of serum-containing media were set to 100%. The down to one-fifth reduced activity of both, MMP9 and MMP2, in the absence of serum was highly significant. Also a predominance of MMP2 towards MMP9 gelatinase activity was seen (densitometric analysis seen in figure 30). The gelatinase activity of MMP2 was set as 100% independently for each serum condition. Under both conditions, with or without serum addition, the MMP9 activity was about 25% of the MMP2 activity. This effect was also highly significant.

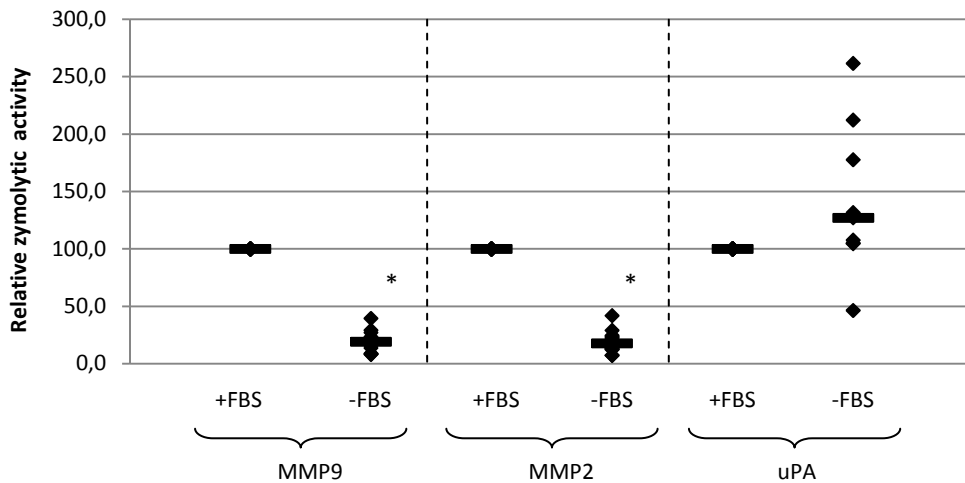


figure 29. Comparison of zymolytic activity of MMP9, MMP2 and uPA when supplemented with or without serum. Diagram represents densitometric analysis of zymographies. Bars indicate median value of seven (MMP9,2) and six (uPA) independent experiments, depicted as spades (Student t-Test: \*  $p < 0.001$  [versus +FBS]). Samples with serum set independently as 100%.

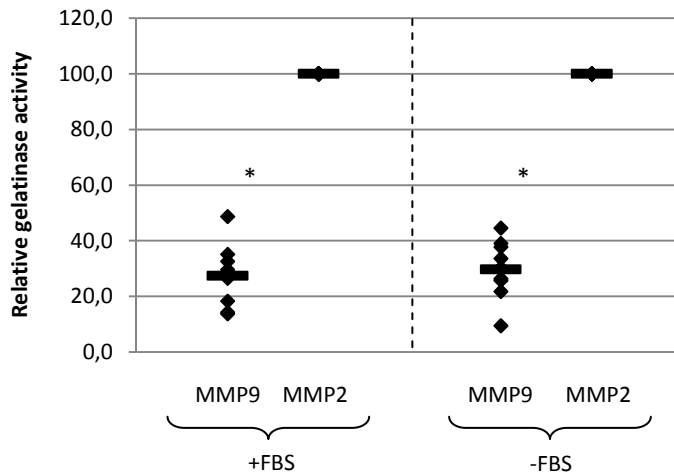


figure 30. Zymolytic gelatinase activity of MMP9 and MMP2 when supplemented with or without serum. Diagram represents densitometric analysis of zymographies. Bars indicate median value of nine independent experiments, depicted as spades (Student t-Test: \*  $p < 0.001$  [versus MMP2]). MMP2 levels set independently as 100%.

In figure 31 the outcome upon Rapamycin treatment on zymolytic activity is demonstrated. There is a decreased activity for all detectable enzymes in the media from cells treated acutely with Rapamycin but only in the absence of serum. The detected changes are not significant as the extent of decreased zymolytic activity varied greatly among experiments (see also densitometric figure 67 to figure 69 in the appendix). Otherwise there were no changes of zymolytic activity perceived.

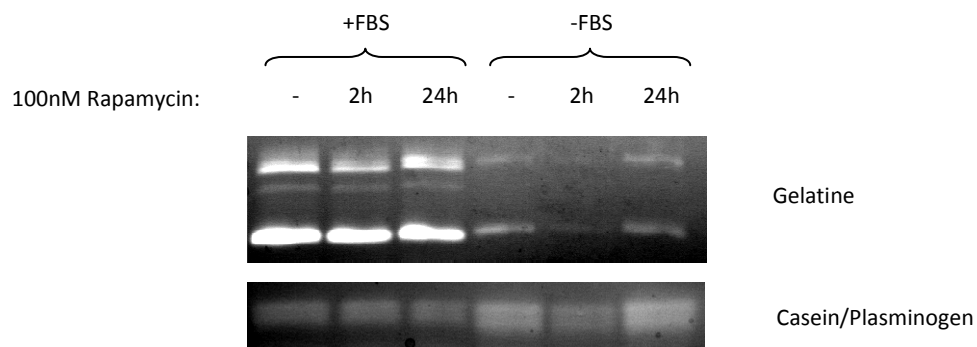


figure 31. Zymography of cell-conditioned media upon Rapamycin treatment, when supplemented with or without serum. Picture represents three independent experiments. (Gelatinase activity: upper band, MMP9 [84kDa], lower band MMP2 [64kDa], uPA activity given by lysed bands of Casein/plasminogen-containing gel)

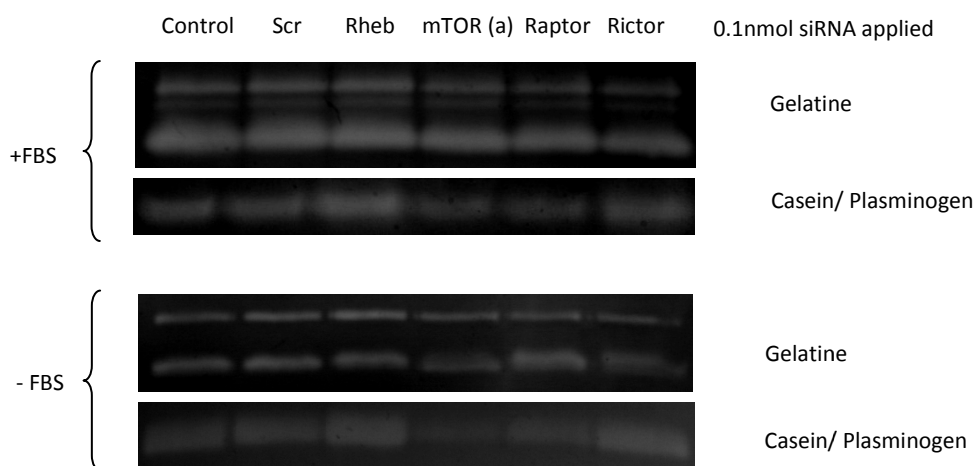


figure 32. Zymography of cell-conditioned media upon siRNA transfection, when supplemented with or without serum. Picture represents at least three independent experiments for each siRNA. (Control: no siRNA, Scr: "scrambled" non-genomic control siRNA, gelatinase activity: upper band, MMP9 [84kDa], lower band MMP2 [64kDa], uPA activity given by lysed bands of casein/plasminogen-containing gel)

Media of transfected cells exhibited mainly changes in uPA activity in absence and presence of serum for mTOR and Raptor knockdown (figure 32). Interestingly, densitometry analysis revealed that mTOR and Raptor also significantly decreased MMP9 activity in the absence of serum about 40% (densitometric analysis see figure 71 in the appendix). The slight decrease in MMP2 activity in serumfree cell-conditioned media upon transfection with mTOR (a), Raptor and Rictor siRNA is not significant due to high variability (densitometric analysis seen in figure 73 in the appendix). The significant about the half lower uPA activity by mTOR (a) and Raptor knockdown is independent from serum availability (densitometric figure 74 and figure 75 in the appendix). For Rheb

knockdown there was a slight, but statistically not significant increase in uPA activity observed under both serum conditions.

In summary, effects upon Rapamycin treatment and siRNA transfection on MMP9 and MMP2 are minor, although for the latter one the results are rather variable. For uPA activity, significant changes could be detected upon cell manipulation through siRNA targeting mTOR and Raptor which both diminished the activity of plasminogen-converting enzyme in cell-conditioned media. A decreasing effect on uPA activity was also seen by acute Rapamycin treatment in the absence of serum which was not significant due to high variability in the degree of reduction. Rheb knockdown tendentially increased uPA activity.

### 3.2.6.2 Expression and secretion of PAI-1

The observation of the influence of Rapamycin and siRNA transfection on uPA secretion raised the question whether the major physiological inhibitor of uPA, which is PAI-1, is affected as well. With several approaches the expression and secretion of PAI-1 was addressed.

When detecting the expression of PAI-1 by Western blot, there were detectable amounts of PAI-1 when cells were cultured without serum (figure 33). It is about half as much as the level of samples which were treated with serum. Interestingly, unlike for serum-conditioned samples, expression of PAI-1 decreased with acute Rapamycin treatment whereas prolonged exposure had no effect. When serum was present, cells expressed slightly more PAI-1 upon Rapamycin.

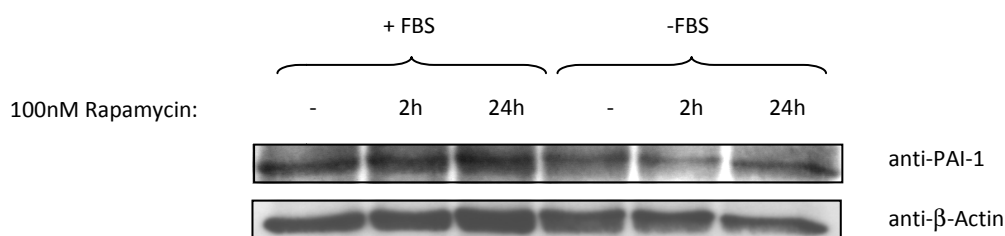


*figure 33. Western blot detection of human PAI-1 expression (cell lysates) upon Rapamycin treatment supplemented with or without serum. Picture represents two independent experiments.*

To further evaluate the expression of PAI-1 and confirm higher expression upon Rapamycin, immunocytochemical staining of cells was performed. Due to methodical issues, only serum-conditioned cells were examined (cells require FBS to attach properly to slides). By indirect labelling PAI-1 was monitored through an RPE-linked antibody by red fluorescence and DNA was obvious as blue fluorescence colour through DAPI staining (see figure 34). Panel with control cells, shows the nuclei with DNA (blue) and a red signal within the cytoplasm. Upon treatment with Rapamycin, there is still a red signal within the cytoplasm but also a pink/violet colour seen which results from the merger of blue (DAPI) and red (RPE) colour indicating either a co-

localization or overlapping of signals. An overlap of signals is probably allowed by “thickness” of samples since it not a cut slice from tissue but a layer of whole cells. It is likely, that there is an induction of a higher PAI-1 expression taking place in the cytoplasm which rather leads to an overlap of signals. However, this method gives no clues about secretion of PAI-1.

Preliminary results of PAI-1 secretion were obtained with Western blot analysis using cell-conditioned media. An increase of PAI-1 level about two-fold upon acute and prolonged Rapamycin treatment in respect to untreated cells when cultured with serum was observed (figure 35). This finding is consistent with the higher PAI-1 expression upon Rapamycin treatment seen in Western blot and by immunocytochemistry. Strikingly, PAI-1 was not detectable within serumfree media.

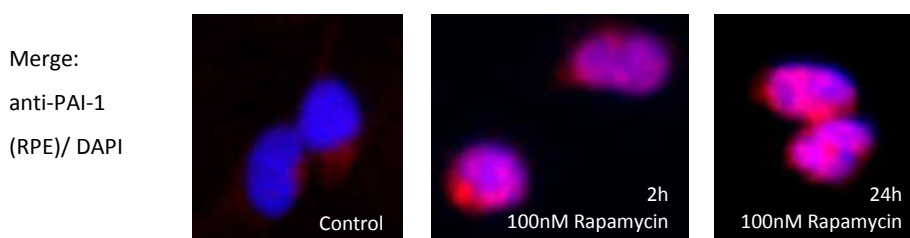


figure 34. Fluorescence-immunocytochemical staining of human PAI-1 upon Rapamycin treatment when supplemented with serum. Pictures represent two independent experiments. (red. PAI-1, blue: DAPI, pink: merge of both signals)

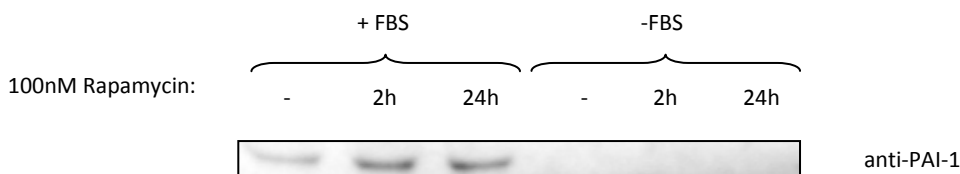


figure 35. Western blot detection of human PAI-1 upon Rapamycin treatment in cell-conditioned media supplemented with or without serum. Picture represents two independent experiments.

For quantification of secreted PAI-1 levels upon Rapamycin treatment and siRNA transfection, an ELISA detecting human PAI-1 to a minimum level of 50 pg/ml was carried out. To be able to calculate concentrations in the cell-conditioned media, a standard curve of known PAI-1 concentrations was set by duplicates for each experiment (presented in figure 66 in the appendix). For low concentrations a linear regression gave the best results with a high coefficient of determination ( $R^2$ ). Diagrams are given with relative values, since concentrations of secreted PAI-1 are cell number-dependent. The approximate detected PAI-1 concentrations lie between 0.5 and 1.5 ng/ml (absolute values are given in figure 40 since it represents one single experiment).

Otherwise, value of untreated control cells was set to 100% for either condition of serum availability within the culture media.

Considering untreated samples, it could be observed that the withdrawal of serum led to a highly significant lower secretion of PAI-1 down to the half which confirms Western blot results of media and cell lysates (figure 36). Here, values of serum-containing media were set as 100%.

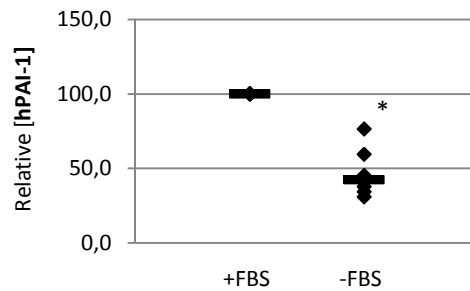


figure 36. Relative level of secreted human PAI-1 in presence and absence of serum measured by ELISA. Bars indicate median value of seven independent experiments, depicted as spades (Student t-Test: \*  $p=0.0001$ ).

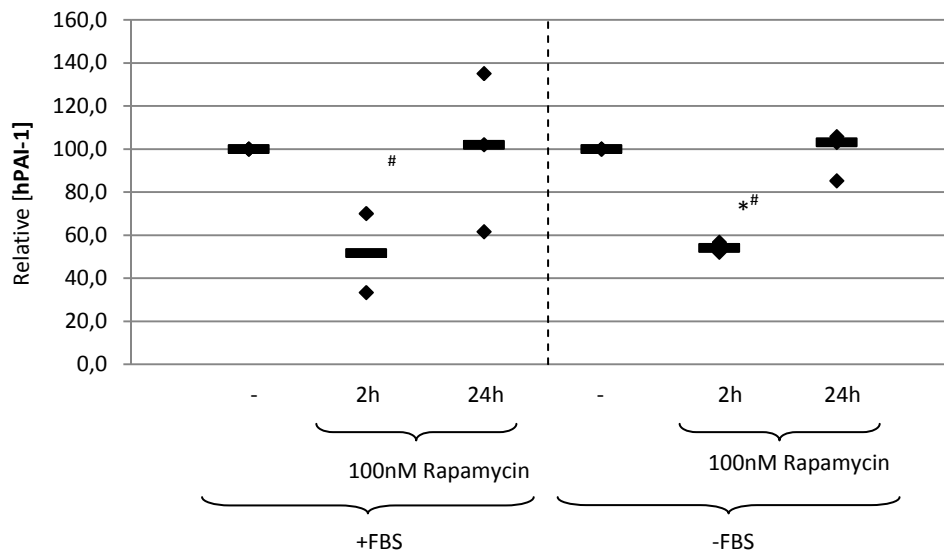


figure 37. Relative level of secreted human PAI-1 upon Rapamycin treatment supplemented with or without serum measured by ELISA. Bars indicate median value of three independent experiments, depicted as spades (Student t-Test: \*  $p=0.001$  [versus control], #  $p<0.02$  [2h versus 24h]). Controls are set independently as 100%.

When cells were treated with acute Rapamycin, there is a decrease about the half in PAI-1 secretion, which is significant under serumfree condition whereas prolonged treatment had no detectable effect (figure 37). The difference in PAI-1 secretion between acute and prolonged exposure of Rapamycin was significant for both conditions.

Transfection of non-genomic siRNA (Scr) showed no effect in PAI-1 secretion with or without supplementation of serum excluding unspecific effects through transfection procedure (figure 38 and figure 39). Significant effects were perceived with mTOR siRNA sequence (a) on PAI-1 secretion, which was reduced about the half with and without presence of serum. There is a slight increase of PAI-1 concentration seen when cells were knocked down for Rheb expression, also under both conditions. Raptor knockdown seems to result tendentially in a decrease of PAI-1 secretion. Rictor siRNA transfection also led to a decrease of PAI-1 concentration but which was only significant in the case of serum-starved cells.

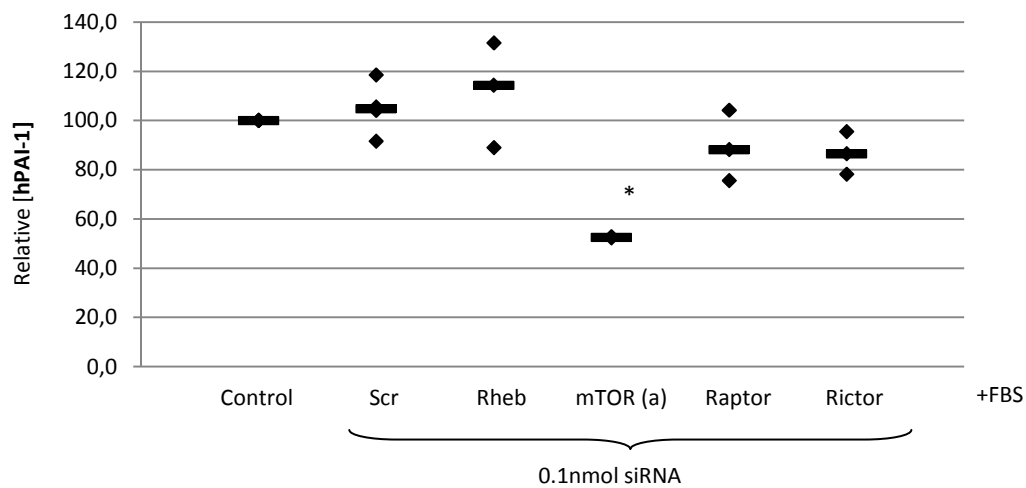


figure 38. Secretion of human PAI-1 upon siRNA transfection supplemented with serum. Bars indicate median value of at least three independent experiments, depicted as spades (Student t-Test: \*  $p=0.003$ ).

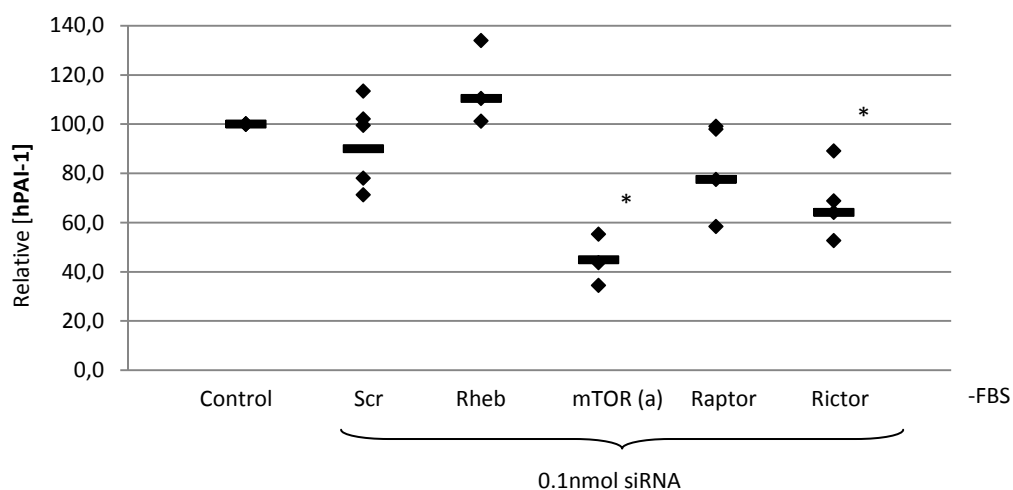


figure 39. Secretion of human PAI-1 upon siRNA transfection in the absence of serum. Bars indicate median value of at least three independent experiments, depicted as spades (Student t-Test: \*  $p<0.03$ ).



Due to too few samples of ELISA kit, samples from treatment with Akt (Akt-I X) and PI3K (LY294002) inhibitors were taken from only a single experiment. The results are demonstrated in figure 40. There seems to be a decrease in PAI-1 secretion when treated with the inhibitors with highest reduction when co-incubated with LY294002 and Rapamycin.

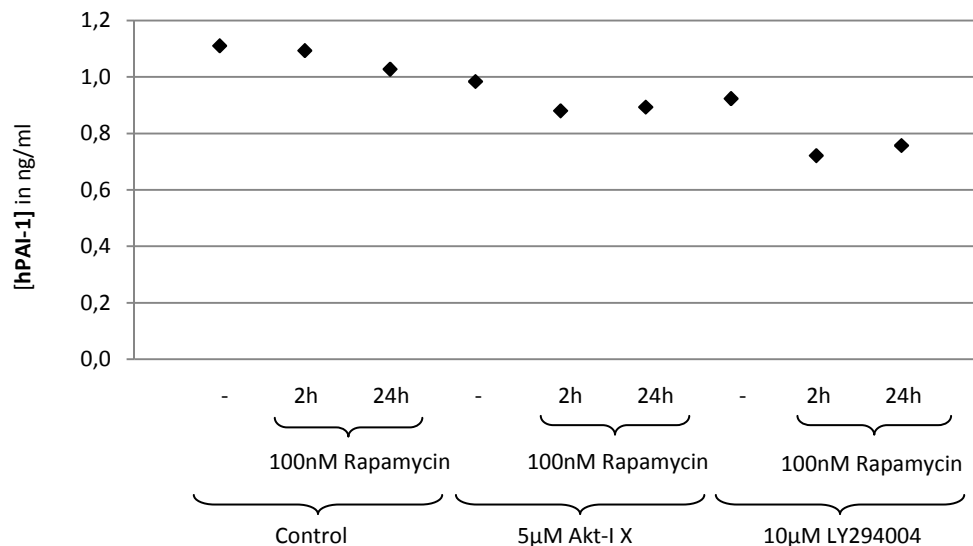


figure 40. Secretion of human PAI-1 upon inhibition of mTOR (Rapamycin), Akt (Akt-I X) or PI3K (LY294002) in the absence of serum. Spades indicate absolute concentration of one experiment.

### 3.2.6.3 Cell invasiveness

With the use of Matrigel-coated well inserts, the potency of cells to invade through extra-cellular matrix can be measured. In general, the *in vitro* Matrigel invasion assay showed very high variability and therefore high standard deviations were obtained which were depicted in the following figures only in upwards direction.

In figure 41 the influence of serum availability is demonstrated. Invasion rate of cells supplemented with serum was set as 100%. In the absence of serum the rate of invasion drops significantly down to 60%. In the figures showing invasion upon Rapamycin treatment and siRNA transfection, invasion rate of control cells were set to 100% for each serum condition.

Upon exposure of Rapamycin, number of invaded cells decreased about 20% with use of serum-containing media and about 60% when cells were serum-deprived (figure 42). Under serumfree condition the decrease of invasion was highly significant. There was no difference seen between acute and prolonged Rapamycin treatment under both conditions.

Invasion assay upon siRNA transfection showed no significant change but it can be noted that mTOR knockdown generally led to a lower level of invaded cells of about 30% to 60% less, whereas Raptor and Rictor

knockdown seemed to have no effect (figure 43). Tendentially, there might be an increase when transfected with Raptor siRNA and no serum added. The non-genomic control (Scr) left cell invasiveness unaffected.

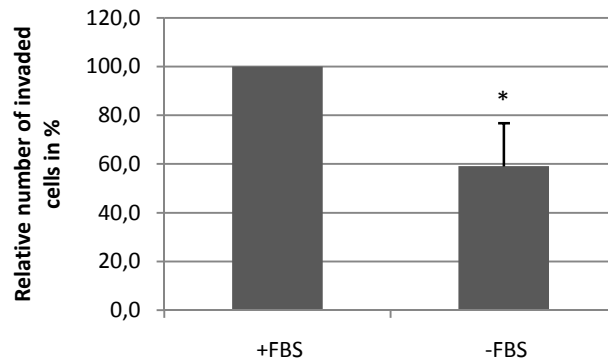


figure 41. Comparison of relative invasion rate when cultured with or in the absence of serum obtained with in vitro Matrigel invasion assay. Error bars indicate standard deviation of five independent experiments with triplicates (Student t-Test: \*  $p=0.007$ )

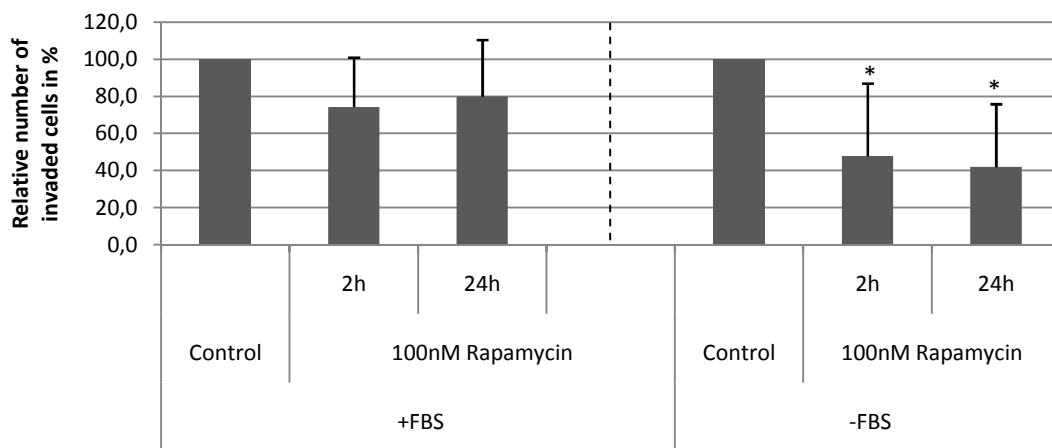


figure 42. Invasion rate upon Rapamycin treatment when cultured with or in the absence of serum. Error bars indicate standard deviation of three independent experiments with triplicates (Student t-Test: \*  $p<0.004$ ).

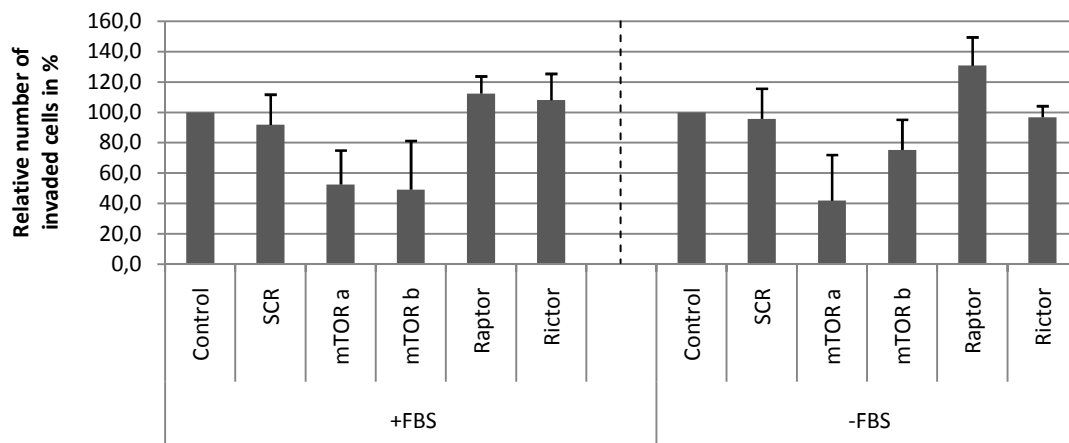
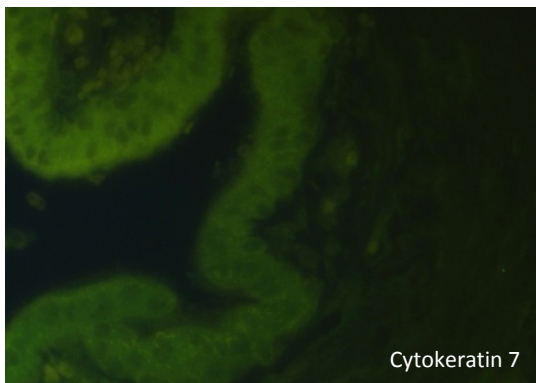


figure 43. Invasion rate upon 0.1nmol siRNA transfection when cultured with or in the absence of serum. Error bars indicate standard deviation of three independent experiments with triplicates. mTOR (a) and mTOR (b) are mTOR-specific siRNAs with different sequence.

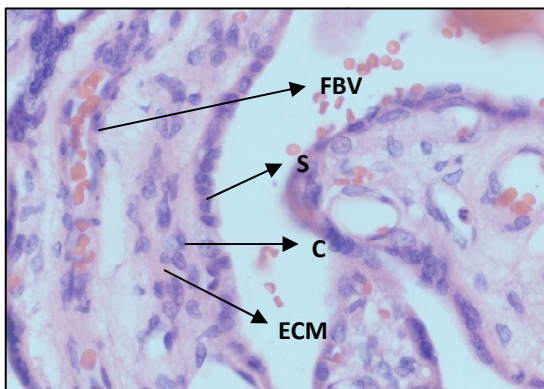
### 3.2.9 Immunohistochemistry of placental tissue

The immunohistochemical staining of tissue from first-trimester (gestational week 11) and term (gestational week 41) placenta revealed the localization of mTOR at the feto-maternal interface. Thereby villous (figure 44) and extra-villous trophoblast (figure 45) were examined. To identify trophoblast cells, the trophoblast marker cytokeratin 7 was applied, which was linked with FITC (green colour).

The hematoxylin-eosin (HE) -staining depicting trophoblast villi, monitored fetal blood vessel containing erythrocytes (red cells), syncytiotrophoblast cells as the outer layer of the villi and cytotrophoblast as well as extra-villous trophoblast cells with surrounding extra-cellular matrix (figure 44 and figure 45). The syncytium showed very high amounts of cytokeratin 7 whereas within the villi, this trophoblast marker was detected with a lower signal. mTOR could be detected by indirect labelling with RPE-conjugated antibody giving a red fluorescent signal. There was a strong signal in the outer layer of the villi implicating a higher expression of mTOR in the syncytial trophoblast than in the cytotrophoblast cells. The signal was localized in the cytoplasm; the nucleus is spared obvious by a dark spot. The mTOR signal might be a bit stronger in the first-trimester placental tissue than in the term placenta. Extra-villous trophoblasts were also positive for cytokeratin 7 and also showed mTOR localized within the cytoplasm. Again the signal for mTOR seemed stronger in the first-trimester placenta.



Gestational week 41:



Gestational week 11:

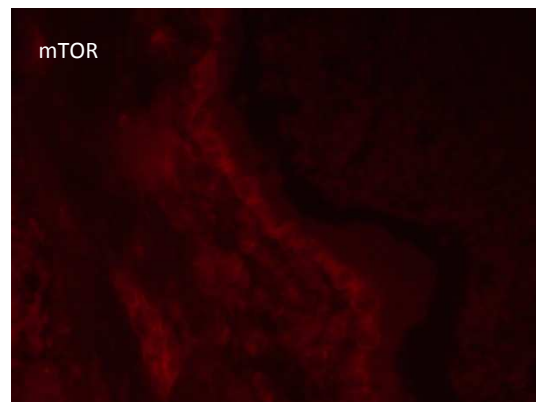
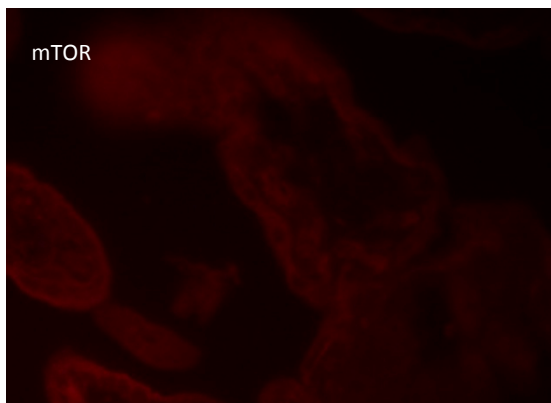
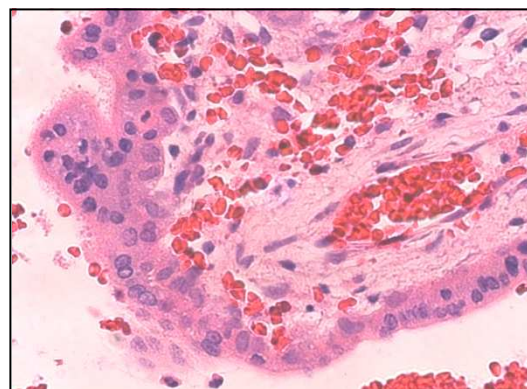
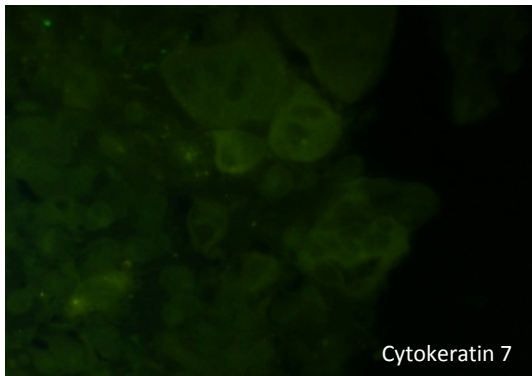
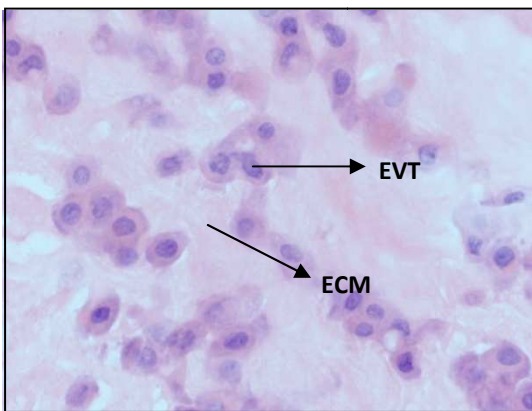


figure 44. Immunohistochemical staining of villous trophoblast cells in placental tissue (decidual side) from gestational week 11 and 41. (FBV: fetal blood vessel, S: syncytiotrophoblast cells, C: villous cytotrophoblast cells, ECM: extracellular matrix)



Gestational week 41:



Gestational week 11:

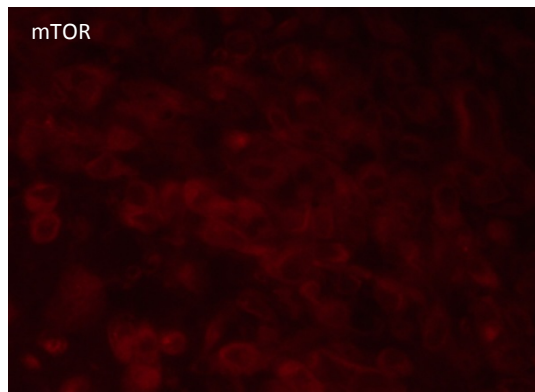
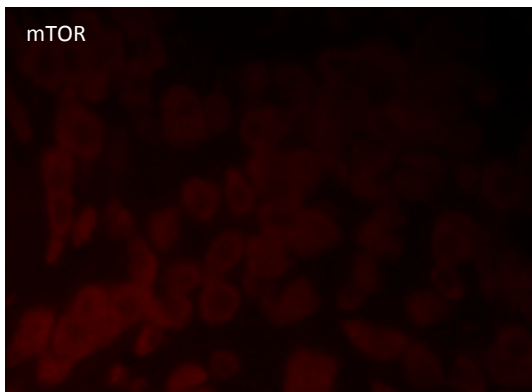
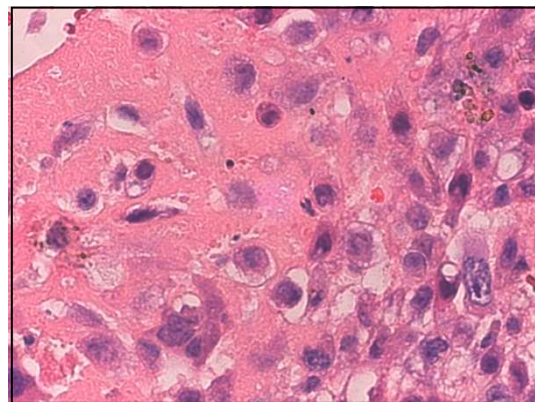


figure 45. . Immunohistochemical staining of extravillous trophoblast cells in placental tissue (decidual side) from gestational week 11 and 41. (EVT: extravillous cytotrophoblast cells, ECM: extracellular matrix)

## Chapter 4 | Discussion

### 4.1 Regulation of mTOR by Rheb in HEK293T

With the obtained constructs, functional and binding assays were carried out, to test the mutants' ability of restoring p70<sup>S6K</sup> phosphorylation upon amino acid withdrawal and their binding to mTOR and its associates, respectively. Results of the functional properties of Rheb mutants will be discussed in the next paragraph (see 4.1.1). However, the analysis of Rheb mutant binding by the chosen experimental design failed. Difficulties were encountered in achieving uniform expression of the GST-tagged constructs within the assay. Therefore, a modified *in vitro* binding assay was performed later on which will be discussed among other approaches in paragraph 4.1.2.

#### 4.1.1 Severe loss-of-function for Rheb switch 1 and 2 mutants

It was found that there are five Rheb mutants, with comparable expression levels, which were unable to rescue p70<sup>S6K</sup> phosphorylation when deprived from amino acids and thus, deficient in function. Interestingly, these mutants contain the mutations close to the switch regions which is not unexpected since the importance of these regions is already known. Switch 1 contains the activation loop and undergoes conformational changes during the GTP/GDP cycle. Switch 2 is the nucleotide binding domain and unlike in other GTPases switch 2 maintains a rather stable conformation [61].

The mutation sites or mutated residues of two of the loss-of-function mutations are located adjacent or within the switch 1 region, whereas the other three mutation sites of loss-of-function mutants are part of the switch 2 region. The mutants (67, 69) and (76, 77) are flanking the short helix (residues 72-74) in switch 2. The mutant (72, 74) was created due to a mistake during primer design, changing amino residue 74 instead of 73. Amino residue 74 is actually predicted to be solvent-inaccessible. Strikingly, unlike the "correct" (72, 73) Rheb mutant the (72, 74) mutant is unable to restore mTOR activity as published by Long *et al.* 2007 [97].

Also some mutants showed ambiguity concerning their ability to rescue p70<sup>S6K</sup> phosphorylation among two independently performed experiments. A verification of conditions is therefore necessary to ensure reproducibility. It is also noteworthy, as it was seen by double bands for the assays of functional analysis, that both S6K isomers were affected by amino acid withdrawal-induced dephosphorylation. This suggests that *in vitro* mTOR kinase activity also comprises phosphorylation of the PI3K subunit p85<sup>S6K</sup>.

#### 4.1.2 The Rheb switch 2 segment is critical for mTORC1

*In reference to the published paper of Long et al. 2007 [97], it follows a discussion of additional results ensuing the scientific residence since results presented in this work are part of the article and the further published data are supplementing and supportive for conclusions and discussion of this study.*

Long *et al.* 2007 showed that by creating a set of Rheb mutants (based on the presented work) and with some additional mutants, Rheb mutants with mutations within the switch region 2 are more severe in the loss of function than those with mutations within the switch 1 region.

Because of the complications arising from the *in vivo* binding assay, the binding properties of the Rheb mutants were analysed by an *in vitro* approach. They could show that Rheb mutants with retained signal activity *in vivo* displayed no diminished ability to bind to mTOR or Raptor. Indeed, switch 2 mutants exhibit 2-fold greater binding than wildtype Rheb. In conclusion, Rheb loss-of-function is not attributable to a deficient mTORC1 binding. Furthermore, wildtype and switch 2 mutants were used to recover mTOR from cells and test its kinase activity *in vitro*. mTOR polypeptides which were retrieved by both switch 2 mutants exhibited nearly equal activity as mTOR retrieved with wildtype Rheb. Hence, Rheb loss-of-function can also not be explained by a deficit in enabling mTOR to acquire kinase activity. All mutants were also tested for their GTP-binding properties by purifying them and binding to radio-labelled GTP *in vitro*. None of the constructs showed moderately decreased binding compared to wildtype Rheb. Both switch 2 mutants were also analysed for their GTP charging during transient expression, and displayed an intact GTP binding. Thus, Rheb loss-of-function is also not a consequence of impaired GTP charging.

In summary, the paper emphasizes a dominant importance of Rheb switch 2 region to signal to mTORC1, which is surprising since it could already been shown that switch 1 Rheb mutants disrupt the ability of mTOR kinase rescue after amino acid deprivation [52]. Despite of the severe loss-of-function by the switch 2 mutants, it could be shown that these mutants are still able to bind GTP *in vitro* and even enhanced *in vivo*. The binding to mTOR was also undisturbed *in vitro* and *in vivo* and the retrieval of bound mTOR polypeptides to the switch 2 mutants still showed intact kinase activity *in vitro*. Hence, the hypothesis that overexpression of Rheb to overcome amino acid depletion is due to an ability of excessive GTP-charging to Rheb and thereby restoring Rheb-mTORC1 interaction by this approach could not be supported, nor was it proven to be false. It was suggested that there is a further requirement for Rheb signalling to mTORC1 *in vivo*. The putative element might operate in close proximity of mTORC1 or further upstream. The identification of this novel Rheb partner is ongoing.

When comparing the results of the discussed paper with the work presented here, it can be noted that there was an improvement of achieving reproducible and equal expression levels. Only one Rheb mutant showed very low expression explainable by protein misfolding or an unknown toxic effect. Regarding the loss-of-function mutants, there were more severe effects by the Rheb switch 1 mutants presented here. This discrepancy might be explained by the sensitivity of the used functional assay, which is only semi-quantitative.

Long *et al.* 2007 also found another loss-of-function mutant (162-165); residues 162 (arginine) and 165 (leucine) substituted with alanine (created afterwards), which is outside of both switch regions close to the C-

terminal part of Rheb. There is no further evaluation of this mutant, but it might imply an important role of the C-terminus for Rheb function. Interestingly, unlike for the other loss-of-function Rheb mutation sites which were solvent-accessible mainly in the GTP-bound Rheb or at least in both forms, both changed amino residues of the (162-165) mutant are only solvent-exposed in Rheb-GDP. That could suggest that the cycling itself from GDP- to GTP-bound form or *vice versa* plays a role in an intact Rheb signalling. This is supported by the fact that strong GTP binding *per se* does not necessarily result in functional Rheb signalling [98].

## 4.2 Role of mTOR in trophoblast invasion

### 4.2.1 Establishment of siRNA transfection in HTR8/SVneo

With the use of various transfection agents such as Oligofectamin (Invitrogen), HiPerfect (Qiagen) and Fugene (Roche) HTR8/SVneo cells were tried to be transfected with siRNA in order to silence the expression of Rheb, mTOR, Raptor and Rictor. Obtained transfection rates were poor (data not shown). By electroporation with the Microporator (PeqLab), transfection could be successfully performed. The parameters of the electroporation process were optimized in order to yield the highest transfection rate. Also the time point of optimal knockdown was verified, which depends on the half-time of target proteins and the cell type. For all targeted proteins, the best silencing effect was observed 48 h after siRNA transfection. Transfection rate upon electroporation was around 80% for all used siRNAs except for Rictor-specific siRNA which showed only a 60% reduction of expression.

Previous studies already presented siRNA-induced protein silencing in HTR8/SVneo cells but with the use of lipophile transfection agents (e.g. DHARMAfect 1 by Meade *et al.* 2007 [36]). To the best knowledge, there is no work showing siRNA transfection in this cell line by electroporation. The existence of unspecific side-effects upon siRNA transfection is well known but its mechanism is poorly understood. Sequence-dependent, unspecific effects of single siRNAs have been reported [99, 100]. A study from Pauls *et al.* 2006 showed that transfection with siRNA stimulates the innate cytokine response, leading to a secretion of IL-1 and IL-8 [101]. Thus, certain cellular functions might be affected and observed effects have to be taken with caution. Meade *et al.* 2007 observed raised levels of PAI-1 with a non-genomic control siRNA and suggested that this siRNA triggered a cytokine response as reported by Pauls and colleagues [36]. PAI-1 secretion can be modulated by IL-1, IL-6 and TNF- $\alpha$  and therefore, the observed effect can be attributed to an unspecific cytokine response. Both groups utilized transfection agents (DHARMAfect 1, Lipofectamin). The question arises whether those effects are solely due to siRNA or also caused by the chosen transfection method. Electroporation is recommended as a good alternative to the commonly used transfection agents and stated to transfect so-called "hard-to-transfect" or primary cells with high cell survival rate. Only little is known about side-effects upon electroporation of eukaryotic cells and it remains to be careful when interpreting data of knockdown experiments.



#### 4.2.2 Rapamycin inhibits proliferation and apoptosis whereas mTOR knockdown promotes apoptosis

In this work a major impact on proliferative activity on HTR8/SVneo without inducing apoptosis upon Rapamycin treatment was observed. Rapamycin as a specific mTOR inhibitor has already been known to decrease cell proliferation. This effect makes it besides its immune-suppressive potential also an interesting target for anti-cancer therapy. Treating patients after transplantation with inhibitors of mTOR showed a lower risk of the development of malignancies than those receiving a calcineurin inhibitor-based immunosuppressant [102]. Here, we observed also that the proliferation rate was different upon Rapamycin in the absence of serum whereas the apoptotic rate was similar between acute and prolonged Rapamycin treatment and also showed no impact of serum availability. Prolonged treatment with Rapamycin increased proliferation in respect to acute exposure. It seems possible that longer Rapamycin-exposure changed the equilibrium of both mTOR complexes towards mTORC2 which in turn led to the negative feedback loop via Akt [71]. Activation of Akt will trigger survival signals independently from the mTOR pathway through inactivation of pro-apoptotic factors such as forkhead transcription factor FOXO and apoptosis regulator BAD [103]. Even though mTORC2 is generally considered to be Rapamycin-insensitive, Sarbassov *et al.* 2006 showed that prolonged treatment disturbs the assembly of the complex with newly expressed proteins [72]. Hence, the negative feedback loop should be abolished upon longer Rapamycin treatment, but it is also likely that the chosen exposure of Rapamycin for 24 h was not long enough in the chosen experimental design to completely rule out this pathway.

Nevertheless, the results hint that inhibition of PI3K rather than of Akt overcomes this feedback since the discrepancy in proliferation rate between acute and prolonged Rapamycin treatment seemed to be abolished. Either used inhibitors are not exclusively specific to their intended targets or the feedback is indeed transmitted via PI3K. It was reported by Vanhaesebroeck *et al.* 1999 that the PI3K inhibitor LY294002 also inhibits mTOR [104]. Thus, it is also possible that LY294002 might just balance out the equilibrium of both mTOR complexes, which is favourable towards mTORC2 upon Rapamycin.

Results of transfected cells undergoing Rapamycin treatment are hard to interpret in regard to overcome the divergence in proliferative activity by acute and prolonged Rapamycin exposure. It seems that knockdown of Rheb, mTOR, Raptor and Rictor could slightly reverse the effect. It also seems plausible that not a single molecule alone within the mTOR pathway determines the direction towards pro-survival or pro-apoptotic signals. The complex interplay of the signal cascades may have led to the observed effects for all performed knockdowns.

It has been reported that mTOR inhibition by Rapamycin induces or facilitates apoptosis in several cell lines [87, 105, 106]. Strikingly, here we observed that Rapamycin could even slightly decrease the apoptotic rate regardless of the exposure time. Yet another study showed by knockdown experiments that the mTORC1-component PRAS40 and mTORC2-component PRR5L regulate apoptosis, and interestingly they also failed to observe Rapamycin-induced apoptosis [107]. PRAS40 is a substrate and inhibitor of mTORC1 and binds to mTOR via Raptor through its TOS motif [108] and upon Rapamycin treatment, PRAS40 dissociates from mTOR

and Raptor [107]. Thedieck *et al.* 2007 suggested that PRAS40 exerts its pro-apoptotic function by binding through another Rapamycin-insensitive molecule [107]. Meanwhile, PRR5L is proposed to promote apoptosis when mTOR is hyperactive which is in contrast to a study from Edinger *et al.* 2004 who observed that constitutively active mTOR reduces apoptosis [48].

Results of this work revealed a high impact on apoptosis when mTOR expression was knocked down whereas silencing of Rheb, Raptor and Rictor expression showed only little effects. SiRNA-induced inhibition of mTOR expression led to a high apoptosis rate which was reflected also in the lower proliferation rate. Proliferation rate was slightly reduced upon Rheb, Raptor and Rictor knockdown, but upon withdrawal of serum proliferation was decreased to a higher extent. Apoptosis rate also increased dramatically in transfected cells when serum was not accessible probably due the transfection procedure itself which may render the cells more susceptible to apoptosis induction. However, these results suggest a higher sensitivity to nutrient availability in terms of proliferative capacity as well as apoptosis induction when the mTOR pathway is disturbed at distinct points. It also supports the idea that both mTOR complexes contribute to the regulation of apoptosis [107] since there could be no difference seen in knockdown of components of either complex. It is also noteworthy to mention that Raptor knockdown tendentially inhibited apoptosis induction in the presence of serum. Thedieck *et al.* 2007 showed that knockdown of Raptor resulted in a decreased association of PRAS40 with mTOR [107]. Thus, one could speculate that PRAS40 promotes apoptosis dependently on mTOR association. This association may be enhanced again by lack of nutrients since upon serum starvation Raptor knockdown showed no more any protective effect on apoptosis induction. As it was mentioned before, upon Rapamycin treatment PRAS40 dissociates from Raptor and mTOR and was shown to have anti-apoptotic potential, supporting the hypothesis, that PRAS40-mediated apoptosis is mTOR-dependent.

Also it is speculative whether the observed phenotypical changes upon mTOR knockdown are due to the higher apoptosis rate or if they indeed derive from structural alterations. It could be assumed that the disruption of mTORC2 by the mTOR knockdown is the cause for the loss of filopodia development since it was described to act on the organization of the cytoskeleton [45].

Overall, there seems to be a delicate balance of mTOR-mediated and -dependent signals which predispose the cells towards apoptosis induction [107]. Additionally, there is a discrepancy of obtained results between inhibition of the mTOR signalling either by use of Rapamycin and inhibition by silencing of crucial signal molecules within the mTOR pathway. Hence, chemical inhibitors of signal molecules seem to provoke a different outcome than siRNA-induced silencing of these molecules. Consequently, the intended comparison of acute Rapamycin treatment with Raptor knockdown and of prolonged Rapamycin treatment with Rictor knockdown was not feasible since the physiological context is naturally more complex.

#### 4.2.3 Role of mTOR signalling in trophoblast invasion through uPA and PAI-1 secretion

Several studies could link p70<sup>S6K</sup> phosphorylation with cell motility [109, 110]. It was demonstrated that upon stimulation with IGF-II, arginine and serum stimulates migration of intestinal cells and that the consequently phosphorylated p70<sup>S6K</sup> distributes to the cell periphery [111]. Berven *et al.* 2000 showed a co-localization of p70<sup>S6K</sup> with actin [112]. This suggests a role of p70<sup>S6K</sup> in cell migration on a structural level. It was reported by Liu *et al.* 2006 that knockdown of Raptor as well as Rictor reduced motility [110]. Rictor is part of the mTOR complex 2 which is generally known to be involved in reorganization of the actin cytoskeleton [45]. Hence, both complexes regulate the migrative potential of the cell.

There are only a few reports that address mTOR signalling in respect to cell invasion. Martin *et al.* 2003 proposed that the triggering of mTOR by exogenous amino acids which is crucial for trophoblast outgrowth is only critical in the implantation window and later on has no or minor effects on trophoblast invasion in mice [93]. Nevertheless, the work by Zhou *et al.* 2006 showed that there is a link between mTOR signalling and cell invasiveness, although it was observed in human ovarian cancer cells [113]. They report that upon HGF stimulation, MMP9 secretion and invasion was mediated through p70<sup>S6K</sup> phosphorylation.

Here, we could show that Rapamycin reduced the invasiveness of HTR8/SVneo, which was even more pronounced when serum was not present. For mTOR siRNA-transfected cells, also a dramatic decrease was observed in the *in vitro* invasion although this effect might be attributed to the observed lower proliferation rate due to enhancement of apoptosis. Strikingly, with knockdown of Raptor and Rictor, a slight increase and no effect, respectively, on invasiveness were detected even though proliferation rate was mildly reduced for both. This would imply that mTOR-mediated cell invasion is independent of Raptor and Rictor. So far, there have been no reports which revealed mTOR function unrelated to its two described complexes. Another explanation for the little effects on invasiveness upon Raptor and Rictor knockdown might be that there is a complementary mechanism between both molecules. It should also be considered that transfection efficiency and rate may have not been sufficient to induce or monitor effects of Raptor and Rictor knockdown. Silencing of mTOR expression might have had a greater impact, since both complexes are disrupted. The idea that only disruption of both complexes interferes with cell invasiveness is supported by the observation that simultaneous silencing of Raptor and Rictor decreased *in vitro* invasion about 30% to 40% (data not shown).

Inhibition of invasion was not further enhanced by prolonged Rapamycin exposure. Thus, one could argue that trophoblast invasion is predominantly regulated via mTORC1 which is acutely Rapamycin-sensitive. This idea is supported by the fact that Raptor knockdown also resulted in a diminished level of secreted uPA but strikingly did not result in lower invasiveness. In contrast to mTOR knockdown, Rheb knockdown displayed higher uPA and PAI-1 level. There might be another interaction partner downstream of Rheb and upstream of mTOR which acts as an inhibitor which would explain the reverse outcome on uPA and PAI-1 secretion. It remains to be determined if this putative molecule is PRAS40.

The invasion of cells is mainly characterized by the secretion of enzymes that degrade the extra-cellular matrix (ECM). Those enzymes comprise matrix-metalloproteases (MMPs) and the urokinase-like plasminogen activator

(uPA) system. The regulation of trophoblast implantation and vascular remodelling was reported to be dependent on the plasminogen activators and their inhibitors [114, 115] and uPA to be a key molecule in the cell-associated degradation of extracellular matrix during invasive growth of trophoblast cells [116]. MMP2 and MMP9 are known to be key regulators of trophoblast invasion and shown to be differentially expressed during pregnancy: MMP2 activity is predominant in gestational week 6 to 8, whereas MMP9 is preferentially secreted in gestational week 9 to 12 [27]. We could observe that the HTR8/SVneo cell line predominantly exhibited MMP2 activity. It was not further specified by Graham *et al.* 1993 from which exact time point in the first trimester of pregnancy the trophoblast cells were isolated to be immortalized and established as a cell line [37]. But it seems likely by the predominant MMP2 secretion that trophoblast originated from early rather than late first-trimester trophoblasts.

It was observed that MMP9 and MMP2 activity was remarkably, and also to the same extent, reduced upon lack of serum. The secretion of uPA was not affected by serum availability, although there was a great variability observed. Rapamycin could strongly reduce uPA, MMP9 and MMP2 activity but only when exposed short-time and in the absence of serum. Hence, additional effects that influence invasive behaviour must account for the decreased invasiveness when cells were treated with Rapamycin for a longer period of time. Knockdown of mTOR or Raptor greatly reduced uPA activity in the presence or absence of serum and showed in tendency to also reduce MMP9 and MMP2. Rheb knockdown showed interestingly an increase in uPA secretion but only when serum was available. Whether the observed decrease of MMP2, MMP9 and uPA secretion accounts for the reduction of invasion when mTOR is knocked down is speculative. Raptor knockdown which also showed impaired secretion of the matrix-degrading enzymes did not exhibit lower invasiveness, suggesting a minor role of these enzymes towards invasion or underlining the before-mentioned effect of apoptosis on the outcome of observed invasion. The used Matrigel mainly contains laminin, collagen IV, heparan sulphate proteoglycans, entactin and nidogen (datasheet of BD Biosciences). Collagen IV is a classical substrate for MMP2 and -9. UPA converts plasminogen in plasmin which, next to its function in fibrinolysis, was shown to be able to degrade laminin 322 [117] and activate MMP2 and -9 [28]. It is likely that other enzymes may also contribute to the invasiveness of the HTR8/SVneo.

Liu *et al.* 2003 showed that uPA stimulates trophoblast migration by using phospholipase C, PI3K and mitogen-activated protein kinase (MAPK) [118]. This study however did not subject an inhibitor of mTOR to the survey but since PI3K is upstream of mTOR it is supportive to the findings presented here. Interestingly, there are recent reports that link the uPA-system to cell proliferation and apoptosis through activation and release of certain growth factor and the dynamic control of cell-matrix interactions [119].

The detected effect on uPA secretion raised the question whether its major inhibitor PAI-1 is also affected by inhibition of mTOR. PAI-1 is the major inhibitor of the plasminogen activator system and prevents excessive matrix destruction by inhibiting the catalytic activity of uPA and thus plasminogen activation [120]. In previous studies, it was already demonstrated that invasiveness of HTR8/SVneo is impaired through reduced uPA and increased PAI-1 secretion which was induced by co-culture with macrophages or incubation with TNF- $\alpha$  [121, 122]. Hu *et al.* 1999 demonstrated in human placenta that PAI-1 is mainly detected in extra-villous and invasive

trophoblasts whereas PAI-2 was found in the syncytiotrophoblasts [33]. HTR8/SVneo cell line is derived from extra-villous trophoblast cells, thus the discovery that HTR8/SVneo cells secrete PAI-1 is not unexpected.

PAI-1 expression as well as its secretion was examined. Preliminary results on PAI-1 secretion revealed an increase of PAI-1 level in response to Rapamycin by Western blot (on conditioned media) whereas the ELISA showed a decrease of PAI-1 level (on conditioned media). This discrepancy can be explained by the reduction of the proliferation rate by Rapamycin which is not taken into account by the ELISA measurement whereas for the Western blot with cell-conditioned media, the protein-concentration was accordingly adjusted. However, we looked at the PAI-1 expression by immunocytochemistry and Western blot (on cell lysates). Western blot with cell-conditioned media without the presence of serum showed no secretion of PAI-1 whatsoever. The used antibody was not favourable for detecting PAI-1 by Western blot, nonetheless it could be seen that there is PAI-1 expression but at a lower level when serum was absent than with presence of serum. Western blot also revealed a slight increase in PAI-1 expression upon Rapamycin treatment when serum was present. The immunocytochemical staining of intracellular PAI-1 also supported the idea that Rapamycin increases PAI-1 levels, at least for the condition under serum accessibility. This finding is in contrast to the work of Pontrelli *et al.* 2008 who observed that Rapamycin reduced PAI-1 expression in proximal tubular epithelial cells [123].

PAI-1 levels in supernatants detected by ELISA of transfected cells showed that there was a strong decrease in secreted PAI-1 level for mTOR knockdown and a minor increase for Rheb knockdown. The decrease in PAI-1 level for mTOR as well as the slight decrease for Raptor and Rictor knockdown correlated with the proliferation rate. It is unclear whether and how PAI-1 accumulates in the media which is determined by its degradation time course. Nevertheless, for Rheb knockdown proliferation rate is not reflected in PAI-1 level since even though there is a decreased proliferation, the level of secreted PAI-1 was raised. Interestingly, the increase of PAI-1 upon Rheb knockdown is associated with an increase also of secreted uPA level. It is also to note that serum availability affects PAI-1 level whereas it has no major effect on the uPA level. This suggests that the regulation of the secretion of PAI-1 and uPA is not necessarily connected with each other but may engage distinct mechanisms; a nutrient-sensitive and a nutrient-insensitive one, respectively. This does not rule out, that those mechanisms interact at some point.

A high level of PAI-1 is known to be a bad prognosis marker in breast cancer [124, 125]. This aspect is a consequence of the dual role of PAI-1. Independently from its characteristic to inhibit uPA activity and thereby invasion through degradation of plasmin and ECM, it also is involved in the detachment of cells from the ECM [126]. This feature is controversial by promoting cell migration and invasion. Planus *et al.* 1997 demonstrated that PAI-1 mediates cell adhesion and spreading and thereby suggesting a mechanism of the dual role of PAI-1 [34]. Increasing levels of PAI-1 after Rapamycin exposure with parallel decrease of invasiveness were found which suggests that, at least in terms of mTOR-mediated signalling, PAI-1 exerts anti-invasive potential in the HTR8/SVneo cells. This finding does not exclude that PAI-1 which is mainly expressed by the invasive type of trophoblasts is required for progression of the invasion process of trophoblast cells *in vivo*.

#### 4.2.4 Cross-talk between mTOR and Stat3 signalling in trophoblast cells

Stat3 is known to be an important signal molecule in order to activate transcription of target genes in a rapid and transient manner upon the according activation. Stat3-induced cell responses include the regulation of survival, proliferation, angiogenesis, invasion and immunosuppression. Constitutively activated Stat3 could be linked with tumourigenesis [127].

Stat3 has two phosphorylation sites, Tyr<sup>705</sup> and Ser<sup>727</sup>. Whereas the role of the tyrosine phosphorylation is well established, it is still somewhat controversial whether the serine phosphorylation has a positive or negative role in the transcriptional activation. The majority of data suggests that the serine phosphorylation leads to a maximal activation of transcription presumably by enhanced recruitment of necessary transcriptional cofactors [79]. Stat3 is also crucial in embryogenesis since it was shown that ablation of Stat3 resulted in early embryonic lethality in mice [128].

To the best knowledge, for the first time the presence of a cross-talk between mTOR and Stat3 in human trophoblast cells is presented with this work. As shown before in a neuroblastoma [77] and hepatocyte carcinoma cell line [129] upon IL-6 stimulation, mTOR phosphorylates Stat3 at the serine residue position 727 (Ser<sup>727</sup>). This finding gave rise to the proposal that mTOR-mediated serine phosphorylation leads together with the Tyr<sup>705</sup> phosphorylation to a maximal transcriptional active Stat3.

Silencing mTOR protein expression by siRNA abolished Stat3 serine phosphorylation in HTR8/SVneo cells whereas tyrosine phosphorylation was only slightly affected by all used siRNAs. The withdrawal of serum had no effect on serine phosphorylation suggesting a basal mTOR kinase activity towards Stat3 regardless of nutrient availability. The knockdown of Raptor and Rictor gave no clue about whether serine phosphorylation is mTORC1 or mTORC2-mediated. Surprisingly, Rapamycin treatment affected serine phosphorylation only upon acute exposure indicating a negative feedback induction by prolonged Rapamycin incubation. This was already considered for the differential outcome on proliferation rate and enzyme secretion. It is tempting to speculate that this cross-talk toward Stat3 may be responsible for the distinct effects upon Rapamycin but it might be rather an effect than the cause.

The benefit of this cross-talk in trophoblast cells is elusive but it could be speculated as a back-up or counterbalance signalling. Interestingly, similar to mTOR, it was hypothesized that Stat3 is involved in the nutritional process supporting the implanting blastocyst [130]. Furthermore, it was shown that target genes of Stat3 are MMP2 [131] and MMP9 [132]. Although, in our laboratory the analysis of the choriocarcinoma cell line JEG-3 whose tyrosine phosphorylation and DNA-binding capacity as well as invasiveness was strongly increased upon leukaemia inhibitory factor (LIF) showed no induction of MMP2 and -9 expression but increased expression of TIMP1 and caspase 4 [96]. In addition, LIF, which was shown to be an important cytokine during pregnancy by regulating proteinase activity in early embryos [133], belongs to the IL-6 family and therefore employs the same receptors as IL-6 which was already mentioned to induce mTOR-mediated Stat3 serine phosphorylation. Little is known whether LIF stimulates mTOR activity but it was already shown that LIF activates PI3K which is upstream of mTOR [134].

#### 4.2.5 No differential expression of mTOR in human first-trimester and term placenta

A recent study by Roos *et al.* 2007 revealed for the first time that mTOR is localized in the transporting epithelium of term placenta [95]. They could also correlate a reduced level of phosphorylated p70<sup>S6K</sup> with intra-uterine growth restriction and therefore proposed mTOR as a placental nutrient sensor. Earlier reports demonstrated already in mice an essential role of mTOR in embryogenesis and trophoblast outgrowth [7, 91]. It was also shown that mTOR is crucial in the implantation window for the transport of exogenous amino acids, particularly leucine and arginine [93, 94].

In this work, we could show localization of mTOR in term as well as in first-trimester placenta (obtained from selective abortion). At both time points, mTOR is expressed in extra-villous trophoblast (EVTs) cells and in the syncytiotrophoblast layer. EVT's display an invasive phenotype and infiltrate and remodel the maternal tissue whereas syncytiotrophoblast cells are non-invasive and are in direct contact with the maternal blood. Both trophoblast types lack any proliferative capacity and are derived from cytotrophoblast cells, which showed low mTOR expression. Hence, along with trophoblast cell differentiation mTOR expression might be enhanced to acquire motility and invasive potential as for EVT's or in the case of the syncytial trophoblasts to gain the capability of endocrine and metabolic exchanges between the mother and the foetus. The latter feature might be achieved through the regulation of amino acid transport systems as demonstrated to be under control of mTOR during implantation in mice [93, 94] and in humans [95]. Since both trophoblast types are terminal differentiated and thus non-proliferative, mTOR is unlikely to play a role in cell cycle progression.

Interestingly, in our laboratory it was found that elevated serine phosphorylation of Stat3 is also localized in the extra-villous and syncytial trophoblast cell of first-trimester and term placenta whereas the tyrosine phosphorylation is not (unpublished observation). This finding underlines the importance of the serine phosphorylation and supports the idea of mTOR regulating Stat3.

### 4.3 Model: Role of mTOR regulation in human reproduction

Findings of this study confirm that mTOR plays a role in human pregnancy. We further propose that mTOR acts not solely as a nutrient sensor but also regulates trophoblast invasion as it was already reported for the murine model. The current knowledge and conclusions drawn from the presented work are portrayed in a simplified schematic presentation of the implanting blastocyst and the foeto-maternal interface in figure 46.

As already mentioned, in mice it was demonstrated that mTOR is critical for implantation as it regulates transporters for the required exogenous amino acids [94] and is also important for trophoblast outgrowth [7, 94]. So far, in the human placenta it has been described that mTOR is a nutrient sensor but its role in the invasion process is largely unknown. It can be proposed that mTOR is also involved in the invasiveness of extra-villous trophoblast cells by regulating the secretion of uPA and PAI-1. mTOR enhances the secretion of uPA and diminishes the secretion of its major physiological inhibitor PAI-1 which promotes cell invasion.

The distinct functions of mTOR may be regulated by various extra- as well as intracellular signals. A difference in cell responses depending on the availability of serum (such as the decrease in uPA activity upon acute Rapamycin treatment) was observed. Fetal bovine serum (FBS) is the most widely used growth supplement for cell culture media. FBS is rich in embryonic growth-promoting factors including growth factors, hormones, attachment and spreading factors, binding proteins, lipids and minerals. It is a complex mixture of many defined and undefined components with different, physiologically balanced growth-promoting and growth-inhibiting activities (Sigma product information). Therefore it is not possible to further characterize the component which is responsible for the observed effects. Since mTOR is well-known to be a nutrient sensor, one could speculate that nutrients account for the reported effects upon mTOR inhibition. One could further hypothesize that the availability of certain factors determines whether mTOR signals aim towards a metabolic response such as the activation of nutrient transporters or towards the induction of invasiveness.

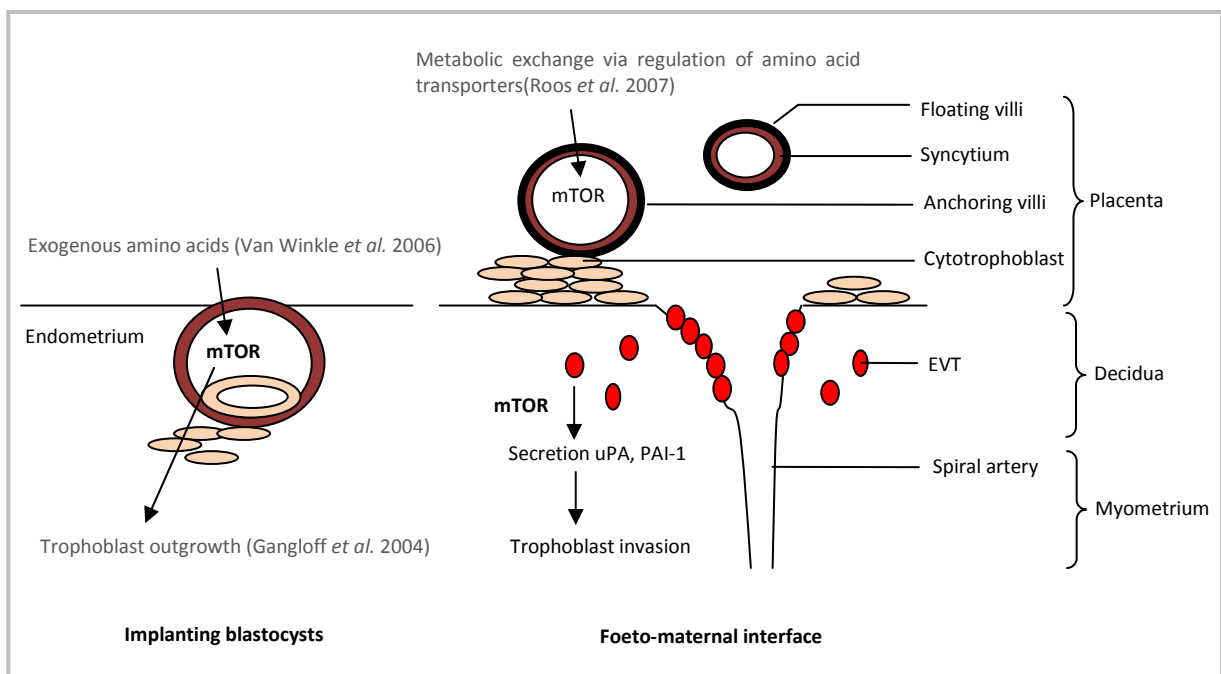


figure 46. Schematic presentation of the role of mTOR during pregnancy in the reproductive tract. Left panel depicts current knowledge of mTOR regulation in murine blastocyst implantation (according literature is indicated (gray)). Right panel shows proposed involvement of mTOR in syncytial and extra-villous trophoblast cells. Bold black circled cells represent cells with elevated mTOR level according to the result of immunohistochemical analysis and according knowledge of mTOR as nutrient sensor (according literature is indicated (gray)). (EVT: extra-villous trophoblasts (red), cytotrophoblasts (pink), syncytium (brown))

In figure 47 the hypothesis of how mTOR regulates different cell responses in a nutrient-dependent manner is schematically depicted. It is tempting to speculate that successful blastocyst implantation is a consequential outcome when the essential nutrients and amino acids are available. Once the embryo is implanted, there might be a lack of nutrients or amino acids in the surrounding tissue and cells start to become invasive.



The lack of nutrients interferes with Rheb activation [52] and may also lead to a change of the balance of both mTOR complexes. The involvement of other signalling molecules, such as PRAS40, Akt and PI3K, on Rheb or mTOR function itself remains yet elusive. It is likely that there is a complex interplay between the signal molecules of the mTOR pathway possibly by negative and positive feedback loops and which is finely regulated by nutrient and amino acid availability and the intracellular energy status.

To further unravel the regulation of signalling events during pregnancy will allow us to get a deeper comprehension of the progression of pathologies such as pre-eclampsia, intra-uterine growth retardation or the development of trophoblastic moles and also of foetal abortion on a molecular basis.

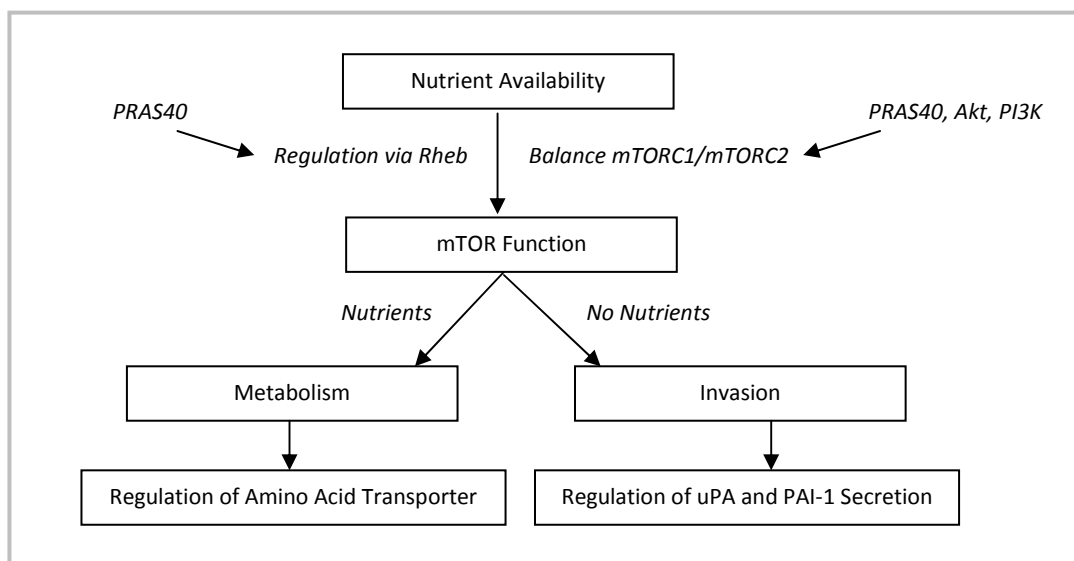


figure 47. Sketch of proposed regulation of mTOR during pregnancy by nutrient availability.

#### 4.4 Perspective

Future directions should address the role of PRAS40 in mTOR-mediated cell response. PRAS40 was initially identified as a substrate of Akt with unknown function [135]. It was then reported that it is phosphorylated by mTORC1 and is an inhibitor of mTORC1 activity [108, 136]. Oshiro *et al.* 2007 observed that amino acid withdrawal inhibited PRAS40 phosphorylation which was reversed by Rheb overexpression [64]. A putative element that binds to Rheb and is involved in regulation of mTOR activity was proposed by Long *et al.* 2007 [97] and so far it is mere speculation if this sought-for molecule is PRAS40. The question whether Rheb binds to PRAS40 and hence affects PRAS40-mediated mTOR inhibition remains to be studied.

It was also mentioned that PRAS40 might display pro-apoptotic function through binding of another Rapamycin-insensitive molecule [107]. If there is indeed an existence of Rheb-PRAS40 binding and Rheb is upstream of mTOR and not affected by Rapamycin, it seems likely that this could also be responsible in the

regulation of apoptosis through mTOR. In addition, in the presented work there was an unsuspected differential outcome on uPA and PAI-1 secretion observed for Rheb and mTOR knockdown which suggested a further interaction partner of Rheb which is upstream of mTOR and presumably acts as an inhibitor to mTOR. A candidate for this proposed molecule could also be PRAS40. Altogether, further analysis of PRAS40 should aim on its ability to bind to Rheb and to affect the regulation of apoptosis and secretion of uPA and PAI-1.

Cytotrophoblast cells as well as *in vitro* propagated EVT cells exhibited an expression of high-affinity uPA receptor (uPAR) [137] and in histochemical and ultrastructural studies demonstrated *in situ* that uPAR is highly expressed at the migration front of EVT cells [138] suggesting a role of the uPA:uPAR interaction in trophoblast migration and invasion [118]. Clinical data revealed that sera from patients with recurrent spontaneous abortions including pre-eclampsia contained antibodies which were reactive to a 62 kDa trophoblast cell surface protein that may be uPAR since these antibodies interfered with uPA:uPAR binding [139]. Therefore, a detailed knowledge of the role and the regulation of the uPA system should be relevant for understanding pregnancy-related pathologies and future studies should address whether mTOR also regulates uPAR expression.

Surprisingly, the absence of serum enhanced the expression of Rictor. It might be of interest to identify molecules which account for the inhibition of Rictor expression. It is unclear whether the nutrient-sensitive pathway via mTORC1 or some other pathway could be involved in the regulation of Rictor expression. There are speculations of how both mTOR complexes regulate each other. It was shown that mTORC1 phosphorylates Rictor and that this phosphorylation was Rapamycin-sensitive and could also be abolished upon knockdown of mTOR [140].

Elevated PAI-1 levels could be associated with pre-eclampsia [141, 142] and the lack of PAI-1 was found together with excessive decidual necrosis and fibrinoid deposition found in complete molar pregnancies, which are manifested by an uncontrolled placental invasion [35]. It is therefore of high interest to unravel the mechanisms involved in the regulation of PAI-1 expression and secretion during pregnancy. Here we used a trophoblast cell line model and even though trophoblasts are the source of secreted PAI-1, it might be beneficial to investigate primary material, particularly from pre-eclamptic patients. But it is to note, that it is hard to isolate and cultivate trophoblast cells. It is also an issue that the first-trimester trophoblasts are of higher importance since placentation is primarily sensitive in the beginning of pregnancy but pre-eclampsia develops later on from 20 weeks of gestation. Pre-eclampsia is a pregnancy-related disorder which is unique to humans [143] and the establishment of a suitable animal model is required and ongoing [144-146]. A mouse model with transferred activated Th1-like cells led to pre-eclampsia symptoms exclusively in pregnant mice in terms of clinical conditions such as hypertension, proteinuria and kidney pathology [144]. The use of this model in the context of altered protease activity has to be elucidated. Mouse models which mimic pre-eclampsia in conjunction with elevated PAI-1 levels might be a useful tool in order to further examine effects of inhibition of mTOR on placentation through regulation of the uPA system.

In general, the question of the worth of cell line models can be raised. Cell lines are immortalized cells derived from primary material and thus cell-specific features might be adverse. Here, it was observed that with the used cell line which is derived from first-trimester EVT<sub>s</sub>, that there is a major effect on proliferation upon mTOR inhibition although *in vivo* EVT<sub>s</sub> are terminal determined and possess no proliferative potential. Nevertheless, studying cellular and molecular mechanisms in human reproduction raises ethical issues and makes *in vivo* studies impossible and therefore the *in vitro* studies an indispensable necessity. Extrapolation from *in vitro* to *in vivo* situation or from animal models to human is consequently the major challenge.

## Chapter 5 | Appendix

### 5.1 Material list

#### *Special technical equipment:*

Bio-imaging system:	DNR MF-ChemiBIS 3.2
Blotting apparatus:	Whatman/Biometra Fastblot
Electrophoresis systems:	Blot-Module Mini-V8x10 (Life Technologies) PerfectBlue Vertical Electrophoresis System Model Twin S (PeqLab) MiniProtean 3 (Bio-Rad)
Electroporation device:	MicroPorator MP-100 (Digital Bio)
Flow cytometer:	FACS Calibur (Becton Dickenson Coulter)
Microplate reader:	MPR A4
Microscope:	Axiovert 25 (Zeiss) Axioplan 2 (Zeiss) with camera: AxioCam HRc (Zeiss) and fluorescence lamp: HBO 100W
PCR machine:	Mastercycler 384 (Eppendorf)
Spectrophotometer:	Cary 50 (Bio Varian)

#### *Cell lines and bacteria strains:*

HEK293T:	ATCC# CRL-11268
HTR8/SVneo:	Kind gift of Charles H. Graham (Queens University, Kingston, Canada) (explained in detail see paragraph 1.2.4 in the introduction chapter)
<i>Escherichia coli</i> :	DH5 $\alpha$ competent cells (Life technologies) (used for subcloning) XL1-Blue supercompetent cells (Stratagene) (provided with PCR kit)

*Special reagents, chemicals and other supplies:*

AssayMax Human PAI-1 ELISA Kit	AssayPro
Cell Lysis Buffer (10x)	Cell Signaling Technology
Chemiluminescent detection reagent	ECL (Amersham Pharmacia Biotech)
Enzymes:	
T4 DNA Ligase	Quick Ligation Kit (New England BioLabs)
Kpn I	Promega
BamH I	Promega
CIAP	Promega
Fetal Bovine Serum (FBS)	BioWhittaker/Cambrex
Film	Hyperfilm 18x24cm (Amersham Pharmacia Biotech)
Gel extraction kit	Marligen
Lipofectamine 2000	Invitrogen
GSH-Sepharose	GE-Healthcare
Maxiprep Kit	High Purity Plasmid Purification Maxiprep System (Marligen)
Miniprep Kit	High Purity Plasmid Purification Miniprep System (Marligen)
Molecular weight marker	PrecisionPlus Protein Standard Dual Color (Bio-Rad)
MTS proliferation assay	CellTiter 96 Aqueous One Solution (Promega)
PCR Kit	QuikChange Site-directed Mutagenesis PCR Kit (Stratagene)
Protease inhibitor cocktail tablet	Roche
Proteinase inhibitor cocktail	Sigma-Aldrich
Protein Assay	BioRad
PVDF Membrane	Hybond-ECL 30cmx3m (Amersham Pharmacia Biotech)
RPMI 1640	with L-glutamine and phenol-red (PAA)
Sepharose Beads	Sigma-Aldrich
Vectors:	
pCMV5-Flag (Flag-tag)	
pEBG (GST-tag)	

*Antibodies:*

Rabbit anti-human Stat3	Cell Signaling Technology
Rabbit anti-human Phospho-(Ser <sup>727</sup> )-Stat3	Cell Signaling Technology
Rabbit anti-human Phospho-(Tyr <sup>705</sup> )-Stat3	Cell Signaling Technology
Rabbit anti-human mTOR	Cell Signaling Technology
Rabbit anti-human Raptor	Cell Signaling Technology
Rabbit anti-human Rictor	Cell Signaling Technology
Rabbit anti-human Rheb	Cell Signaling Technology
Rabbit anti-human $\beta$ -Actin	Cell Signaling Technology
Mouse anti-human Phospho-(Thr <sup>389</sup> )-p70 <sup>S6K</sup>	Cell Signaling Technology
Mouse anti-human cleaved PARP	Cell Signaling Technology
Mouse anti-Flag M2	Sigma-Aldrich
Rabbit anti-GST	Santa Cruz Biotechnology
Goat-anti-rabbit IgG, HRP-conjugated	Cell Signaling Technology
Goat-anti-mouse IgG, HRP-conjugated	Cell Signaling Technology
Mouse anti-human PAI-1	American Diagnostics Inc.
Mouse anti-human cleaved PARP, Fluorescein-conjugated	Cell Signaling Technology

Vector map:

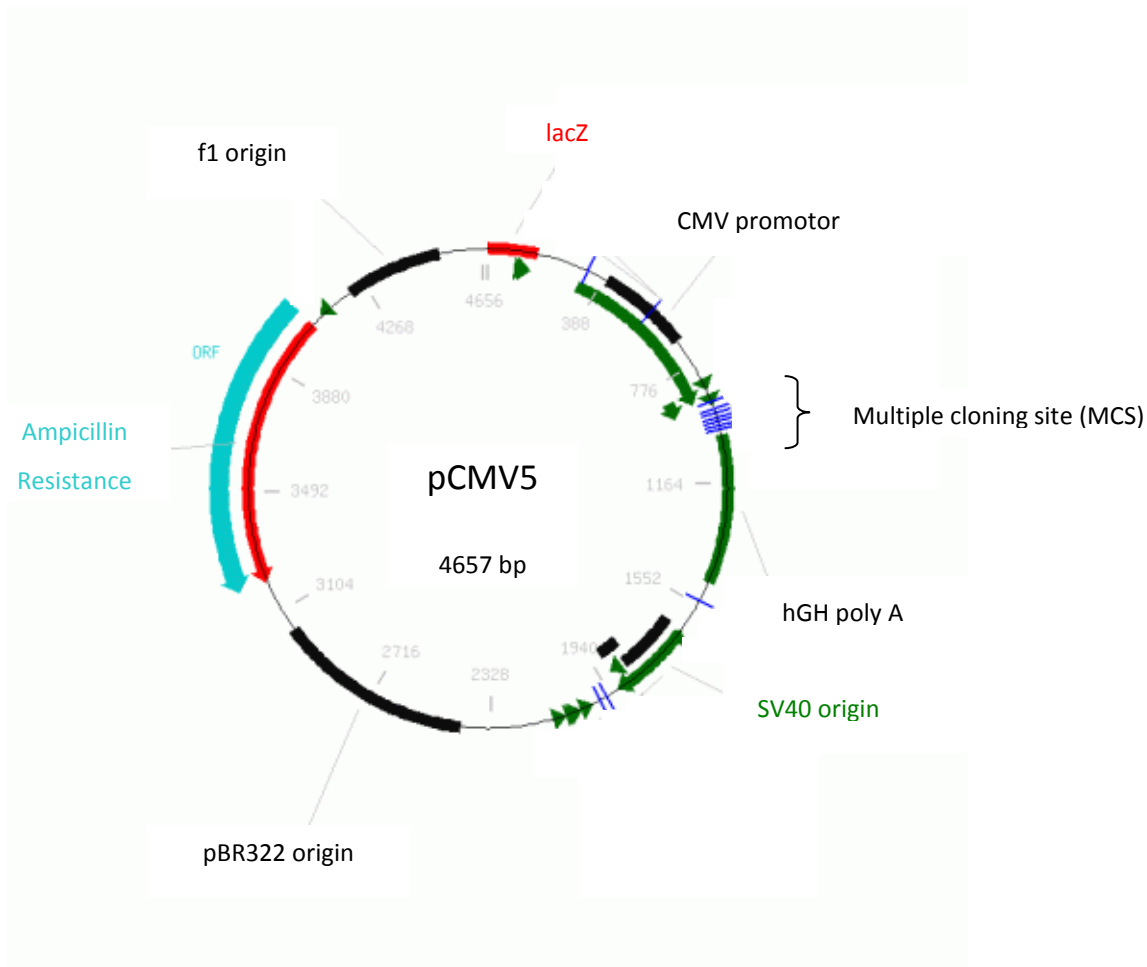


figure 48. Vector map of pCMV5-Flag (modified from Addgene). Restriction sites for insertion of Rheb wildtype or mutants are highlighted in the red rectangle. (hGH poly A: human growth hormone poly A-tail, SV40: simian virus 40, lacZ encodes b-galactosidase, f1 is a bacteriophage)

Restriction sites: 5' gca GGA / TCC cgG GT / A Cct cta 3'

┌──────────┐
┌──────────┐  
*BamH I*
*Kpn I*

Flag-Rheb junction: 5' acc ATG GAC TAC AAG GAC GAC GAT GAC AAG aat tct gca GGA TCC ATG CCG ... 3'

┌──────────────────────────────────┐
┌──────────┐  
*Flag-tag* (DYKDDDDK)
*BamH I* *Rheb1*

(ATG: start codon for methionine, A: adenosine, T: thymidine, G: guanosine, C: cytosine, D: aspartic acid, Y: tyrosine, K: lysine)

## 5.2 Supplementary densitometric analysis

Western blots:

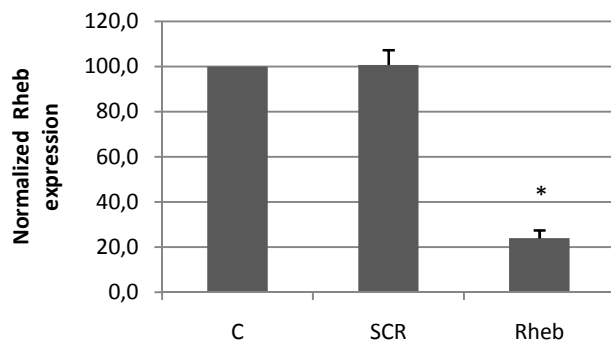


figure 49. Relative expression of Rheb, normalized to  $\beta$ -Actin, upon 0.1nmol siRNA transfection after 48h, representing two independent experiments (Student t-Test: \*  $p=0.02$ ).

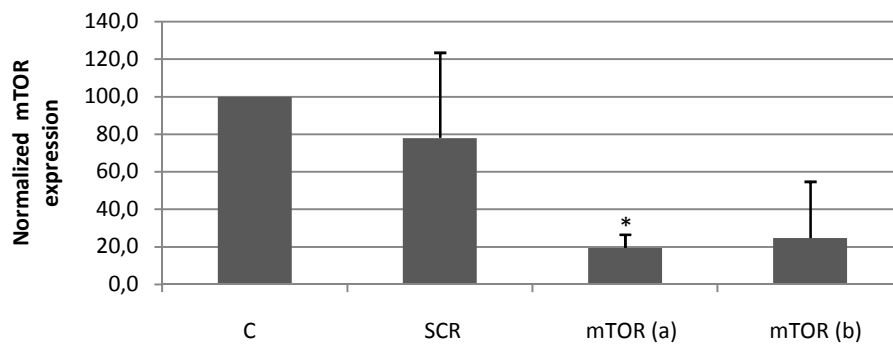


figure 50. Relative expression of mTOR, normalized to  $\beta$ -Actin, upon 0.1nmol siRNA transfection after 48h. Error bars indicate standard deviation of two independent experiments (Student t-Test: \*  $p=0.04$ ).

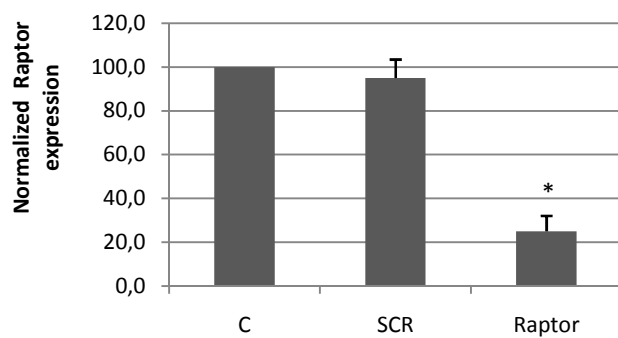


figure 51. Relative expression of Raptor, normalized to  $\beta$ -Actin, upon 0.1nmol siRNA transfection after 48h. Error bars indicate standard deviation of four independent experiments (Student t-Test: \*  $p=0.0005$ ).



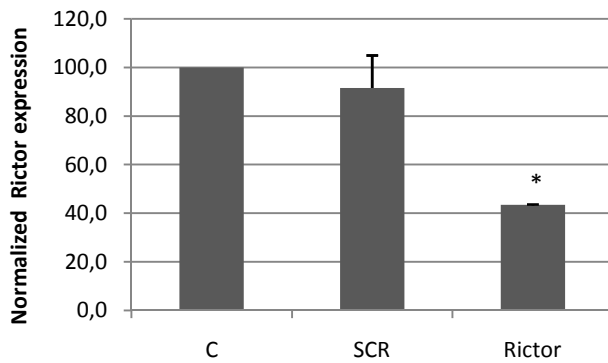


figure 52. Relative expression of Rictor, normalized to  $\beta$ -Actin, upon 0.1nmol siRNA transfection after 48h. Error bars indicate standard deviation of two independent experiments (Student t-Test: \*  $p=0.002$ ).

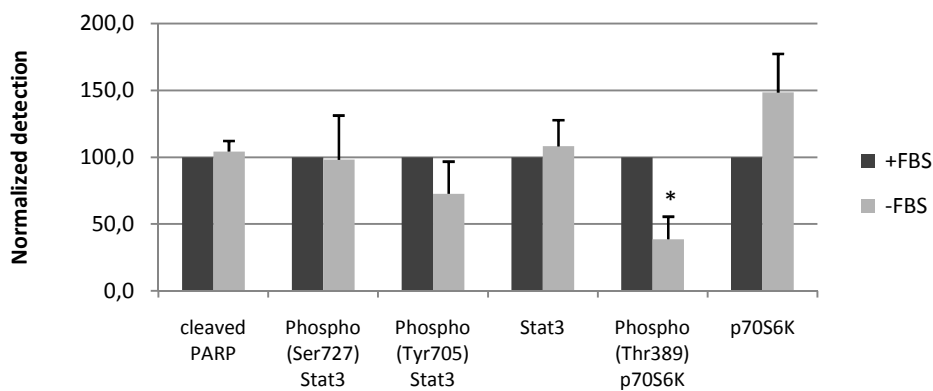


figure 53. Relative detection of cleaved PARP, phosphorylated Stat3 and  $p70^{S6K}$  and total Stat3 and  $p70^{S6K}$  expression in the presence and absence of serum. Error Bars indicate standard deviation of at least two experiments (Student t-Test: \*  $p=0.02$ ). Samples with serum supplementation were set independently as 100%.

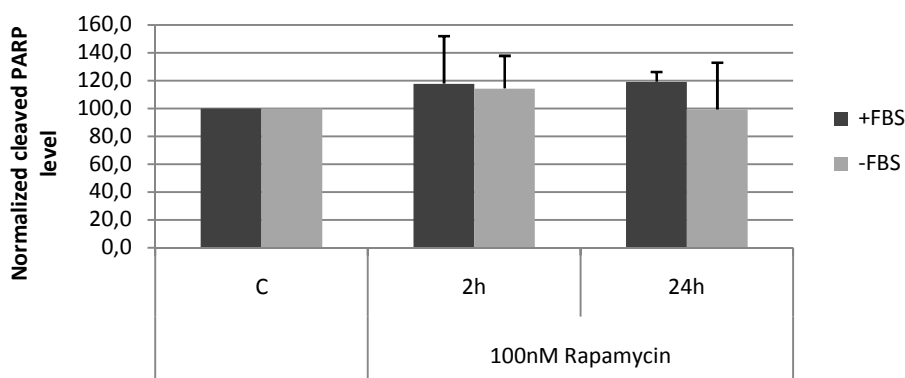


figure 54. Relative level of cleaved PARP, normalized to  $\beta$ -Actin, upon treatment with Rapamycin. Error bars indicate standard deviation of at least three experiments. Controls are set independently as 100%.

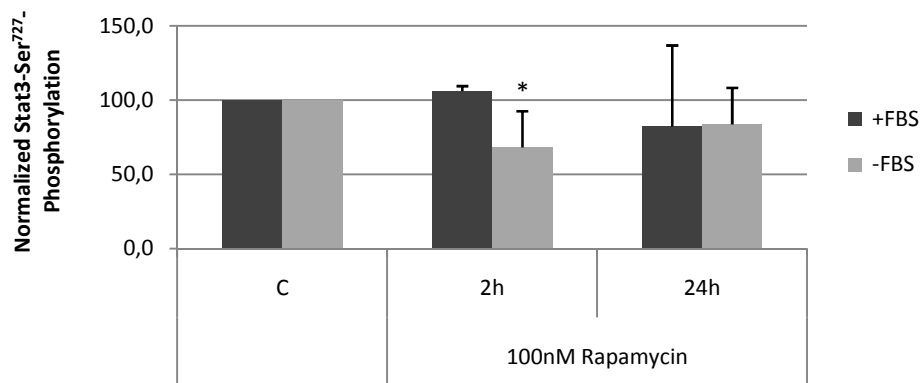


figure 55. Relative phosphorylation of Stat3 at Ser<sup>727</sup>, normalized to total Stat3 expression, upon treatment with Rapamycin. Error bars indicate standard deviation of at least four experiments (Student T-test: \* p=0.04, n=4). Controls are set independently as 100%.

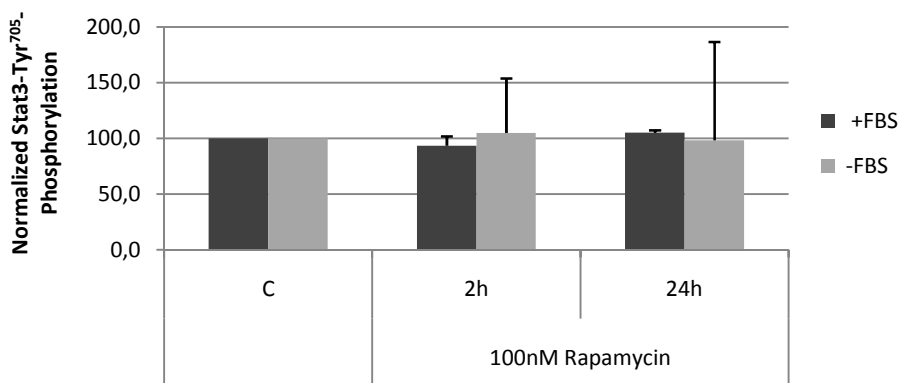


figure 56. Relative phosphorylation of Stat3 at Tyr<sup>705</sup>, normalized to total Stat3 expression, upon treatment with Rapamycin. Error bars indicate standard deviation of two independent experiments. Controls are set independently as 100%.

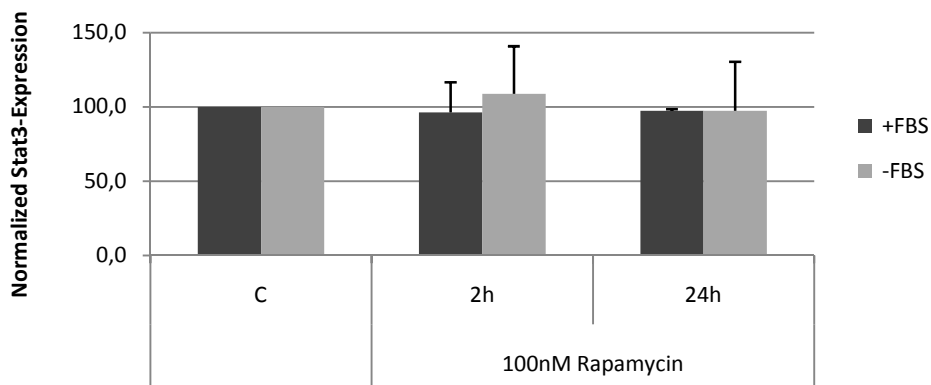


figure 57. Relative expression of Stat3, normalized to  $\beta$ -Actin, upon treatment with Rapamycin. Error bars indicate standard deviation of at least two experiments. Controls are set independently as 100%.

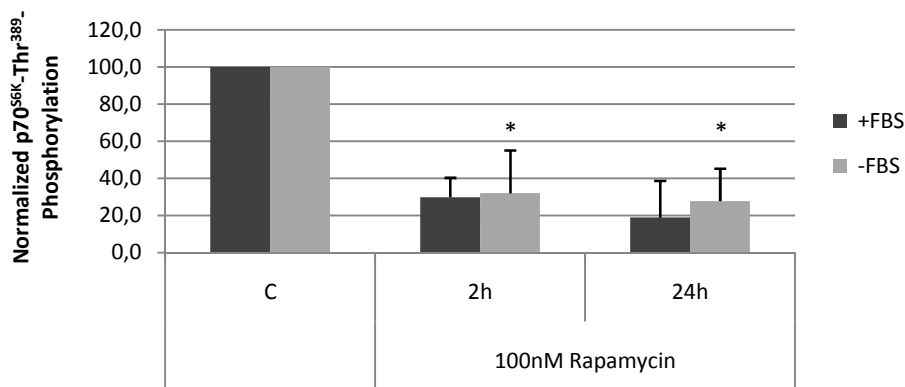


figure 58. Relative phosphorylation of  $p70^{S6K}$ , normalized to total  $p70^{S6K}$  expression, upon treatment with Rapamycin. Error bars indicate standard deviation of at least two experiments (Student T-test: \*  $p < 0.04$ ). Controls are set independently as 100%.

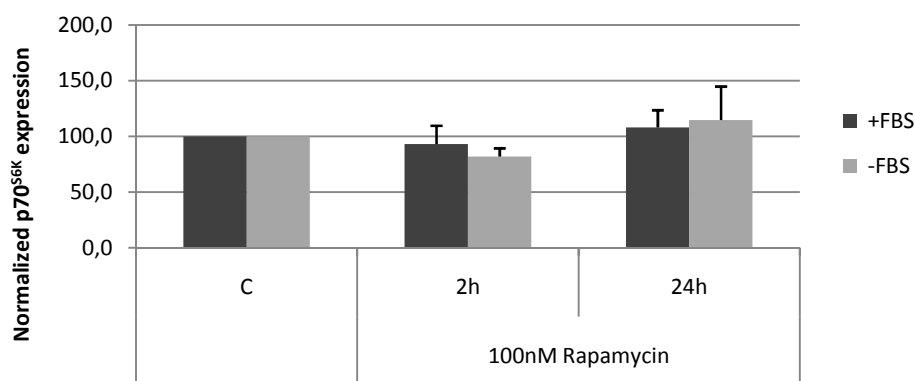


figure 59. Relative expression of  $p70^{S6K}$ , normalized to  $\beta$ -Actin, upon treatment with Rapamycin. Error bars indicate standard deviation of at least two experiments.

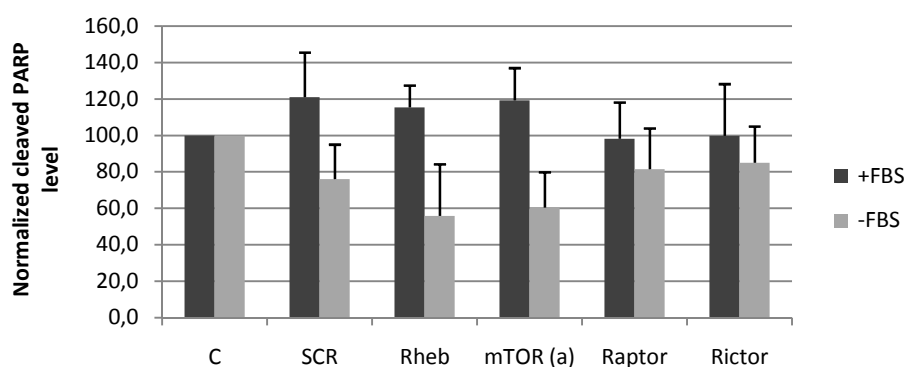


figure 60. Relative level of cleaved PARP, normalized to  $\beta$ -Actin, upon 0.1nmol siRNA transfection after 48h. Error bars indicate standard deviation of at least four independent experiments. Controls set independently as 100%.

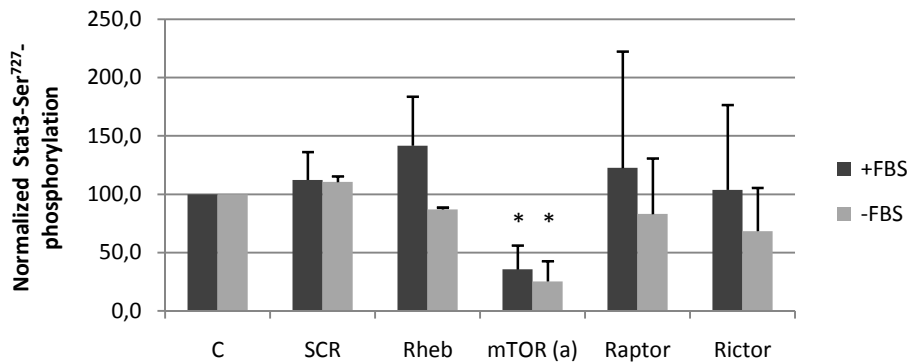


figure 61. Relative phosphorylation of Stat3 at Ser<sup>727</sup>, normalized to total Stat3 expression, upon 0.1nmol siRNA transfection. Error bars indicate standard deviation of at least two independent experiments (Student t-Test: \* p<0.05). Controls set independently as 100%.

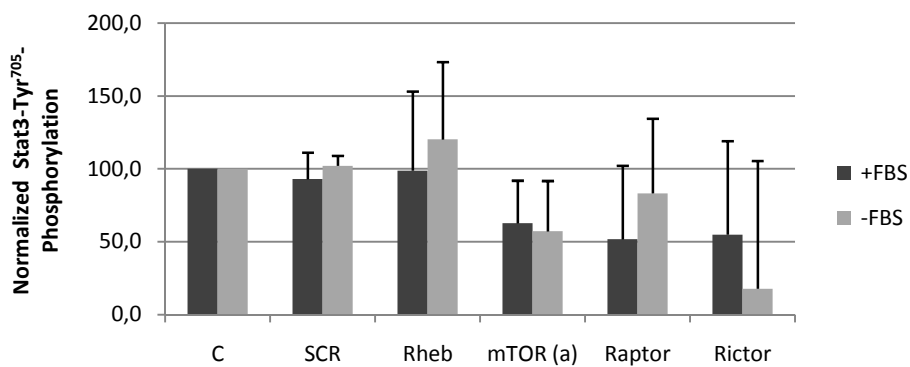


figure 62. Relative phosphorylation of Stat3 at Tyr<sup>705</sup>, normalized to total Stat3 expression, upon 0.1nmol siRNA transfection. Error bars indicate standard deviation of two independent experiments. Controls set independently as 100%.

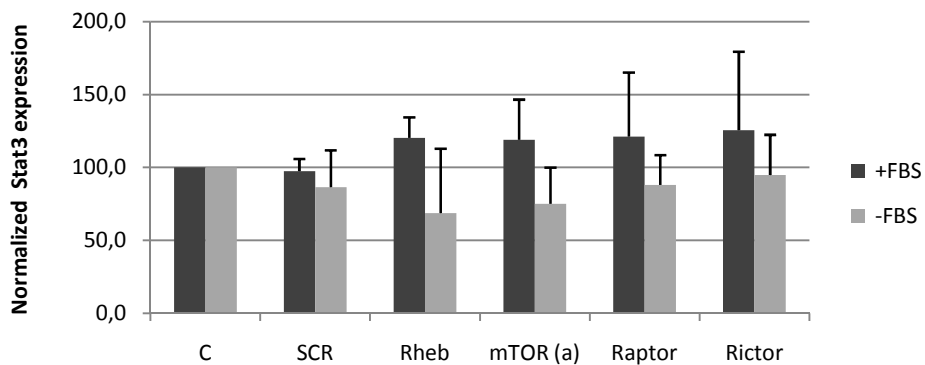


figure 63. Relative expression of Stat3, normalized to β-Actin, upon 0.1nmol siRNA transfection after 48h. Error bars indicate standard deviation of at least two independent experiments. Controls set independently as 100%.

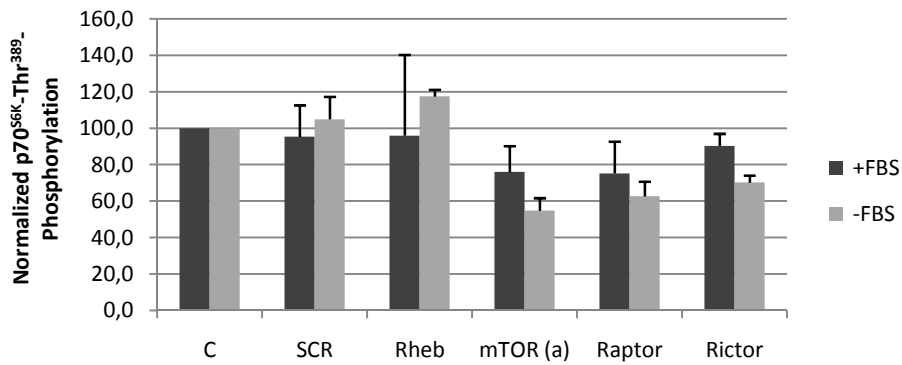


figure 64. Relative phosphorylation of p70<sup>S6K</sup> at position Thr<sup>389</sup>, normalized to total p70<sup>S6K</sup>, upon 0.1nmol siRNA transfection after 48h. Error bars indicate standard deviation of two independent experiments. Controls set independently as 100%.

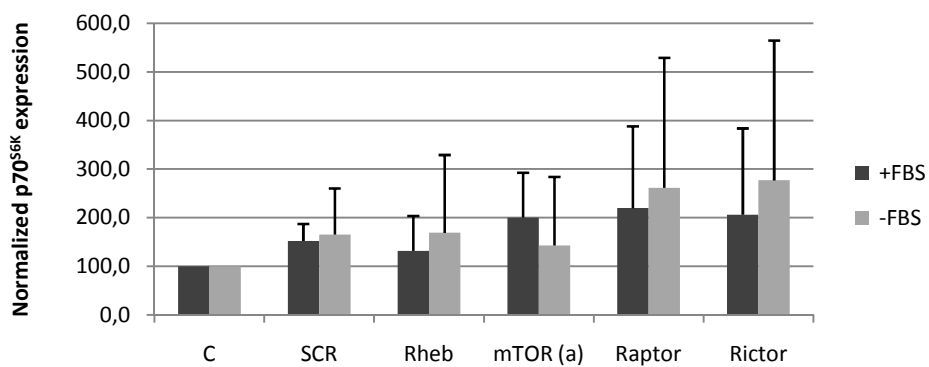


figure 65. Relative expression of p70<sup>S6K</sup>, normalized to  $\beta$ -Actin, upon 0.1nmol siRNA transfection after 48h. Error bars indicate standard deviation of two independent experiments. Controls set independently as 100%.

PAI-1 ELISA standard curve:

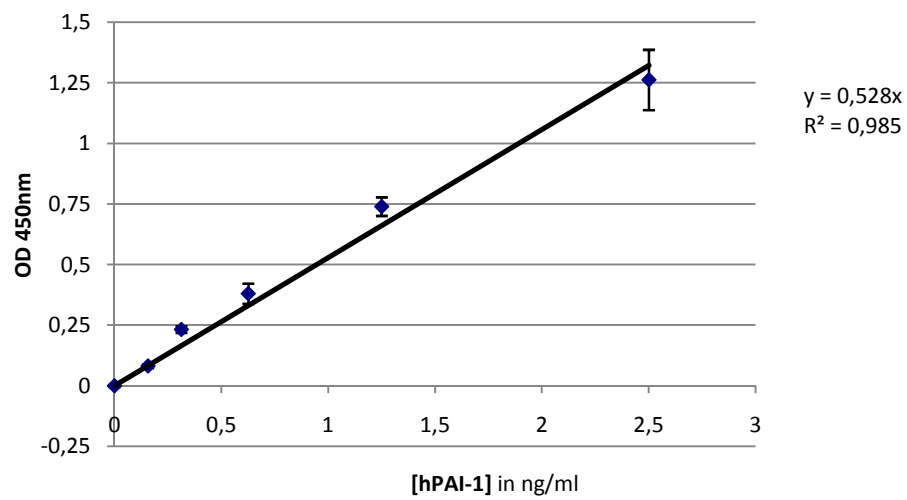


figure 66. Standard curve of known concentrations of human PAI-1 measured by ELISA. Error bars indicate standard deviation of duplicates. Equation of linear regression and coefficient of determination ( $R^2$ ) is shown in the diagram.

Zymography:

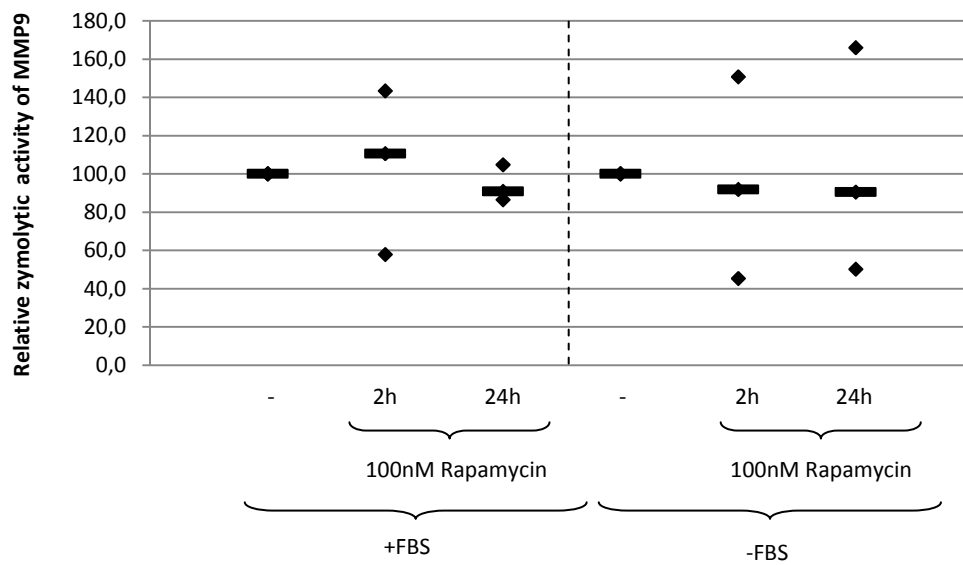


figure 67. Zymolytic activity of MMP9 when supplemented with or without serum. Bars indicate median value of three independent experiments, depicted as spades. Controls set independently as 100%.

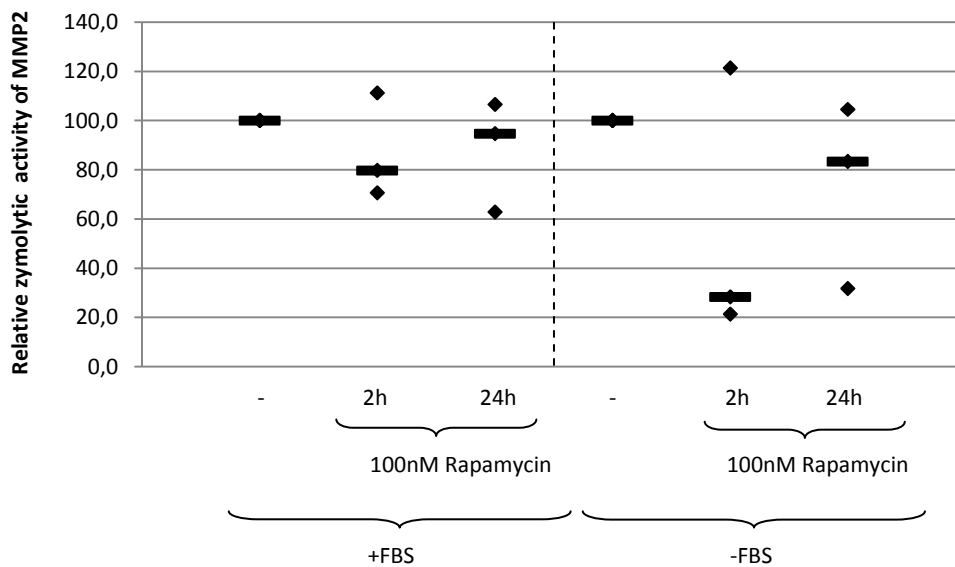


figure 68. Zymolytic activity of MMP2 when supplemented with or without serum. Bars indicate median value of three independent experiments, depicted as spades. Controls set independently as 100%.

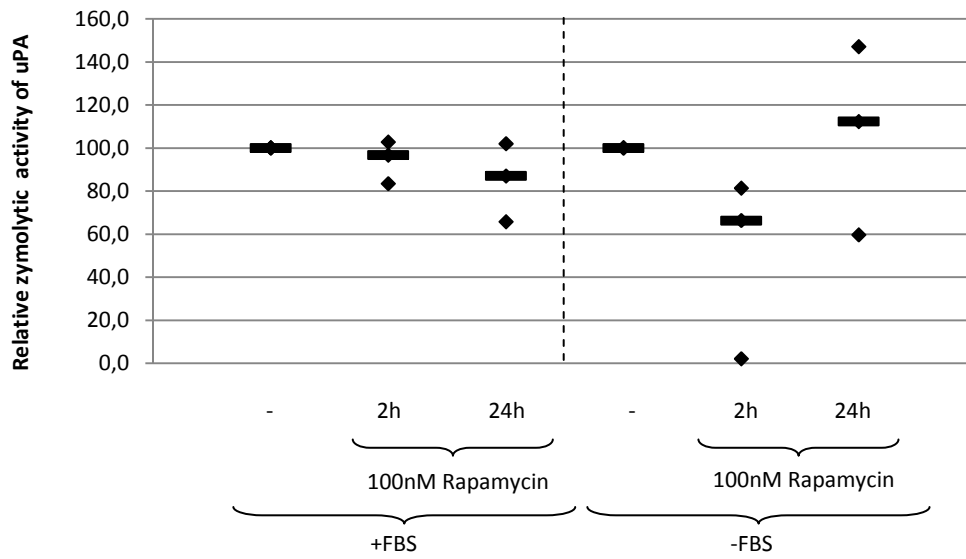


figure 69. Zymolytic activity of uPA when supplemented with or without serum. Bars indicate median value of three independent experiments, depicted as spades. Controls set independently as 100%.

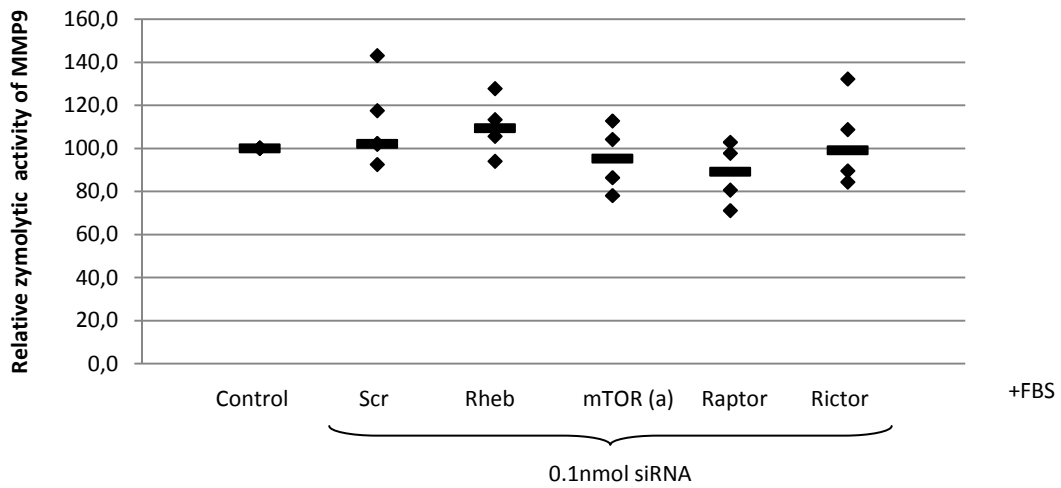


figure 70. Zymolytic activity of MMP9 when supplemented with serum. Bars indicate median value of at least four independent experiments, depicted as spades.



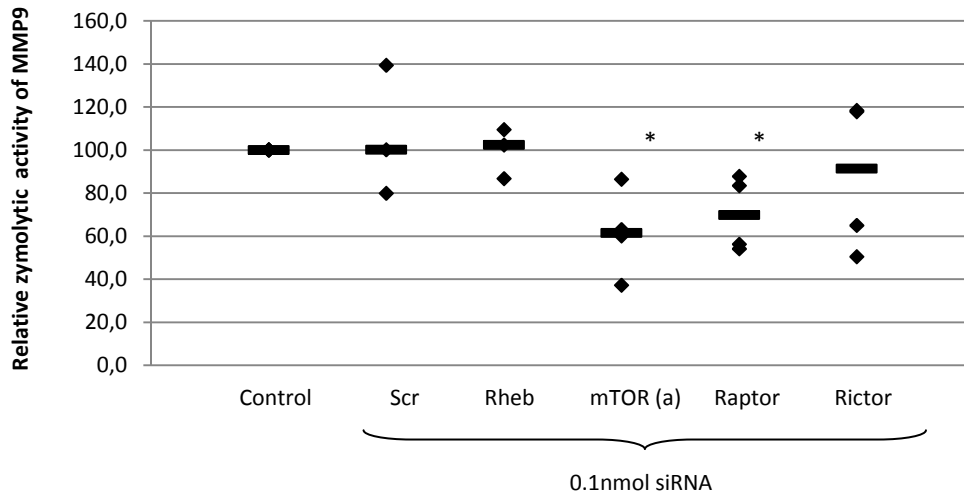


figure 71. Zymolytic activity of MMP9 when supplemented without serum. Bars indicate median value of at least four independent experiments, depicted as spades (Student t-test: \*  $p < 0.05$ ).

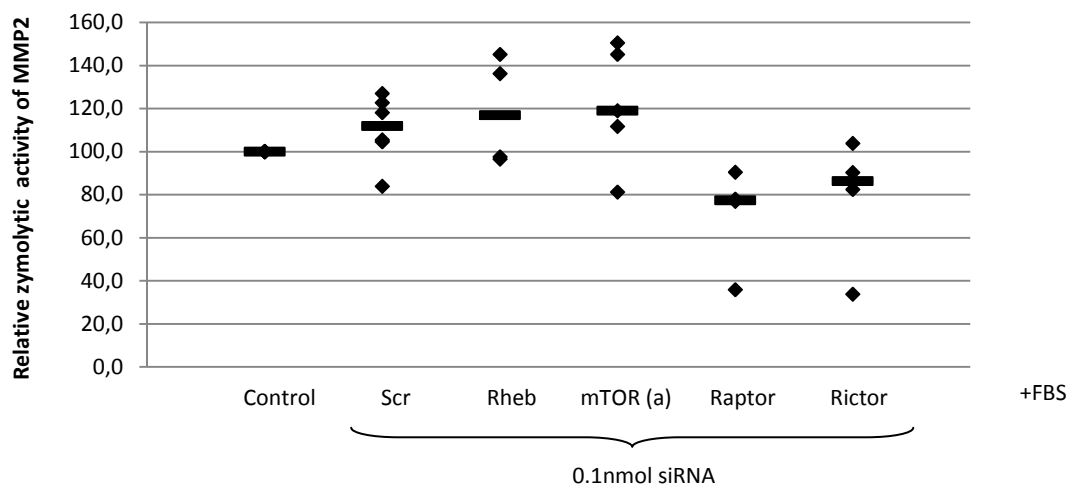


figure 72. Zymolytic activity of MMP2 when supplemented with serum. Bars indicate median value of at least four independent experiments, depicted as spades.

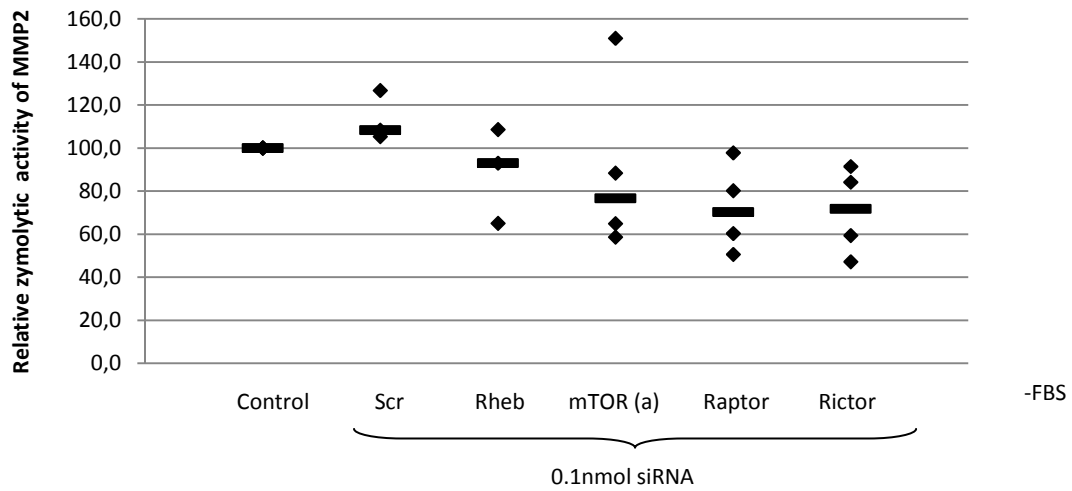


figure 73. Zymolytic activity of MMP2 when supplemented without serum. Bars indicate median value of at least four independent experiments, depicted as spades.

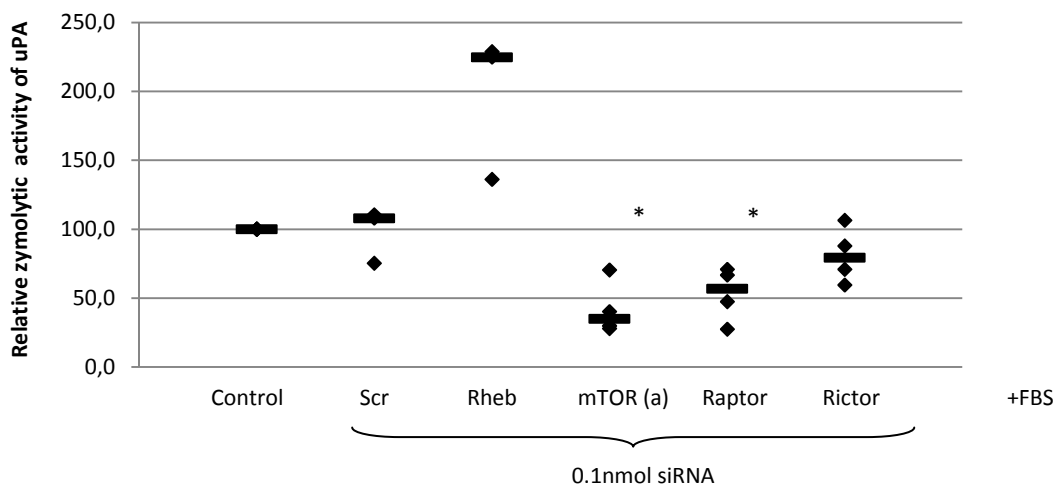


figure 74. Zymolytic activity of uPA when supplemented with serum. Bars indicate median value of at least four independent experiments, depicted as spades (Student t-Test: \*  $p < 0.02$ ).

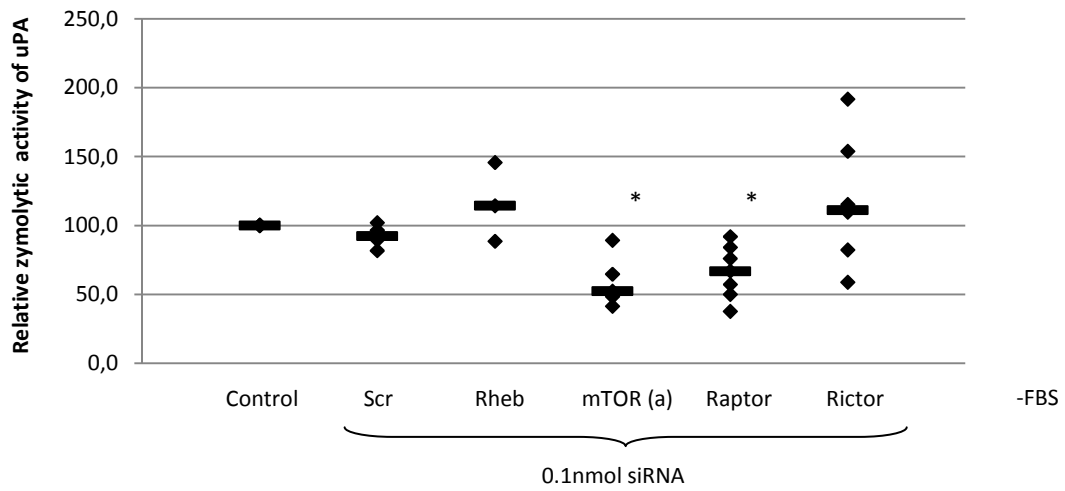


figure 75. Zymolytic activity of uPA when supplemented without serum. Bars indicate median value of at least four independent experiments, depicted as spades (Student t-Test: \*  $p < 0.03$ ).

### 5.3 Summary

In this study the regulation of the signal molecule mTOR by the GTPase Rheb and the role of this signaling pathway in respect to the invasive behaviour of human trophoblast cells, which is a critical feature in pregnancy, was examined.

Trophoblast cells are cells from foetal origin and upon implantation of the blastocyst, they infiltrate the maternal tissue and blood vessels and remodel it. In concert with maternal cells such as stromal and immune cells, they form the placenta. The placenta is a self-sufficient unit, which anchors the foetus and guarantees the required supply of nutrients and oxygen. At the foeto-maternal interface, the maternal immune system comes into contact with the semi-allogenic "foreign" trophoblasts. A variety of immune-suppressive mechanisms prevents a rejection of the foetus. The progression of the differentiation and invasion of the trophoblast cells even require a cellular and molecular contact between both individuals.

The secretion of extra-cellular matrix degrading enzymes enables cells to invade. The activity of those enzymes is controlled by secretion of inhibitors. Key enzymes for degrading the extra-cellular matrix during pregnancy are the matrix-metalloproteases (MMP) -2 and -9. Another enzyme which essentially influences invasiveness is the urokinase-like plasminogen activator (uPA) which major inhibitor is PAI-1. Trophoblast invasion is in many aspects similar to that of tumor cells but is physiologically restricted in terms of temporal and spatial limitations. The exact mechanism by which trophoblast invasion is regulated is largely unknown.

Several signalling pathways were linked to the invasive behaviour of cells. In mice models, the mammalian target of Rapamycin was discovered as an important molecule within embryogenesis and trophoblast outgrowth and migration. MTOR is a serine/threonine kinase and involved in the initiation of protein translation and thereby also in cell proliferation. MTOR is downstream in the PI3K/Akt pathway and is present in two complexes. Its binding partners are distinct in both complexes and determine Rapamycin-sensitivity and substrate specificity and thereby the functional outcome. In mTOR complex 1 (mTORC1), one component is Raptor and in complex 2 (mTORC2) is Rictor. The latter complex seems to be involved in the regulation of the cytoskeleton organization. The microbial product Rapamycin inhibits the kinase activity of mTORC1 and only upon prolonged exposure it inhibits the assembly of newly synthesized mTORC2 components. The kinase activity of mTOR is stimulated by various growth factors, extracellular amino acids and the intracellular energy level. In general, mTOR is described as sensor of the energy status. An overexpression of Rheb overcomes the sensitivity of mTOR kinase activity towards nutrient availability.

In order to unravel the exact mechanism how Rheb activates mTOR kinase activity, a set of 25 Rheb mutants was generated. Thereby, distinct, solvent-exposed amino acid residues of Rheb were substituted to the small, apolar amino acid alanine. Five loss-of-function mutants could be identified. An overexpression of those mutants *in vitro* could not overcome mTOR sensitivity upon amino acid withdrawal anymore. The mutation sites of these mutants were positioned within or adjacent to two functional important structures of Rheb,

named switch 1 and switch 2. The loss of function was not associated with an impaired binding property towards mTOR.

As model for trophoblasts, the cell line HTR8/SVneo, which originates from extra-villous first-trimester trophoblast cells, were chosen. It was focussed on functional analysis relevant to invasiveness such as the secretion of matrix-degrading enzymes (MMP2, -9, uPA) and one of its inhibitor (PAI-1) as well as the *in vitro* invasion behaviour upon manipulation of the cells. Those investigations were performed by substrate zymography, ELISA, immunocytochemistry and Matrigel invasion assays. Additionally, the effects on proliferation and apoptosis were checked. The expression of certain molecules within the mTOR signal cascade (Rheb, mTOR, Raptor, Rictor) was silenced by siRNA-induced RNA interference which is a post-transcriptional mRNA-degrading process. Also the mTOR kinase activity was inhibited by Rapamycin and serum-starvation.

As conclusion, it was seen that mTOR mainly influences proliferation and apoptosis. Nevertheless, there is a hint that there is a minor impact on invasiveness through regulation of uPA and PAI-1 secretion. The question whether the observed effects are mediated by mTORC1 or mTORC2 could not be fully resolved. Results implicate a pre-dominant role of mTORC1. In addition, a signal cross-talk between mTOR and Stat3 in human trophoblast cells could be demonstrated. The expression of mTOR in human term as well as first-trimester placenta could be confirmed by immunohistochemical staining and revealed elevated mTOR level in extra-villous and syncytial trophoblast cells.

Further studies should aim on the impact of recently identified mTOR complex 1 component and mTOR kinase inhibitor PRAS40. The unexpected outcome of loss-of-function Rheb binding to mTOR and also the opposing effects of Rheb and mTOR “knock-down” might be explained with this new discovered mTOR interaction partner. A further analysis of the role and regulation of uPA, its receptor of uPA (uPAR) and its major inhibitor PAI-1 on trophoblast invasiveness might be valuable in order to elucidate the clinical link of the uPA system to pregnancy-related disorders such as pre-eclampsia which is due hypoinvasiveness.

## 5.4 Bibliography and Index of Tables

Page II	Picture taken from <a href="http://pages.ca.inter.net">http://pages.ca.inter.net</a>	
Figure 1.	Schematic presentation of an implanting blastocyst. taken from Staun-Ram and Shalev 2005	[25]
Figure 2.	Schematic presentation of signaling pathways stimulating trophoblast migration. modified from Pollheimer <i>et al.</i> 2004	[23]
Figure 3.	Placental implantation site. modified after Lunghi <i>et al.</i> 2007	[16]
Figure 4.	Schematic structure of mTOR complex components. taken from Yang <i>et al.</i> 2008	[44]
Figure 5.	TOR signalling network. modified after Martin and Hall 2005	[147]
Figure 6.	Overall structure of Rheb-GppNHp complex taken from Yu <i>et al.</i> 2005	[61]
Figure 7.	Structure of Rapamycin. taken from <a href="http://www.molcan.com/rapamycin.htm">www.molcan.com/rapamycin.htm</a>	
Figure 8.	Sequence of human Rheb1. taken from Long <i>et al.</i> 2007	[97]
Figure 9.	Schematic presentation of experimental design.	
Figure 48.	Vector map. Modified from <a href="http://www.addgene.org/pgvec1?f=c&amp;cmd=showvecinfo&amp;vectorid=5578">www.addgene.org/pgvec1?f=c&amp;cmd=showvecinfo&amp;vectorid=5578</a>	
Table 1.	Some of the key factors regulating EVT cell function. taken from Lunghi <i>et al.</i> 2007	[16]
Table 2.	Set of Rheb1 mutants.	
Table 3.	Combination and incubation time of used inhibitors.	
Table 4.	Summary of results from two functional analysis experiments of Rheb mutant expression and their mTOR kinase rescue ability.	

## 5.5 References

- [1] Croy, B.A., et al., *Characterization of murine decidual natural killer (NK) cells and their relevance to the success of pregnancy*. Cell Immunol, 1985. 93(2): p. 315-26.
- [2] Szekeres-Bartho, J., *Immunological relationship between the mother and the fetus*. Int Rev Immunol, 2002. 21(6): p. 471-95.
- [3] Schmitt, C., B. Ghazi, and A. Bensussan, *NK cells and surveillance in humans*. Reprod Biomed Online, 2008. 16(2): p. 192-201.
- [4] Soundararajan, R. and A.J. Rao, *Trophoblast 'pseudo-tumorigenesis': significance and contributory factors*. Reprod Biol Endocrinol, 2004. 2: p. 15.
- [5] Mutter, W.P. and S.A. Karumanchi, *Molecular mechanisms of preeclampsia*. Microvasc Res, 2008. 75(1): p. 1-8.
- [6] Driscoll, S.G., *Gestational trophoblastic neoplasms: morphologic considerations*. Hum Pathol, 1977. 8(5): p. 529-39.
- [7] Gangloff, Y.G., et al., *Disruption of the mouse mTOR gene leads to early postimplantation lethality and prohibits embryonic stem cell development*. Mol Cell Biol, 2004. 24(21): p. 9508-16.
- [8] Manaseki, S. and R.F. Searle, *Natural killer (NK) cell activity of first trimester human decidua*. Cell Immunol, 1989. 121(1): p. 166-73.
- [9] Tabiasco, J., et al., *Human decidual NK cells: unique phenotype and functional properties -- a review*. Placenta, 2006. 27 Suppl A: p. S34-9.
- [10] Hiby, S.E., et al., *Combinations of maternal KIR and fetal HLA-C genes influence the risk of preeclampsia and reproductive success*. J Exp Med, 2004. 200(8): p. 957-65.
- [11] Thellin, O., et al., *Tolerance to the foeto-placental 'graft': ten ways to support a child for nine months*. Curr Opin Immunol, 2000. 12(6): p. 731-7.
- [12] Sargent, I.L., A.M. Borzychowski, and C.W. Redman, *Immunoregulation in normal pregnancy and preeclampsia: an overview*. Reprod Biomed Online, 2006. 13(5): p. 680-6.
- [13] Wegmann, T.G., et al., *Bidirectional cytokine interactions in the maternal-fetal relationship: is successful pregnancy a TH2 phenomenon?* Immunol Today, 1993. 14(7): p. 353-6.
- [14] Blois, S.M., et al., *A pivotal role for galectin-1 in fetomaternal tolerance*. Nat Med, 2007. 13(12): p. 1450-7.
- [15] Huppertz, B., *The feto-maternal interface: setting the stage for potential immune interactions*. Semin Immunopathol, 2007. 29(2): p. 83-94.
- [16] Lunghi, L., et al., *Control of human trophoblast function*. Reprod Biol Endocrinol, 2007. 5: p. 6.
- [17] Kauma, S., N. Hayes, and S. Weatherford, *The differential expression of hepatocyte growth factor and met in human placenta*. J Clin Endocrinol Metab, 1997. 82(3): p. 949-54.

- [18] Duan, C., J.R. Bauchat, and T. Hsieh, *Phosphatidylinositol 3-kinase is required for insulin-like growth factor-I-induced vascular smooth muscle cell proliferation and migration*. *Circ Res*, 2000. 86(1): p. 15-23.
- [19] McKinnon, T., et al., *Stimulation of human extravillous trophoblast migration by IGF-II is mediated by IGF type 2 receptor involving inhibitory G protein(s) and phosphorylation of MAPK*. *J Clin Endocrinol Metab*, 2001. 86(8): p. 3665-74.
- [20] Bass, K.E., et al., *Human cytotrophoblast invasion is up-regulated by epidermal growth factor: evidence that paracrine factors modify this process*. *Dev Biol*, 1994. 164(2): p. 550-61.
- [21] Lysiak, J.J., V.K. Han, and P.K. Lala, *Localization of transforming growth factor alpha in the human placenta and decidua: role in trophoblast growth*. *Biol Reprod*, 1993. 49(5): p. 885-94.
- [22] Athanassiades, A. and P.K. Lala, *Role of placenta growth factor (PlGF) in human extravillous trophoblast proliferation, migration and invasiveness*. *Placenta*, 1998. 19(7): p. 465-73.
- [23] Pollheimer, J. and M. Knofler, *Signalling pathways regulating the invasive differentiation of human trophoblasts: a review*. *Placenta*, 2005. 26 Suppl A: p. S21-30.
- [24] Uehara, Y., et al., *Placental defect and embryonic lethality in mice lacking hepatocyte growth factor/scatter factor*. *Nature*, 1995. 373(6516): p. 702-5.
- [25] Staun-Ram, E. and E. Shalev, *Human trophoblast function during the implantation process*. *Reprod Biol Endocrinol*, 2005. 3: p. 56.
- [26] Hirata, M., et al., *Differential regulation of the expression of matrix metalloproteinases and tissue inhibitors of metalloproteinases by cytokines and growth factors in bovine endometrial stromal cells and trophoblast cell line BT-1 in vitro*. *Biol Reprod*, 2003. 68(4): p. 1276-81.
- [27] Staun-Ram, E., et al., *Expression and importance of matrix metalloproteinase 2 and 9 (MMP-2 and -9) in human trophoblast invasion*. *Reprod Biol Endocrinol*, 2004. 2: p. 59.
- [28] Vassalli, J.D., A.P. Sappino, and D. Belin, *The plasminogen activator/plasmin system*. *J Clin Invest*, 1991. 88(4): p. 1067-72.
- [29] Vassalli, J.D., D. Baccino, and D. Belin, *A cellular binding site for the Mr 55,000 form of the human plasminogen activator, urokinase*. *J Cell Biol*, 1985. 100(1): p. 86-92.
- [30] Blasi, F., *The urokinase receptor. A cell surface, regulated chemokine*. *APMIS*, 1999. 107(1): p. 96-101.
- [31] Tecimer, C., et al., *Clinical relevance of urokinase-type plasminogen activator, its receptor, and its inhibitor type 1 in endometrial cancer*. *Gynecol Oncol*, 2001. 80(1): p. 48-55.
- [32] Andreasen, P.A., R. Egelund, and H.H. Petersen, *The plasminogen activation system in tumor growth, invasion, and metastasis*. *Cell Mol Life Sci*, 2000. 57(1): p. 25-40.
- [33] Hu, Z.Y., et al., *Expression of tissue type and urokinase type plasminogen activators as well as plasminogen activator inhibitor type-1 and type-2 in human and rhesus monkey placenta*. *J Anat*, 1999. 194 ( Pt 2): p. 183-95.
- [34] Planus, E., et al., *Binding of urokinase to plasminogen activator inhibitor type-1 mediates cell adhesion and spreading*. *J Cell Sci*, 1997. 110 ( Pt 9): p. 1091-8.
- [35] Floridon, C., et al., *Localization and significance of urokinase plasminogen activator and its receptor in placental tissue from intrauterine, ectopic and molar pregnancies*. *Placenta*, 1999. 20(8): p. 711-21.



- [36] Meade, E.S., Y.Y. Ma, and S. Guller, *Role of hypoxia-inducible transcription factors 1alpha and 2alpha in the regulation of plasminogen activator inhibitor-1 expression in a human trophoblast cell line.* Placenta, 2007. 28(10): p. 1012-9.
- [37] Graham, C.H., et al., *Establishment and characterization of first trimester human trophoblast cells with extended lifespan.* Exp Cell Res, 1993. 206(2): p. 204-11.
- [38] Chiu, M.I., H. Katz, and V. Berlin, *RAPT1, a mammalian homolog of yeast Tor, interacts with the FKBP12/rapamycin complex.* Proc Natl Acad Sci U S A, 1994. 91(26): p. 12574-8.
- [39] Schmelzle, T. and M.N. Hall, *TOR, a central controller of cell growth.* Cell, 2000. 103(2): p. 253-62.
- [40] Brunn, G.J., et al., *The mammalian target of rapamycin phosphorylates sites having a (Ser/Thr)-Pro motif and is activated by antibodies to a region near its COOH terminus.* J Biol Chem, 1997. 272(51): p. 32547-50.
- [41] Isotani, S., et al., *Immunopurified mammalian target of rapamycin phosphorylates and activates p70 S6 kinase alpha in vitro.* J Biol Chem, 1999. 274(48): p. 34493-8.
- [42] Andrade, M.A. and P. Bork, *HEAT repeats in the Huntington's disease protein.* Nat Genet, 1995. 11(2): p. 115-6.
- [43] Sekulic, A., et al., *A direct linkage between the phosphoinositide 3-kinase-AKT signaling pathway and the mammalian target of rapamycin in mitogen-stimulated and transformed cells.* Cancer Res, 2000. 60(13): p. 3504-13.
- [44] Yang, X., et al., *The mammalian target of rapamycin-signaling pathway in regulating metabolism and growth.* J Anim Sci, 2008. 86(14 Suppl): p. E36-50.
- [45] Jacinto, E., et al., *Mammalian TOR complex 2 controls the actin cytoskeleton and is rapamycin insensitive.* Nat Cell Biol, 2004. 6(11): p. 1122-8.
- [46] Kuruvilla, F.G. and S.L. Schreiber, *The PIK-related kinases intercept conventional signaling pathways.* Chem Biol, 1999. 6(5): p. R129-36.
- [47] Wullschleger, S., R. Loewith, and M.N. Hall, *TOR signaling in growth and metabolism.* Cell, 2006. 124(3): p. 471-84.
- [48] Edinger, A.L. and C.B. Thompson, *Akt maintains cell size and survival by increasing mTOR-dependent nutrient uptake.* Mol Biol Cell, 2002. 13(7): p. 2276-88.
- [49] Cheadle, J.P., et al., *Molecular genetic advances in tuberous sclerosis.* Hum Genet, 2000. 107(2): p. 97-114.
- [50] Manning, B.D. and L.C. Cantley, *Rheb fills a GAP between TSC and TOR.* Trends Biochem Sci, 2003. 28(11): p. 573-6.
- [51] Hay, N. and N. Sonenberg, *Upstream and downstream of mTOR.* Genes Dev, 2004. 18(16): p. 1926-45.
- [52] Long, X., et al., *Rheb binding to mammalian target of rapamycin (mTOR) is regulated by amino acid sufficiency.* J Biol Chem, 2005. 280(25): p. 23433-6.
- [53] Gao, X., et al., *Tsc tumour suppressor proteins antagonize amino-acid-TOR signalling.* Nat Cell Biol, 2002. 4(9): p. 699-704.
- [54] Kim, D.H., et al., *mTOR interacts with raptor to form a nutrient-sensitive complex that signals to the cell growth machinery.* Cell, 2002. 110(2): p. 163-75.

- [55] Inoki, K., T. Zhu, and K.L. Guan, *TSC2 mediates cellular energy response to control cell growth and survival*. Cell, 2003. 115(5): p. 577-90.
- [56] Shen, C., et al., *TOR signaling is a determinant of cell survival in response to DNA damage*. Mol Cell Biol, 2007. 27(20): p. 7007-17.
- [57] Reiling, J.H. and D.M. Sabatini, *Stress and mTOR signaling*. Oncogene, 2006. 25(48): p. 6373-83.
- [58] Yamagata, K., et al., *rheb, a growth factor- and synaptic activity-regulated gene, encodes a novel Ras-related protein*. J Biol Chem, 1994. 269(23): p. 16333-9.
- [59] Castro, A.F., et al., *Rheb binds tuberous sclerosis complex 2 (TSC2) and promotes S6 kinase activation in a rapamycin- and farnesylation-dependent manner*. J Biol Chem, 2003. 278(35): p. 32493-6.
- [60] Inoki, K., et al., *Rheb GTPase is a direct target of TSC2 GAP activity and regulates mTOR signaling*. Genes Dev, 2003. 17(15): p. 1829-34.
- [61] Yu, Y., et al., *Structural basis for the unique biological function of small GTPase RHEB*. J Biol Chem, 2005. 280(17): p. 17093-100.
- [62] Burnett, P.E., et al., *RAFT1 phosphorylation of the translational regulators p70 S6 kinase and 4E-BP1*. Proc Natl Acad Sci U S A, 1998. 95(4): p. 1432-7.
- [63] Nojima, H., et al., *The mammalian target of rapamycin (mTOR) partner, raptor, binds the mTOR substrates p70 S6 kinase and 4E-BP1 through their TOR signaling (TOS) motif*. J Biol Chem, 2003. 278(18): p. 15461-4.
- [64] Oshiro, N., et al., *The proline-rich Akt substrate of 40 kDa (PRAS40) is a physiological substrate of mammalian target of rapamycin complex 1*. J Biol Chem, 2007. 282(28): p. 20329-39.
- [65] Fonseca, B.D., et al., *PRAS40 is a target for mammalian target of rapamycin complex 1 and is required for signaling downstream of this complex*. J Biol Chem, 2007. 282(34): p. 24514-24.
- [66] Wang, L., T.E. Harris, and J.C. Lawrence, Jr., *Regulation of Proline-Rich Akt Substrate of 40 kDa function by mammalian target of rapamycin complex 1-mediated phosphorylation*. J Biol Chem, 2008.
- [67] Jefferies, H.B., et al., *Rapamycin suppresses 5'TOP mRNA translation through inhibition of p70s6k*. EMBO J, 1997. 16(12): p. 3693-704.
- [68] Jefferies, H.B., et al., *Rapamycin selectively represses translation of the "polypyrimidine tract" mRNA family*. Proc Natl Acad Sci U S A, 1994. 91(10): p. 4441-5.
- [69] Rousseau, D., et al., *The eIF4E-binding proteins 1 and 2 are negative regulators of cell growth*. Oncogene, 1996. 13(11): p. 2415-20.
- [70] Lawrence, J.C., Jr. and R.T. Abraham, *PHAS/4E-BPs as regulators of mRNA translation and cell proliferation*. Trends Biochem Sci, 1997. 22(9): p. 345-9.
- [71] Sarbassov, D.D., et al., *Phosphorylation and regulation of Akt/PKB by the rictor-mTOR complex*. Science, 2005. 307(5712): p. 1098-101.
- [72] Sarbassov, D.D., et al., *Prolonged rapamycin treatment inhibits mTORC2 assembly and Akt/PKB*. Mol Cell, 2006. 22(2): p. 159-68.
- [73] Sarbassov, D.D., et al., *Rictor, a novel binding partner of mTOR, defines a rapamycin-insensitive and raptor-independent pathway that regulates the cytoskeleton*. Curr Biol, 2004. 14(14): p. 1296-302.

- [74] Um, S.H., D. D'Alessio, and G. Thomas, *Nutrient overload, insulin resistance, and ribosomal protein S6 kinase 1, S6K1*. *Cell Metab*, 2006. 3(6): p. 393-402.
- [75] Chiang, G.G. and R.T. Abraham, *Phosphorylation of mammalian target of rapamycin (mTOR) at Ser-2448 is mediated by p70S6 kinase*. *J Biol Chem*, 2005. 280(27): p. 25485-90.
- [76] Holz, M.K. and J. Blenis, *Identification of S6 kinase 1 as a novel mammalian target of rapamycin (mTOR)-phosphorylating kinase*. *J Biol Chem*, 2005. 280(28): p. 26089-93.
- [77] Yokogami, K., et al., *Serine phosphorylation and maximal activation of STAT3 during CNTF signaling is mediated by the rapamycin target mTOR*. *Curr Biol*, 2000. 10(1): p. 47-50.
- [78] Decker, T. and P. Kovarik, *Serine phosphorylation of STATs*. *Oncogene*, 2000. 19(21): p. 2628-37.
- [79] Levy, D.E. and C.K. Lee, *What does Stat3 do?* *J Clin Invest*, 2002. 109(9): p. 1143-8.
- [80] Heitman, J., N.R. Movva, and M.N. Hall, *Targets for cell cycle arrest by the immunosuppressant rapamycin in yeast*. *Science*, 1991. 253(5022): p. 905-9.
- [81] Koltin, Y., et al., *Rapamycin sensitivity in Saccharomyces cerevisiae is mediated by a peptidyl-prolyl cis-trans isomerase related to human FK506-binding protein*. *Mol Cell Biol*, 1991. 11(3): p. 1718-23.
- [82] Brown, E.J., et al., *A mammalian protein targeted by G1-arresting rapamycin-receptor complex*. *Nature*, 1994. 369(6483): p. 756-8.
- [83] Guertin, D.A. and D.M. Sabatini, *An expanding role for mTOR in cancer*. *Trends Mol Med*, 2005. 11(8): p. 353-61.
- [84] Vivanco, I. and C.L. Sawyers, *The phosphatidylinositol 3-Kinase AKT pathway in human cancer*. *Nat Rev Cancer*, 2002. 2(7): p. 489-501.
- [85] Im, E., et al., *Rheb is in a high activation state and inhibits B-Raf kinase in mammalian cells*. *Oncogene*, 2002. 21(41): p. 6356-65.
- [86] Noh, W.C., et al., *Determinants of rapamycin sensitivity in breast cancer cells*. *Clin Cancer Res*, 2004. 10(3): p. 1013-23.
- [87] Treeck, O., et al., *Effects of a combined treatment with mTOR inhibitor RAD001 and tamoxifen in vitro on growth and apoptosis of human cancer cells*. *Gynecol Oncol*, 2006. 102(2): p. 292-9.
- [88] Sifontis, N.M., et al., *Pregnancy outcomes in solid organ transplant recipients with exposure to mycophenolate mofetil or sirolimus*. *Transplantation*, 2006. 82(12): p. 1698-702.
- [89] McKay, D.B., et al., *Reproduction and pregnancy in transplant recipients: current practices*. *Prog Transplant*, 2006. 16(2): p. 127-32.
- [90] Hentges, K.E., et al., *FRAP/mTOR is required for proliferation and patterning during embryonic development in the mouse*. *Proc Natl Acad Sci U S A*, 2001. 98(24): p. 13796-801.
- [91] Murakami, M., et al., *mTOR is essential for growth and proliferation in early mouse embryos and embryonic stem cells*. *Mol Cell Biol*, 2004. 24(15): p. 6710-8.
- [92] Wen, H.Y., et al., *mTOR: a placental growth signaling sensor*. *Placenta*, 2005. 26 Suppl A: p. S63-9.
- [93] Martin, P.M., A.E. Sutherland, and L.J. Van Winkle, *Amino acid transport regulates blastocyst implantation*. *Biol Reprod*, 2003. 69(4): p. 1101-8.

- [94] Van Winkle, L.J., et al., *System B0,+ amino acid transport regulates the penetration stage of blastocyst implantation with possible long-term developmental consequences through adulthood*. Hum Reprod Update, 2006. 12(2): p. 145-57.
- [95] Roos, S., et al., *Mammalian target of rapamycin in the human placenta regulates leucine transport and is down-regulated in restricted fetal growth*. J Physiol, 2007. 582(Pt 1): p. 449-59.
- [96] Fitzgerald, J.S., et al., *Leukemia inhibitory factor triggers activation of signal transducer and activator of transcription 3, proliferation, invasiveness, and altered protease expression in choriocarcinoma cells*. Int J Biochem Cell Biol, 2005. 37(11): p. 2284-96.
- [97] Long, X., et al., *The Rheb switch 2 segment is critical for signaling to target of rapamycin complex 1*. J Biol Chem, 2007. 282(25): p. 18542-51.
- [98] Long, X., et al., *Rheb binds and regulates the mTOR kinase*. Curr Biol, 2005. 15(8): p. 702-13.
- [99] Jackson, A.L., et al., *Expression profiling reveals off-target gene regulation by RNAi*. Nat Biotechnol, 2003. 21(6): p. 635-7.
- [100] Sledz, C.A., et al., *Activation of the interferon system by short-interfering RNAs*. Nat Cell Biol, 2003. 5(9): p. 834-9.
- [101] Pauls, E., et al., *Induction of interleukins IL-6 and IL-8 by siRNA*. Clin Exp Immunol, 2007. 147(1): p. 189-96.
- [102] Gutierrez-Dalmau, A. and J.M. Campistol, *The role of proliferation signal inhibitors in post-transplant malignancies*. Nephrol Dial Transplant, 2007. 22 Suppl 1: p. i11-6.
- [103] Burgering, B.M. and R.H. Medema, *Decisions on life and death: FOXO Forkhead transcription factors are in command when PKB/Akt is off duty*. J Leukoc Biol, 2003. 73(6): p. 689-701.
- [104] Vanhaesebroeck, B., et al., *Autophosphorylation of p110delta phosphoinositide 3-kinase: a new paradigm for the regulation of lipid kinases in vitro and in vivo*. EMBO J, 1999. 18(5): p. 1292-302.
- [105] Thimmaiah, K.N., et al., *Insulin-like growth factor I-mediated protection from rapamycin-induced apoptosis is independent of Ras-Erk1-Erk2 and phosphatidylinositol 3'-kinase-Akt signaling pathways*. Cancer Res, 2003. 63(2): p. 364-74.
- [106] Hahn, M., et al., *Rapamycin and UCN-01 synergistically induce apoptosis in human leukemia cells through a process that is regulated by the Raf-1/MEK/ERK, Akt, and JNK signal transduction pathways*. Mol Cancer Ther, 2005. 4(3): p. 457-70.
- [107] Thedieck, K., et al., *PRAS40 and PRR5-like protein are new mTOR interactors that regulate apoptosis*. PLoS ONE, 2007. 2(11): p. e1217.
- [108] Sancak, Y., et al., *PRAS40 is an insulin-regulated inhibitor of the mTORC1 protein kinase*. Mol Cell, 2007. 25(6): p. 903-15.
- [109] Rhoads, J.M., et al., *Role of mTOR signaling in intestinal cell migration*. Am J Physiol Gastrointest Liver Physiol, 2006. 291(3): p. G510-7.
- [110] Liu, L., et al., *Rapamycin inhibits cell motility by suppression of mTOR-mediated S6K1 and 4E-BP1 pathways*. Oncogene, 2006. 25(53): p. 7029-40.
- [111] Rhoads, J.M., et al., *Arginine stimulates intestinal cell migration through a focal adhesion kinase dependent mechanism*. Gut, 2004. 53(4): p. 514-22.

- [112] Berven, L.A. and M.F. Crouch, *Cellular function of p70S6K: a role in regulating cell motility*. Immunol Cell Biol, 2000. 78(4): p. 447-51.
- [113] Zhou, H.Y. and A.S. Wong, *Activation of p70S6K induces expression of matrix metalloproteinase 9 associated with hepatocyte growth factor-mediated invasion in human ovarian cancer cells*. Endocrinology, 2006. 147(5): p. 2557-66.
- [114] Fazleabas, A.T., S.L. Everly, and R. Lottenberg, *Immunological and molecular characterization of plasminogen activator inhibitors 1 and 2 in baboon (Papio anubis) placental tissues*. Biol Reprod, 1991. 45(1): p. 49-56.
- [115] Estelles, A., et al., *Altered expression of plasminogen activator inhibitor type 1 in placentas from pregnant women with preeclampsia and/or intrauterine fetal growth retardation*. Blood, 1994. 84(1): p. 143-50.
- [116] Blasi, F., J.D. Vassalli, and K. Dano, *Urokinase-type plasminogen activator: proenzyme, receptor, and inhibitors*. J Cell Biol, 1987. 104(4): p. 801-4.
- [117] Ogura, Y., et al., *Plasmin induces degradation and dysfunction of laminin 332 (laminin 5) and impaired assembly of basement membrane at the dermal-epidermal junction*. Br J Dermatol, 2008.
- [118] Liu, J., et al., *Noncatalytic domain of uPA stimulates human extravillous trophoblast migration by using phospholipase C, phosphatidylinositol 3-kinase and mitogen-activated protein kinase*. Exp Cell Res, 2003. 286(1): p. 138-51.
- [119] Hildenbrand, R., et al., *The urokinase-system--role of cell proliferation and apoptosis*. Histol Histopathol, 2008. 23(2): p. 227-36.
- [120] Pepper, M.S., et al., *Proteolytic balance and capillary morphogenesis in vitro*. EXS, 1992. 61: p. 137-45.
- [121] Renaud, S.J., et al., *Activated macrophages inhibit human cytotrophoblast invasiveness in vitro*. Biol Reprod, 2005. 73(2): p. 237-43.
- [122] Huber, A.V., et al., *TNFalpha-mediated induction of PAI-1 restricts invasion of HTR-8/SVneo trophoblast cells*. Placenta, 2006. 27(2-3): p. 127-36.
- [123] Pontrelli, P., et al., *Rapamycin inhibits PAI-1 expression and reduces interstitial fibrosis and glomerulosclerosis in chronic allograft nephropathy*. Transplantation, 2008. 85(1): p. 125-34.
- [124] Foekens, J.A., et al., *Plasminogen activator inhibitor-1 and prognosis in primary breast cancer*. J Clin Oncol, 1994. 12(8): p. 1648-58.
- [125] Knoop, A., et al., *Prognostic significance of urokinase-type plasminogen activator and plasminogen activator inhibitor-1 in primary breast cancer*. Br J Cancer, 1998. 77(6): p. 932-40.
- [126] Czekay, R.P., et al., *Plasminogen activator inhibitor-1 detaches cells from extracellular matrices by inactivating integrins*. J Cell Biol, 2003. 160(5): p. 781-91.
- [127] Yu, H., M. Kortylewski, and D. Pardoll, *Crosstalk between cancer and immune cells: role of STAT3 in the tumour microenvironment*. Nat Rev Immunol, 2007. 7(1): p. 41-51.
- [128] Takeda, K., et al., *Targeted disruption of the mouse Stat3 gene leads to early embryonic lethality*. Proc Natl Acad Sci U S A, 1997. 94(8): p. 3801-4.
- [129] Kim, J.H., et al., *Regulation of interleukin-6-induced hepatic insulin resistance by mammalian target of rapamycin through the STAT3-SOCS3 pathway*. J Biol Chem, 2008. 283(2): p. 708-15.

- [130] Duncan, S.A., et al., *STAT signaling is active during early mammalian development*. Dev Dyn, 1997. 208(2): p. 190-8.
- [131] Xie, T.X., et al., *Stat3 activation regulates the expression of matrix metalloproteinase-2 and tumor invasion and metastasis*. Oncogene, 2004. 23(20): p. 3550-60.
- [132] Dechow, T.N., et al., *Requirement of matrix metalloproteinase-9 for the transformation of human mammary epithelial cells by Stat3-C*. Proc Natl Acad Sci U S A, 2004. 101(29): p. 10602-7.
- [133] Harvey, M.B., et al., *Proteinase expression in early mouse embryos is regulated by leukaemia inhibitory factor and epidermal growth factor*. Development, 1995. 121(4): p. 1005-14.
- [134] Takahashi, K., M. Murakami, and S. Yamanaka, *Role of the phosphoinositide 3-kinase pathway in mouse embryonic stem (ES) cells*. Biochem Soc Trans, 2005. 33(Pt 6): p. 1522-5.
- [135] Kovacina, K.S., et al., *Identification of a proline-rich Akt substrate as a 14-3-3 binding partner*. J Biol Chem, 2003. 278(12): p. 10189-94.
- [136] Vander Haar, E., et al., *Insulin signalling to mTOR mediated by the Akt/PKB substrate PRAS40*. Nat Cell Biol, 2007. 9(3): p. 316-23.
- [137] Zini, J.M., et al., *Characterization of urokinase receptor expression by human placental trophoblasts*. Blood, 1992. 79(11): p. 2917-29.
- [138] Mulhaupt, H.A., et al., *Expression of urokinase receptors by human trophoblast. A histochemical and ultrastructural analysis*. Lab Invest, 1994. 71(3): p. 392-400.
- [139] McCrae, K.R., et al., *Detection of antitrophoblast antibodies in the sera of patients with anticardiolipin antibodies and fetal loss*. Blood, 1993. 82(9): p. 2730-41.
- [140] Akcakanat, A., et al., *Rapamycin regulates the phosphorylation of rictor*. Biochem Biophys Res Commun, 2007. 362(2): p. 330-3.
- [141] Jorgensen, M., et al., *Plasminogen activator inhibitor-1 is the primary inhibitor of tissue-type plasminogen activator in pregnancy plasma*. Thromb Haemost, 1987. 58(3): p. 872-8.
- [142] Gao, M., et al., *The imbalance of plasminogen activators and inhibitor in preeclampsia*. J Obstet Gynaecol Res, 1996. 22(1): p. 9-16.
- [143] Rosenberg, K.R. and W.R. Trevathan, *An anthropological perspective on the evolutionary context of preeclampsia in humans*. J Reprod Immunol, 2007. 76(1-2): p. 91-7.
- [144] Zenclussen, A.C., et al., *Introducing a mouse model for pre-eclampsia: adoptive transfer of activated Th1 cells leads to pre-eclampsia-like symptoms exclusively in pregnant mice*. Eur J Immunol, 2004. 34(2): p. 377-87.
- [145] Nishizawa, H., et al., *Mouse model for allogeneic immune reaction against fetus recapitulates human pre-eclampsia*. J Obstet Gynaecol Res, 2008. 34(1): p. 1-6.
- [146] Davisson, R.L., et al., *Discovery of a spontaneous genetic mouse model of preeclampsia*. Hypertension, 2002. 39(2 Pt 2): p. 337-42.
- [147] Martin, D.E. and M.N. Hall, *The expanding TOR signaling network*. Curr Opin Cell Biol, 2005. 17(2): p. 158-66.

## Zusammenfassung

In der vorliegenden Arbeit wurde die Regulation des Signalmoleküls mTOR durch die GTPase Rheb und die Rolle dieses Signalweges in Bezug auf das Invasionsverhalten von humanen Trophoblasten, welches ein kritisches Merkmal in der Schwangerschaft darstellt, näher untersucht.

Trophoblasten sind fetale Zellen, die nach Implantation der Blastocyste in das mütterliche Gewebe einwachsen. Sie infiltrieren und remodelieren das umliegende Gewebe und Blutgefäße und zusammen mit mütterlichen Zellen (Stroma-, Immunzellen) bilden sie die Plazenta. Die Plazenta ist ein eigenständiges Organ, welche den Fetus verankert und die Versorgung mit lebenswichtigen Elementen wie Nährstoffe und Sauerstoff gewährleistet. An der fetal-maternalen Grenzfläche kommt es zum Kontakt zwischen mütterlichen Immunzellen und den semi-allogenen, „fremden“ Trophoblast-Zellen. Eine Vielzahl an immunsuppressiven Mechanismen verhindert eine Abstoßungsreaktion. Weiterhin wird dieser Kontakt benötigt, um die Differenzierung und die Invasion der Trophoblasten voranzutreiben.

Die Sekretion von Enzymen, die die extrazelluläre Matrix abbauen, befähigt die Trophoblasten zur Invasion. Die Aktivität dieser Enzyme wird durch Sekretion von Inhibitoren kontrolliert. Als Schlüsselenzyme für die Degradation der extrazellulären Matrix wurden die Matrixmetalloproteasen (MMP)-2 und -9 in der Plazenta entdeckt. Ein weiteres Enzym, das Zellinvasion wesentlich beeinflusst, ist urokinase-ähnliche Plasminogenaktivator (uPA). Die Trophoblast-Invasion ähnelt in vielen Merkmalen denen von Tumorzellen, mit dem Unterschied, dass die Invasivität von Trophoblasten zeitlich und räumlich begrenzt ist. Die genauen physiologischen Mechanismen, die die Trophoblasten-Invasion regulieren und einschränken, sind weitestgehend unbekannt.

Verschiedene Signalwege wurden mit Invasivität von Zellen in Verbindung gebracht. In Mausmodellen konnte mammalian target of Rapamycin (mTOR) als essentielles Molekül in Embryogenese und Trophoblasten-Auswuchs und -Migration aufgedeckt werden. mTOR ist eine Serin/Threonin-Kinase und wesentlich an der Initiation der Proteintranslation und damit der Zellproliferation und des Zellwachstums beteiligt. mTOR befindet sich downstream im PI3K/Akt Signalweg und kommt in zwei Komplexen vor. Die Bindungspartner von mTOR unterscheiden sich in beiden Komplexen und bestimmen die Substratspezifität als auch die Sensitivität zu Rapamycin. Im mTOR Komplex 1 (mTORC1) ist mTOR im Verbund mit Raptor und im Komplex 2 (mTORC2) mit Rictor. Das mikrobielle Produkt Rapamycin hemmt die Kinaseaktivität von mTORC1 und verhindert erst nach längerer Gabe die Neuformation von mTORC2. Die Kinaseaktivität wird über verschiedene Wachstumsfaktoren, extrazelluläre Aminosäuren und dem intrazellulären Energiestatus reguliert. mTOR wird als Sensor des Energielevels im Allgemeinen beschrieben. Eine Überexpression des mTOR Regulators Rheb kann diese Empfindlichkeit gegenüber dem verfügbaren Energielevel aufheben.

Um den genauen Mechanismus der Regulation von Rheb in der Aktivierung der mTOR-Kinaseaktivität zu klären, wurden 25 Rheb-Mutanten generiert. Dabei wurden verschiedene, exponierte Aminosäurereste von Rheb mit der unpolaren, einfachen Aminosäure Alanin substituiert. Es wurden fünf Mutanten mit Funktionsverlust

identifiziert. Eine Überexpression dieser Mutanten *in vitro* konnte die Sensitivität von mTOR nach Entzug extrazellulärer Aminosäuren nicht aufheben. Die Mutationen dieser Mutanten lag innerhalb oder benachbart der zwei funktionellen Strukturen von Rheb, die als Switch 1 und Switch 2 bezeichnet werden. Der Funktionsverlust ging unerwarteterweise nicht mit einer verminderten Bindung zu mTOR einher.

Als Modell für Trophoblasten diente die Zelllinie HTR8/SVneo, die aus extravillösen Ersttrimester-Trophoblasten erhalten und immortalisiert wurde. Im Fokus standen funktionelle Analysen, die relevant für die Zellinvasion sind. Darunter zählten Untersuchungen *in vitro*, die die Sekretion von Enzymen, die die extrazelluläre Matrix verdauen können (MMP2, MMP9, uPA), und des Inhibitors eines solchen Enzyms (PAI-1), als auch die Invasivität einschlossen. Methodisch wurde dies ermöglicht durch Substrat-Zymographie, ELISA, Immunzytochemie und Matrigel Invasionsassay-Experimente. Weiterhin wurde auch das Proliferation- und Apoptoseverhalten geprüft. Um die Einflüsse einzelner Moleküle des mTOR Signalweges (Rheb, mTOR, Raptor, Rictor) auf die genannten Eigenschaften zu untersuchen, wurde deren Expression mit Hilfe durch siRNA-induzierter RNA-Interferenz post-transkriptional gehemmt. Zusätzlich wurde durch Inkubation mit Rapamycin und durch Serumentzug die Kinaseaktivität von mTOR inhibiert. Es wurde festgestellt, dass mTOR hauptsächlich in Proliferation und Apoptose der gewählten Zelllinie involviert ist. Gemessene Unterschiede im Invasions- und Sekretionsverhalten konnten auf diese Effekte zurückgeführt werden. Dennoch gibt es einen Einfluss auf die Invasivität vermutlich über die Regulation der Sekretion von uPA und dessen Inhibitor PAI-1. Zusätzlich konnte nachgewiesen werden, dass Rapamycin und mTOR Silencing die Serin-Phosphorylierung von Stat3 negativ beeinflussen.

Generell konnte gezeigt werden, dass mTOR hauptsächlich die Proliferation- und Apoptoserate in der gewählten Trophoblastzelllinie beeinflusst. Es konnte auch nachgewiesen werden, dass mTOR die Trophoblastinvasion durch Regulation der Sekretion von uPA and PAI-1 beeinflusst. Die Frage, ob diese Regulation über mTORC1 oder mTORC2 vermittelt wird, konnte nicht vollständig geklärt werden. Die Ergebnisse deuten auf eine größere Rolle für mTORC1. Zusätzlich konnte ein Cross-talk zwischen mTOR und Stat3 in humanen Trophoblasten bestätigt werden. Die Expression von mTOR konnte in humanen Plazenten aus dem ersten und dritten Trimester nachgewiesen werden. Immunhistochemische Analysen zeigten eine erhöhte mTOR Expression in extravillösen und synzytialen Trophoblasten für beide Zeitpunkte.

Zukünftige Studien sollten den Einfluss von PRAS40 auf mTOR-vermittelte Signale klären. PRAS40 ist kürzlich als integraler Bestandteil mTORC1, der die Kinaseaktivität von mTOR inhibiert, entdeckt worden. Mithilfe dieses Proteins könnte die unerwartete Bindung von funktionsverlustigen Rheb-Mutanten an mTOR als auch die gegenteilige Effekte von Rheb und mTOR knockdown erklärt werden. Weiterhin sollte die Bedeutung des uPA-Systems in Hinsicht auf die Regulation der Trophoblasteninvasion entschlüsselt werden, um klinische Ansätze zu Schwangerschafts-assoziierten Pathologien wie Prä-Eklampsie zu finden.



## Danksagung/Acknowledgement

Ich danke meiner Familie, ganz besonders meinen Eltern, die mir stets und zweifelsfrei beiseite stehen!

Ich danke meine Freunden, die immer ein offenes Ohr für mich haben und mich unterstützen. Besonderen Dank an Conni, Jasmin, Anne (extra Danke für Korrekturlesen), Astrid (ebenfalls extra Danke für Korrekturlesen), Julia, Karin, Frauke, Sandra, Ina, Conny, Matthias, Steffen und Antje.

Ich bedanke mich beim gesamten Team des Placentalabors für die nette und angenehme Zusammenarbeit: Stefan, Maja, Conny, André, Mike, Torben, Levon, Uta, Diana, Constance, Astrid, Cilia, Justine, Tobias und Lydia. Besonderen Dank an Maja mit meinen immunhistochemischen Fragen und der Mikroskophandhabung und an Stefan mit meinen statistischen Fragen.

I would like to thank Prof. Joseph Avruch for introducing me to mTOR and allowing me to be part of his team for half a year. My special thanks to Xiaomeng who was supervising me. Also special thanks to Matt, Joey, Maria, Florin, Dave, Changfeng, Ulla, Tom and Tania for making my stay, not just scientifically enormously worthwhile, but also very enjoyable.

I would also like to thank Prof. Charles Graham for sending the cells and for having me in his lab. Special thanks to Steve who supervised me and gave good ideas, and also to the rest of the team for their help and kindness.

Meinen herzlichen Dank an Prof. Claus Liebmann, der sich freundlicherweise als Zweitgutachter zur Verfügung stellte.

Meinen besonderen Dank an meinen Betreuer PD Udo Markert, der mich unterstützte und es mir ermöglichte auch außerhalb des eigenen Labors neue Methoden und Techniken zu erlernen.

Die vorliegende Arbeit wurde im Labor von Herrn PD  
*Dr. med.* Udo R. Markert im Klinikum der Friedrich-  
Schiller-Universität Jena, Abteilung für Gynäkologie und  
Geburtshilfe angefertigt.

#### **Ehrenwörtliche Erklärung**

Hiermit erkläre ich, dass mir die geltende Promotionsordnung der Biologisch-Pharmazeutischen Fakultät bekannt ist und ich die vorliegende Dissertation selbst verfasst habe und keine anderen als die angegebenen Quellen und Hilfsmittel verwendet habe und, dass alle Stellen, die dem Wortlaut oder Sinn nach, anderen Werken entnommen sind, durch Angaben deren Quellen kenntlich gemacht wurden. Folgende Personen haben mich bei der Auswertung von Ergebnissen und der Erstellung des Manuskriptes unterstützt: PD Dr. med. Udo R. Markert, Prof. Dr. rer. nat. Claus Liebmann, Prof. Joseph Avruch MD PhD, Prof. Charles Graham PhD, Prof. Sebastian San Martin, Xiaomeng Long PhD, Steven Renaud, Anne Braunschweig, Stefan Neubeck, Maja Weber. Die Hilfe eines Promotionsberaters wurde nicht Anspruch genommen. Dritte haben keine geldwerte Leistungen im Zusammenhang mit der vorgelegten Arbeit erhalten. Weiterhin wurde die vorliegende Dissertation oder Teile daraus keiner weiteren Institution/Universität als Prüfungsarbeit vorgelegt.

Jena, 05.06.2008

---

Diplom-Biochemikerin Susann Busch